

UC Irvine

UC Irvine Electronic Theses and Dissertations

Title

The KCNE2 potassium channel subunit in metabolic syndrome

Permalink

<https://escholarship.org/uc/item/2t30h8pp>

Author

Lee, Soomin

Publication Date

2016

Supplemental Material

<https://escholarship.org/uc/item/2t30h8pp#supplemental>

Peer reviewed|Thesis/dissertation

UNIVERSITY OF CALIFORNIA,
IRVINE

The KCNE2 potassium channel subunit in metabolic syndrome

DISSERTATION

submitted in partial satisfaction of the requirements
for the degree of

DOCTOR OF PHILOSOPHY

in Pharmacology

by

Soo-Min Lee

Dissertation Committee:
Professor Geoffrey W. Abbott, Chair
Professor Olivier Civelli
Professor Frederick J. Ehlert

2016

Chapter 1 © 2015 Elsevier Ltd.
Chapter 2 © 2016 Nature Publishing Group
All other materials © 2016 Soo-Min Lee

DEDICATION

To

my family and friends,

in recognition of their worth and love

Elizabeth and Charlotte,

In my whole life, you will always be what I wanted most.

TABLE OF CONTENTS

	Page
LIST OF FIGURES	v
ACKNOWLEDGMENTS	vii
CURRICULUM VITAE	ix
ABSTRACT OF THE DISSERTATION	xiii
INTRODUCTION	1
References	5
CHAPTER 1: <i>Kcne2</i> deletion promotes atherosclerosis and diet-dependent sudden death	
Abstract	10
Introduction	11
Methods	13
Results	15
Discussion	17
References	25

CHAPTER 2: *Kcne2* deletion causes early-onset nonalcoholic fatty liver disease via iron deficiency

Abstract	31
Introduction	32
Methods	34
Results and Discussion	38
References	53

CHAPTER 3: *Kcne2* deletion Type II Diabetes Mellitus via a primary defect in insulin secretion

Abstract	59
Introduction	60
Methods	63
Results	69
Discussion	72
References	94

CONCLUSION 102

References	105
------------	-----

LIST OF FIGURES

	Page
Chapter 1- Figure 1	19-21
Chapter 1- Figure 2	22-24
Chapter 2 – Figure 1	43-44
Chapter 2 – Figure 2	45
Chapter 2 – Figure 3	46-47
Chapter 2 – Figure 4	48
Chapter 2 – Figure 5	49-51
Chapter 2 – Figure 6	52
Chapter 3 – Figure 1	77
Chapter 3 – Figure 2	78
Chapter 3 – Figure 3	79
Chapter 3 – Figure 4	80-82
Chapter 3 – Figure 5	83
Chapter 3 – Figure 6	84
Chapter 3 – Figure 7	85
Chapter 3 – Figure 8	86
Chapter 3 – Supplementary Figure 1	87-89
Chapter 3 – Supplementary Figure 2	90

Chapter 3 – Supplementary Figure 3	91
Chapter 3 – Supplementary Figure 4	92
Chapter 3 – Supplementary Figure 5	93

ACKNOWLEDGMENTS

This thesis has become a reality with the kind support and help of many individuals. I would like to extend my sincere thanks to all of them.

I would like to express my deepest appreciation to my committee chair, Professor Geoffrey W. Abbott, who has the attitude and the substance of a genius. Without his guidance and persistent help, this dissertation would not have been possible. He has always been the greatest mentor and it is by his example that I have become the scientist that I am.

I would like to thank my committee members, Professor Olivier Civelli and Professor Frederick J. Ehlert. Both whom demonstrated the scientific enthusiasm, supported my study and provided valuable advice upon my thesis work during departmental presentations and routine lab meetings.

I would also like to thank our lab members including the other graduate student, Dan Neverisky, who is a kind friend, and post-Doc, Shawn Crump for their helpful discussions and technical support.

I would like to thank our lab technicians, Ritu Kant and Dara Nguyen who contributed to my work.

I would like to thank my undergraduate students Raquel Rios, Jasmine Baik, Vicky Nguyen, Thien Nguyen and Araxi Zakarian for their assistance with my experiments.

I would like to thank my current student colleagues Candice Gellner, Nayna Sanathara, Derek Greene, and Steve Liu and previous student colleagues JP David, Lien Wang, Peter Yu, John Park, Anastasia Kosenko, and Seungwoo Kang, and friends GyoungYoung Seok, Hong Yeol ,and SungYong Lee.

I thank my American cousins Junie, Ray, Mattew, Ruth, David, and Adam. I had a great time with them while I have stayed in the states.

I would like to thank my company, SK chemicals for support.

Finally, and most importantly, I would like to express my gratitude towards my family for the encouragement which helped me complete this work. I thank my beloved wife, JeeAh who is a strong and great mother. She has taken care of our first daughter, Elizabeth, without me in Korea. As my soulmate, best friend and life partner, she strengthens me.

I thank my lovely children Elizabeth SeoHa Lee and Charlotte JuHa Lee who are the greatest things that ever happened to me.

I thank my parents, JungYong Lee and JaeSoon Chang, for their support and faith in me and allowing me to be as ambitious as I wanted. It was under their guidance that I gained so much drive and an ability to tackle challenges head on. I thank my brother, SooHyen Lee, my sister in law, AhGyeong Cho and my two lovely nephews, SangMook Lee and YoungMook Lee who had a great time with me in the states. Also, I thank my mother in law, BumSook Lee who has helped take care of my children from the bottom of her heart.

CURRICULUM VITAE

Soo-Min Lee

Graduate Student, Department of Pharmacology, School of Medicine
University of California, Irvine, 389 Med Surge II, Irvine, CA 92697-4625

EDUCATION HISTORY

**University of California,
Irvine,US**

09/2012-07/2016

Graduate Student

**Seoul National University, Seoul,
Korea**

03/2002-02/2004

Master of Science

**Seoul National University, Seoul,
Korea**

03/1996-02/2002

Bachelor of Science

**RESEARCH
EXPERIENCE**

**University of California,
Irvine,US**

09/2012-07/2016

Graduate Student

**SK CHEMICALS,
Korea**

03/2004-08/2012

Associate Research Scientist, Life Science R&D Center Pharmacology Lab (01/2011-08/2012)

Conducted research on pharmacology and molecular biology

Research Scientist, Life Science R&D Center Pharmacology Lab (01/2006-12/2010)

Conducted research on pharmacology and molecular biology

Assistant Research Scientist, Life Science R&D Center Pharmacology Lab (03/2004-12/2005)

Conducted research on pharmacology, pharmacokinetics, and toxicology

**Seoul National University, Seoul,
Korea**

05/2001-02/2004

Researcher, Molecular Biology Lab, Dept. of Biological Science

Acquired molecular biology related research skills in the Molecular Biology Lab

PUBLICATIONS

“Kcne2 deletion causes early-onset nonalcoholic fatty liver disease via iron deficiency anemia.” Lee SM, Nguyen D, Anand M, Kant R, Kohncke C, Lisewski U, Roepke TK, Hu Z, Abbott GW. *Scientific Reports* 2016, 6, 23118

“Kcne2 deletion promotes atherosclerosis and diet-dependent sudden death.” Lee SM, Nguyen D, Hu Z, Abbott GW. *J Mol Cell Cardiol.* 2015,87:148-151.

“SK-PC-B70M alleviates neurologic symptoms in G93A-SOD1 amyotrophic lateral sclerosis mice.” Seo JS, Baek IS, Leem YH, Kim TK, Cho Y, Lee SM, Park YH, Han PL. *Brain Res.* January 2011, 12; 1368: 299-307.

“SK-PC-B70M confers anti-oxidant activity and reduces Abeta levels in the brain of Tg2576 mice.” Seo JS, Kim TK, Leem YH, Lee KW, Park SK, Baek IS, Kim KS, Im GJ, Lee SM, Park YH, Han PL. *Brain Res.* March 2009, 19; 1261: 100-8.

“The penile erection efficacy of a new phosphodiesterase type 5 inhibitor, mirodenafil (SK3530), in rabbits with acute spinal cord injury.” Jung JY, Kim SK, Kim BS, Lee SH, Park YS, Kim SJ, Choi C, Yoon SI, Kim JS, Cho SD, Im GJ, Lee SM, Jung JW, Lee YS. *J Vet Med Sci.* November 2008, 70(11): 1199-204.

“Dose-linear pharmacokinetics of oleanolic acid after intravenous and oral administration in rats.” Eong DW, Kim YH, Kim HH, Ji HY, Yoo SD, Choi WR, Lee SM, Han CK, Lee HS. *Biopharm Drug Dispos.* March 2007, 28(2): 51-7.

“The 113th and 117th charged amino acids in the 5th alpha-helix of the HBV core protein are necessary for pgRNA encapsidation.” Lee SM, Park SG, Park E, Lee JY, Jung G. *Virus Genes.* December 2003, 27(3): 227-35.

“Antisense oligodeoxynucleotides targeted against molecular chaperonin Hsp60 block human hepatitis B virus replication.” Park SG, Lee SM, Jung G. *J Biol Chem.* October 2003, 278(41): 39851-7.

POSTER PRESENTATION

The American Heart Association Basic Cardiovascular Sciences (BCVS) 2014 Conference 07/2014

Poster Title: *Kcne2* gene deletion combines with a Western diet to cause early-onset diabetes mellitus and atherosclerosis in mice

*Authors: **Soo-Min Lee**, Ritu Kant, Geoffrey W. Abbott.*

The Federation of American Societies for Experimental Biology (FASEB) 2013 Science Research Conference on Ion Channel Regulation 07/2013

Poster Title: Potential roles for KCNE subunits in the brain

*Authors: **Soo-Min Lee**, Ritu Kant, Geoffrey W. Abbott.*

The Pharmaceutical Society of Korea 2011 conference

11/2011

Poster Title: SK-PC-B70M, the New Herbal Medicinal Product for the Treatment of Alzheimer's Disease

*Authors: **Soo-Min Lee**, Won-Rack Choi, Jung-soo Han, Pyung-Lim Han, Bong-Yong Lee, Yang Hae Park.*

And many others

ABSTRACT OF THE DISSERTATION

The KCNE2 potassium channel subunit in metabolic syndrome

By

Soo-Min Lee

Doctor of Philosophy in Pharmacology

University of California, Irvine, 2016

Professor Geoffrey W. Abbott, Chair

Coronary artery disease (CAD) is the number 1 cause of death in the U.S and globally. The traditional risk factors for CAD are hypercholesterolemia, hypertriglyceridemia, hypertension including high levels of angiotensin, diabetes, aging, and smoking. Non-traditional risk factors are chronic inflammation, hyperhomocysteinemia, high levels of C-reactive protein (CRP) and left ventricular hypertrophy (LVH). We previously found that *Kcne2* deletion causes hypercholesterolemia, high levels of angiotensin, glucose intolerance and LVH. Here, we show that *Kcne2* deletion promotes CAD including hypertriglyceridemia, diabetes, hyperhomocysteinemia, elevated CRP. In female western diet-fed mice, *Kcne2* deletion increases plaque deposition and also causes premature ventricular complexes and sudden death. Nonalcoholic fatty liver disease (NAFLD) is the most common cause of chronic liver disease in Western countries. NAFLD displays not only increases liver-related complications but also increases risk of developing diabetes and atherosclerosis. We discovered that *Kcne2* deletion in mice causes early-onset NAFLD via iron deficiency arising from KCNE2-dependent achlorhydria, while two other KCNE2-dependent defects, cardiac dysfunction and hypothyroidism, do not contribute to early-onset NAFLD in *Kcne2*^{-/-} mice. Last, we also found

that *Kcne2* deletion causes Type II diabetes mellitus (T2DM) via a primary defect in insulin secretion. *Kcne2* deletion in mice impairs glucose tolerance as early as 5 weeks of age in pups fed on a western diet, ultimately causing diabetes. In adult mice fed a normal diet, skeletal muscle insulin receptor β and IRS-1 expression were downregulated by *Kcne2* deletion, characteristic of T2DM. *Kcne2* deletion also caused extensive pancreatic transcriptome changes consistent with T2DM, which included ER stress, inflammation and hyperproliferation. *Kcne2* deletion impaired isolated β -cell insulin secretion and diminished β -cell peak outward K^+ current at positive membrane potentials, but also left-shifted its voltage dependence and reduced inactivation. Metabolic syndrome refers to a clustering of the following medical conditions: hypertension, insulin resistance, and hypertriglyceridemia. Metabolic syndrome is associated with the risk of developing CAD, NAFLD and T2DM. The work described herein demonstrates that *Kcne2* disruption is a novel genetic predisposing factor for elements of metabolic syndrome including CAD, NAFLD and T2DM.

Introduction

Potassium channels are one of the most widely distributed types of membrane proteins and they can be found in virtually all prokaryotic and eukaryotic cell types and control a wide variety of cell functions (1,2). These channels selectively permit potassium ions to flow down their electrochemical gradient (1,3). Potassium channels can be divided into four main classes based on their domain structure and activation mechanisms: voltage-gated potassium (Kv) channels, calcium-activated potassium (KCa) channels, inwardly rectifying potassium (Kir) channels and two-pore domain potassium (K2P) channels (1,3,4,5). Among them, Kv channels are the largest subset of potassium channels and play important roles in restoring the membrane potential and returning the depolarized cell to its resting state (3,4,5). Kv channels play a critical role in cellular signaling processes regulating neurotransmitter release, heart rate, hormone secretion, neuronal excitability, epithelial electrolyte transport, and smooth muscle contraction (3,5). Kv channels are a tetramer of alpha subunits forming a water-filled permeation pore. Alpha subunits of Kv channels contain cytoplasmic N and C terminus domains and six transmembrane segments (TM1–TM6) and a pore loop between TM5 and TM6. TM4 contains a stretch with positively charged amino acids that is considered a key element for the voltage sensor function (3,4,6).

Beta subunits are regulatory subunits that associate with alpha subunits and alter their functions (8,9). One family of beta subunits is the KCNE family, comprising five known members, KCNE1-5. All KCNEs contain a single TM segment, an extracellular N-terminus and an intracellular C-terminus. KCNEs have been shown to modify several Kv channels via direct interaction (8,9) but

may also modulate non-channel proteins through macromolecular complexes (10).

Stoichiometry between KCNE and alpha subunits are still a matter of extensive debate. Current data indicates a probable 4:2 KCNQ1-KCNE1 subunit stoichiometry (11,12,13), or 4:4 KCNQ1-KCNE1 depending on expression levels (14). NMR studies of KCNQ1-KCNE1 suggests that KCNE1 interacts with pore helix residues of KCNQ1 and that the TM segment of the KCNE1 is located in a cleft between the voltage sensor domain of one KCNQ1 subunit and the pore helix of a neighboring KCNQ1 subunit (15,16).

One of the KCNE family, KCNE2 markedly modifies Kv channel gating, conductance, regulation, trafficking, and pharmacology (17, 18). KCNE2 regulates multiple types of cardiac voltage-gated cation channels such as Kv1.5 (19), Kv4.2 (20), human ether-à-go-go-related gene (hERG) (21), KCNQ1 (22) and HCN (23). Dysregulation of KCNE2 can cause ventricular arrhythmia and Long QT Syndrome (LQTS) (21,24,25). Analysis of ventricular myocytes from *Kcne2*^{-/-} mice shows about 50% reduction in the 4-aminopyridine-sensitive I_{Kslow} current, mediated by Kv1.5, and approximately 25% reduction in the I_(to,f) current, mediated by Kv4.2 (19). KCNE2 also governs hERG. In *Xenopus laevis* oocytes, KCNE2 appears to accelerate deactivation, shift the activation curve to more positive membrane potentials, and decrease hERG current amplitude (21). A variety of missense mutations in KCNE2 have been found in patients suffering from inherited or acquired arrhythmia (21,26,27,28,29). Mutations to the *KCNE2* gene have shown that KCNE2 is critical for hERG channel normal activity, reduces I_{Kr} current, and causes LQTS. For example, KCNE2-V65M and M54T show an acceleration of hERG channel inactivation resulting in a decrease in I_{Kr} (27,30). N-terminus KCNE2 mutations (T8A, Q9E) greatly alter hERG channel drug sensitivity, which correlates with drug-induced LQTS in respective mutation carriers (21, 28, 30). KCNE2 co-localizes with KCNQ1 in cardiac myocytes (31, 32), dramatically reducing the current amplitude of KCNQ1 in vitro, while also introducing a constitutive component present even at hyperpolarized voltages (22, 32). In addition to the

heart, KCNE2 has been detected in a variety of other organs including stomach, lung, kidney, choroid plexus epithelium (CPE) and thyrocytes. KCNE2 plays an important role in gastric acid secretion (33). KCNQ1-KCNE2 is typically expressed on the apical membrane of gastric parietal cells (34) and regulates gastric H⁺/K⁺-ATPase transporter through a luminal potassium recycling mechanism (33). On the other hand, KCNE2 is highly expressed in the choroid plexus epithelium (CPE), which is the major site of cerebrospinal fluid (CSF) production, secretion and regulation (35). An important function of the CPE is to maintain physiological levels of potassium in the CSF. Our lab recently identified KCNE2 to be prominently expressed in the apical membrane of the CPE and interact with KCNQ1 subunits to regulate anion secretion into the CSF (35). In *Kcne2*^{-/-} mice, KCNQ1 traffics incorrectly to the basolateral instead of the apical membrane of the CPE and this consequently leads to an increase CSF chloride concentration compared to *Kcne2*^{+/+} mouse (35,36). KCNE2 also is expressed in thyrocytes. Moving of I⁻ from the blood into the central colloid is required for biosynthesis of thyroid hormones, triiodothyronine (T3) and thyroxine (T4). This is mediated by the sodium iodide symporter (NIS) (37). KCNE2 may play a critical role for NIS-mediated iodide uptake; *Kcne2*^{-/-} mice have impaired thyroid iodide accumulation, and have a phenotype consistent with hypothyroidism, including cardiac hypertrophy, alopecia, dwarfism, and goiter (38). Furthermore, our lab has shown that *Kcne2* deletion creates a multifactorial substrate for sudden cardiac death (SCD) that includes diabetes mellitus and dyslipidemia, showing impaired glucose tolerance and high blood LDL level, respectively, in mouse models (39). In this study, *Kcne2*^{-/-} mice also displayed anemia, lowered mean corpuscular hemoglobin, lowered mean corpuscular volume, and enlarged spleen - all symptoms of iron deficiency anemia (39). Interestingly, a single nucleotide polymorphism (SNP) near the human *KCNE2* locus was also previously linked to early-onset myocardial infarction (MI) (40). Anemia, hypercholesterolemia, and diabetes mellitus all diminish myocardial oxygen supply and can cause MI (41).

Because a Western diet is one of the major risk factors for MI and diabetes, we have investigated the effect of KCNE2 on atherosclerosis and diabetes using *Kcne2*^{-/-} mice and analyzed the impact of a Western diet in Chapter 1 and Chapter 3, respectively. Also, we have studied potential metabolic defects in the liver and pancreas, aiming to gain a better understanding of the molecular mechanisms for atherosclerosis, NAFLD, and T2DM caused by *Kcne2* deletion, in Chapters 2 and 3.

References

1. Choe S. et al., Potassium channel structures. *Nature Reviews Neuroscience*, 2002,**3**: 115-121
2. Littleton J.T. et al., Ion channels and synaptic organization: analysis of the *Drosophila* genome. *Neuro*, 2000, **26** (1): 35–43
3. Shieh C. C. et al., Potassium Channels: Molecular Defects, Diseases, and Therapeutic Opportunities. *Pharmacological Reviews*, 2000, **52**(4): 557-594
4. Tian C. et al., Potassium Channels: Structures, Diseases, and Modulators. *Chemical Biology & Drug Design*, 2014, **83** (1): 1-26.
5. Wulff H. et al., Voltage-gated Potassium Channels as Therapeutic Drug Targets. *Nat Rev Drug Discov.* 2009, **8**(12): 982–1001.
6. Yellen G. et al., The voltage-gated potassium channels and their relatives. *Nature*. 2002, **419**(5): 35-42.
7. Papazian D.M. et al., Alteration of voltage dependence of Shaker potassium channel by mutations in the S4 sequence. *Nature*, 1991.**349**:305–310.
8. Pongs O. et al., Functional and molecular aspects of voltage-gated K⁺ channel beta subunits. *Ann N Y Acad Sci*, 1999.**868**(30):344–55.
9. Li Y. et al., Voltage-gated potassium channels: regulation by accessory subunits. *Neuroscientist*, 2006.**12**(3):199–210.
10. Abbott G.W. et al, KCNQ1, KCNE2, and Na⁺-Coupled Solute Transporters Form Reciprocally Regulating Complexes that Affect Neuronal Excitability. *Science Signaling*. 2014. **7**(315):ra22.
11. Chen H. et al., Charybdotoxin binding in the I(Ks) pore demonstrates two MinK subunits in each channel complex. *Neuron*, 2003. **40**:15-23.

12. Sesti F. et al., Single-channel characteristics of wild-type IKs channels and channels formed with two minK mutants that cause long QT syndrome. *J Gen Physiol*, 1998. **112**:651-63.
13. Wang K.W. et al., Subunit composition of minK potassium channels. *Neuron*, 1995. **14**:1303-9.
14. Nakajo K. et al., Stoichiometry of the KCNQ1 - KCNE1 ion channel complex. *Proc Natl Acad Sci USA*, 2010. **107**:18862-7.
15. Kang C. et al, Structure of KCNE1 and implications for how it modulates the KCNQ1 potassium channel. *Biochemistry*, 2008.**47**: 7999–8006,
16. Wrobel.E. et al., The KCNE tango – how KCNE1 interacts with Kv7.1. *Front. Pharmacol.*, 2012.**2**(3):142.
17. Abbott. G.W., KCNE2 and the K (+) channel: the tail wagging the dog. *Channels*, 2012.**6**(1):1-10.
18. McCrossan Z.A. et al., The MinK-related peptides. *Neuropharmacology*, 2004.**47**:787–821.
19. Roepke T.K. et al., Targeted deletion of *kcne2* impairs ventricular repolarization via disruption of I(K,slow1) and I(to,f). *FASEB J*, 2008.**22**:3648–60.
20. Zhang, M. et al., MinK-related peptide 1 associates with Kv4.2 and modulates its gating function: potential role as beta subunit of cardiac transient outward channel? *Circ Res*, 2001.**88**: 1012–1019.
21. Abbott, G. W. et al., MiRP1 Forms IKr Potassium Channels with HERG and Is Associated with Cardiac Arrhythmia. *Cell*, 1999.**97**:175–87.
22. Tinel N. et al., KCNE2 confers background current characteristics to the cardiac KCNQ1 potassium channel. *EMBO J*, 2000.**19**(23):6326-30.
23. Wu Y.H. et al., MinK-related peptide 1: a beta subunit for the HCN ion channel subunit family enhances expression and speeds activation. *Circ Res*, 2001.**88**: E84–7.

24. Curran, M. E. et al., A molecular basis for cardiac arrhythmia: HERG mutations cause long QT syndrome. *Cell*, 1995.**80**:795–803.
25. Isbrandt, D. et al., Identification and functional characterization of a novel KCNE2 (MiRP1) mutation that alters HERG channel kinetics. *J Mol Med*, 2002.**80**:524–32.
26. Curran M.E. et al, A molecular basis for cardiac arrhythmia: HERG mutations cause long QT syndrome. *Cell*, 1995.**80**: 795–803.
27. Isbrandt D. et al., Identification and functional characterization of a novel KCNE2 (MiRP1) mutation that alters HERG channel kinetics. *J Mol Med*, 2002.**80**: 524–32.
28. Sesti F. et al, A common polymorphism associated with antibiotic-induced cardiac arrhythmia. *Proc Natl Acad Sci USA*, 2000.**97**: 10613–8.
29. Trudeau M.C., HERG, a human inward rectifier in the voltage-gated potassium channel family. *Science*, 1995.**269**: 92–5.
30. Lu Y. et al., Mutant MiRP1 subunits modulate HERG K⁺ channel gating: a mechanism for pro-arrhythmia in long QT syndrome type 6. *J Physiol*, 2003.**551**: 253–62.
31. Wu D.M., et al., KCNE2 is colocalized with KCNQ1 and KCNE1 in cardiac myocytes and may function as a negative modulator of IKs current amplitude in the heart. *Heart Rhythm*, 2006.**3**(12):1469-80.
32. Bendahhou. S. et al, *In vitro* molecular interactions and distribution of KCNE family with KCNQ1 in the human heart. *Cardiovasc Res*, **2005**.**67**: 529–38.
33. Roepke.T.K. et al., The KCNE2 potassium channel ancillary subunit is essential for gastric acid secretion. *J.BIOL CHEM*, 2006.**281**(33):23740–7.
34. Dedek K. et al., Colocalization of KCNQ1/KCNE channel subunits in the mouse gastrointestinal tract. *Pflügers Arch*, 2001.**442**: 896–902.
35. Roepke T.K. et al, KCNE2 forms potassium channels with KCNA3 and KCNQ1 in the choroid plexus epithelium. *FASEB J*, 2011. **25**:4264-73.

36. Roepke T.K. et al., Genetic dissection reveals unexpected influence of beta subunits on KCNQ1 K⁺ channel polarized trafficking *in vivo*. *FASEB J*, 2011. **25**:727-36.
37. De. L. V. A et al., Molecular analysis of the sodium/iodide symporter: impact on thyroid and extrathyroid pathophysiology. *Physiol Rev*, 2000. **80**:1083-105.
38. Roepke T.K., et al. *Kcne2* deletion uncovers its crucial role in thyroid hormone biosynthesis. *Nat Med*, 2009. **15**:1186-94.
39. Hu Z et al., *Kcne2* deletion creates a multisystem syndrome predisposing to sudden cardiac death. *Circ Cardiovasc Genet*, 2014.**7**(1):33-42.
40. Myocardial Infarction Genetics Consortium, Kathiresan S. et al., Genome-wide association of early-onset myocardial infarction with common single nucleotide polymorphisms, common copy number variants, and rare copy number variants. *Nat Genet*, 2009.**41**(3): 334–341.
41. Pepine C.J. et al., The pathophysiology of chronic ischemic heart disease. *Clin Cardiol*, 2007.**30**(2 Suppl 1):I4–I9.

Chapter 1

***Kcne2* deletion promotes atherosclerosis and diet-dependent sudden death**

ABSTRACT

Coronary artery disease (CAD) is the leading cause of death worldwide. An estimated half of cases involve genetic predisposition. Sequence variants in human *KCNE2*, which encodes a cardiac and epithelial K⁺ channel β subunit, cause inherited cardiac arrhythmias. Unexpectedly, human *KCNE2* polymorphisms also associate with atherosclerosis predisposition, with unestablished causality or mechanisms. In Chapter 1, we show that germline *Kcne2* deletion promotes atherosclerosis in mice, overcoming the relative resistance of this species to plaque deposition. In female western diet-fed mice, *Kcne2* deletion increased plaque deposition >6-fold and also caused premature ventricular complexes and sudden death. The data establish causality for the first example of ion channel-linked atherosclerosis, and demonstrate that the severity of *Kcne2*-linked cardiac arrhythmias is strongly diet-dependent.

Introduction

CAD results in higher mortality in the United States and globally each year than any other single cause of death (1). An estimated half of CAD cases involve genetic predisposition, yet it is predicted that reduction of other risk factors could reduce CAD mortality and morbidity by >30% (2). It is therefore crucial to develop more comprehensive prevention and treatment strategies for both genetic and environmental risk factors for CAD (2), necessitating a fuller mechanistic understanding of CAD.

Another form of fatal heart disorder, Sudden Cardiac Death (SCD), accounts for ~1000 deaths per day in the United States. SCD is proposed to require an electric substrate, an ischemic substrate, and perhaps a trigger (3). Despite significant advances in our mechanistic understanding of SCD, there is still much to learn. Because most of the 25 genes linked to SCD also serve roles outside the heart, the possibility arises that even monogenic forms of SCD may involve complex, multi-system disease pathogenesis not confined to direct dysfunction of cardiac myocyte electrical activity.

Many SCD-linked genes encode ion channel pore-forming (α) subunits, but the rest encode proteins that regulate them (3, 4). KCNE2 (which we originally named MiRP1) is a relatively promiscuous, single-transmembrane span ion channel β subunit best known for its ability to co-assemble with and alter the trafficking and functional properties of voltage-gated potassium (Kv) channels (5). Human KCNE2 mutations that result in impaired function of ventricular myocyte Kv channels are linked to cardiac arrhythmias including Long QT syndrome (LQTS) (5, 7), which predisposes to ventricular fibrillation and SCD.

In addition to the heart, *KCNE2* is expressed in a variety of secretory epithelia (8-11), raising the possibility of extracardiac effects of human *KCNE2* disruption. Indeed, a SNP near the human *KCNE2* locus is associated with early onset (12), prevalence, and subsequent mortality (13) of myocardial infarction (MI); a different SNP within the human *KCNE2* gene itself is associated with predisposition to CAD (14). These findings suggested the possibility of a causal link between *KCNE2* disruption and CAD/MI, which we investigated here using germline *Kcne2* deletion in mice.

Methods

All mice were housed in pathogen-free facilities and the study was approved by the Animal Care and Use Committee at University of California, Irvine, in strict accordance with the recommendations in the Guide for the Care and Use of Laboratory Animals of the National Institutes of Health. The *Kcne2*^{-/-} mouse line was generated as we previously described (9), and mice used in this study were bred by crossing *Kcne2*^{+/-} mice which had been backcrossed >10 times into the C57BL/6 strain. After being genotyped and weaned at 3 weeks of age, mice pups were assigned to, and maintained on, either a control diet (2020X, Harlan, 16% kcal from fat; 19.1% protein, 2.7% crude fiber, 12.3% neutral detergent fiber and 0% cholesterol) or western diet (TD.88137, Harlan, 42% kcal from fat, >60% of which is saturated; 34% sucrose; 0.2% cholesterol). Detailed methods appear in the online supplement.

Plaque quantification

Mice were fed either a control or western diet starting at 3 weeks of age. All mice were subjected to fortnightly 6-hr fasts prior to glucose tolerance tests. Some cohorts, including mice used for plaque quantification, had an additional fortnightly 20 to 24-hour fast commencing the morning after glucose tolerance tests, between weeks 5 through 15-17, with similar fasting protocols for mice of each diet and genotype. After euthanasia, perfusion to the left ventricle with cold PBS and subsequently with cold buffered formalin, aortas were dissected. After removing the external adipose tissue, aortas were placed in 10% neutral buffered formalin overnight, then opened lengthwise the following day. The tissue was then stained for 15 minutes with 0.5% Sudan IV solution in acetone and 70% ethanol (1:1), followed by decolorization for 5 minutes using 80% ethanol, and gently washing with water for several minutes. The *en face* preparations were digitally photographed and then the percentage of aortic plaque deposition

was calculated by quantification of Sudan IV staining using ImageJ, by an individual blinded to the genotype, sex and diet of the mice from which the aorta were harvested.

Electrocardiography

Mice were anesthetized with 2 % isoflurane then maintained under 1% isoflurane and surgical anesthesia was verified by a lack of response to toe pinch. The standard limb lead II configuration electrocardiographic system was inserted subcutaneously to limbs by needle electrodes, and electrocardiograms (ECGs) were recorded in mice 5-7 months of age. QT and QRS intervals and heart rate (HR) were analyzed offline after acquisition. QT_c was calculated based on Mitchell's formula specifically for mice (37): $QT_c = QT/(RR/100)^{1/2}$. The real-time data were collected by Powerlab/8sp system (AD Instruments, Colorado Springs, CO). LabChart 7.2.1 software (AD Instruments, Colorado Springs, CO) was used for ECG data acquisition and analysis. PVC frequency was quantified manually from 30 s ECG recordings.

Statistical analysis

Statistical analyses (student's t-test or ANOVA, as indicated in the figure legends) were performed assuming significance with p values < 0.05. Bonferroni and Holm corrections were used for multiple comparisons. Survival curves were compared using the log rank test.

Results

3.1. *Kcne2* deletion promotes atherosclerosis

We first quantified plaque deposition as a percentage of aortic surface area in mice fed regular mouse chow (normal diet), or a high-fat, high-cholesterol, high sugar (western) diet, comparing *Kcne2*^{+/+} and *Kcne2*^{-/-} mice matched for age and sex. Plaques were visible in the aorta of *Kcne2*^{-/-} mice fed a western diet, suggesting a predisposition to atherosclerosis (**Figure 1A,B**). We confirmed this by *en face* quantification of Sudan IV-stained plaques in the aorta of 5-7 month-old mice. In mice fed a control diet, plaque deposition was relatively low, but female and male *Kcne2*^{-/-} mice exhibited 10.2-fold ($p = 0.035$) and 2.5-fold ($p = 0.1$) increases in mean plaque surface area respectively, at 5-7 months of age ($n = 4-7$). In mice fed a western diet, *Kcne2* deletion increased plaque deposition 6.2-fold ($p = 8 \times 10^{-6}$) in females and 3.2-fold ($p = 0.049$) in males (**Figure 1C,D**).

3.2. A western diet potentiates the effects of *Kcne2* deletion on arrhythmogenesis and mortality

Human *KCNE2* gene variants cause LQTS (5, 23, 24), and *Kcne2* deletion lengthens the QTc interval in aging mice fed a normal diet (8, 22). Here, we discovered particularly prominent effects of *Kcne2* deletion on arrhythmogenesis and sudden death in female mice fed a western diet. In *Kcne2*^{+/+} mice, and in male *Kcne2*^{-/-} mice, the western diet had negligible effects on mortality during the study. In contrast, 4/7 western diet-fed female *Kcne2*^{-/-} mice died suddenly by the age of 15 weeks. In normal diet-fed *Kcne2*^{-/-} mice, the first mortality was observed at 18 weeks (**Figure 2A**).

Electrocardiographic analysis of surviving mice revealed that *Kcne2* deletion increased the QTc interval in male mice on a western diet, and in female mice on a control diet, the latter recapitulating our previous findings (8, 22) (**Figure 2B,C**). The western diet did not greatly

extend the already-long QTc in female *Kcne2*^{-/-} mice, but it induced frequent premature ventricular complexes (PVCs) in all 3 female mice still alive for testing beyond 15 weeks, at a mean frequency of 4 PVCs per 100 beats (**Figure 2B-E**). The PVCs were typically immediately followed by full compensatory pauses that were double the length of the preceding R-R interval (**Figure 2E, blue arrows**), highly characteristic of PVCs observed on human ECGs. In contrast, PVCs were not observed in any of the other groups (**Figure 2B,D**), nor in our previous studies of normal diet-fed *Kcne2*^{-/-} mice (8, 22).

Discussion

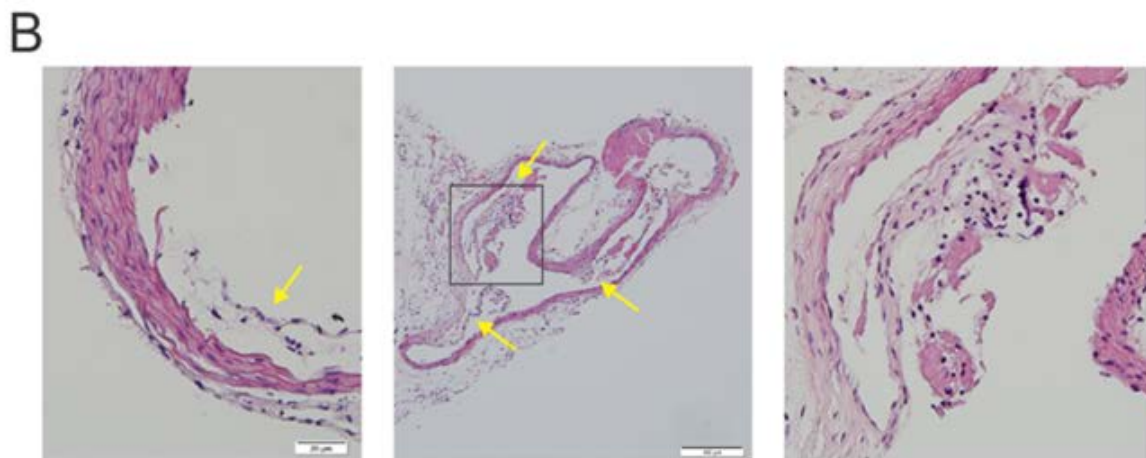
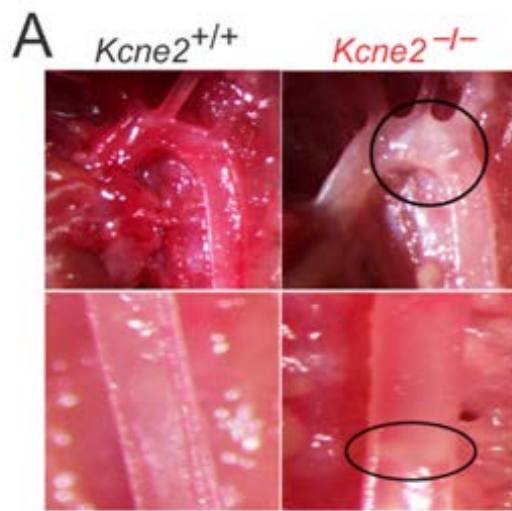
Our findings demonstrate for the first time that genetic disruption of an ion channel subunit gene can cause atherosclerosis, and support recent human genetics studies in which polymorphisms in or near the *KCNE2* locus were associated with increased predisposition to atherosclerosis and early-onset myocardial infarction (12-14). Mice are inherently resistant to development of atherosclerosis. To our knowledge, only two other single-gene knockout mouse lines (*ApoE*^{-/-} and *Ldlr*^{-/-}) develop spontaneous atherosclerotic lesions, the Apolipoprotein E gene (*ApoE*) knockout being the most striking (25, 26). Unlike *ApoE*^{-/-} mice, *Ldlr*^{-/-} mice typically only develop substantial plaques when fed an elevated cholesterol or a western diet (27), although a semi-synthetic diet induced modest plaque development in *Ldlr*^{-/-} mouse aortic root (28).

Future studies targeted toward delineating other aspects of metabolic syndrome that may contribute to the mechanistic basis for *KCNE2*-linked atherosclerosis are described in Chapters 2 and 3. We previously found that *Kcne2* deletion raises serum LDL and impairs glucose tolerance, by unknown mechanisms. *Kcne2* deletion also causes hypothyroidism (11), which can predispose to hyperlipidemia (30), and elevates serum Angiotensin II (8), which can cause vascular injury by a number of pathways (32). We suspect that *Kcne2* deletion results in a spectrum of factors, each either impairing lipid or carbohydrate metabolism, or favoring plaque development through other mechanisms.

Human *KCNE2* sequence variants predispose to LQTS arising from loss of function of ventricular Kv channels formed with hERG (*KCNH2*) (29). In adult mice, *Kcne2* deletion prolongs the QTc because of loss of function of Kv4.2 and Kv1.5 channels, which it normally

regulates in mouse ventricles. In *Kcne2*^{-/-} mice fed normal chow, QTc prolongation is not observed until 7 months of age, unless facilitated by a QTc-prolonging medication (22). Here, premature mortality and PVCs occurred only in female mice fed a western diet. The increased susceptibility for *Kcne2*-linked atherosclerosis, PVCs and premature mortality in female versus male mice we observed may be linked to estrogen regulation of KCNE2 expression, which is presumed to make females more reliant than males upon KCNE2 (36).

When K⁺ channel loss-of-function delays ventricular repolarization to the extent that an action potential fires during phase 2 or 3 of the previous action potential, early afterdepolarizations (EADs) can arise, and in turn cause PVCs. While human PVCs are in general not particularly uncommon and often benign, when occurring in combination with LQTS they are highly problematic as they promote potentially lethal polymorphic ventricular tachycardias including *torsades de pointes* (33). Although it is possible that PVCs contributed to premature mortality in western diet-fed female *Kcne2*^{-/-} mice, the PVCs could alternatively represent solely an electrocardiographic marker of their CAD (**Figure 2A**). Human PVCs are associated with increased risk of coronary heart disease (34) and incidence of SCD (35). Our preliminary findings suggest that, in addition to avoiding drugs known to prolong the QT interval, diet management may be of paramount importance in individuals harboring potentially pathogenic *KCNE2* sequence variants.



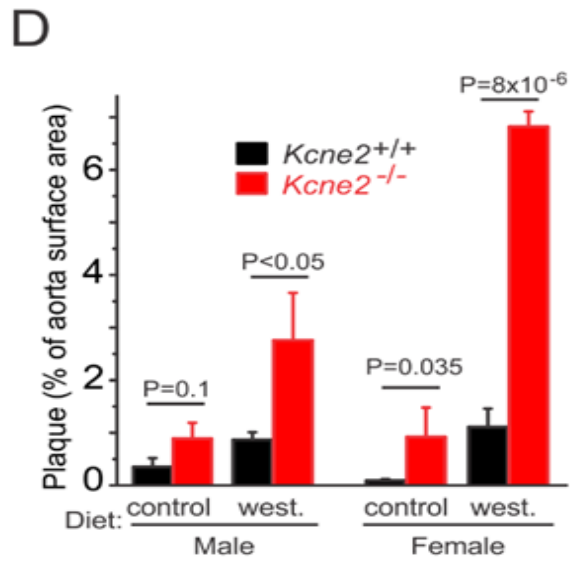
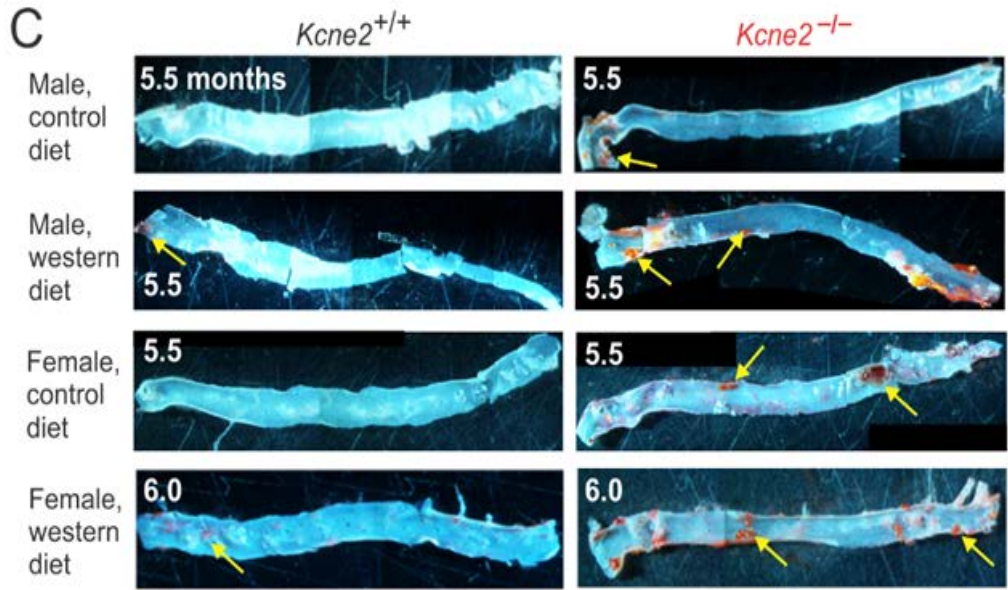
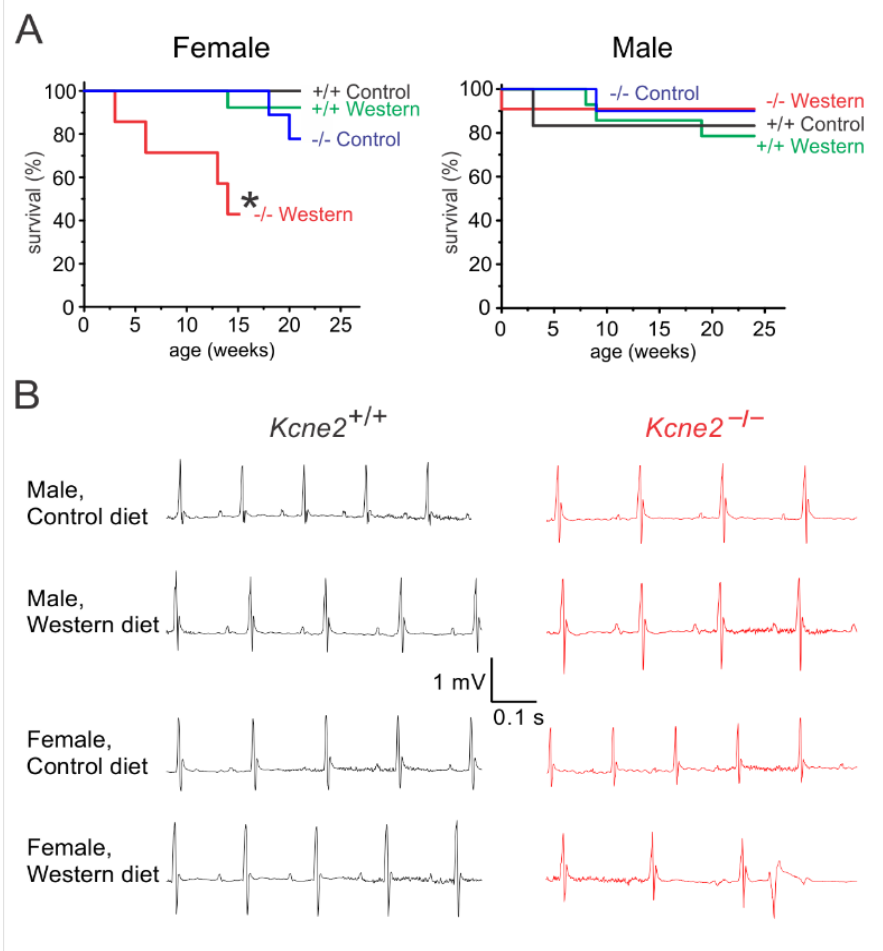


Figure 1. *Kcne2* deletion promotes atherosclerosis.

- A. External images of 9-10 month-old, western diet-fed *Kcne2*^{+/+} (*left*) and *Kcne2*^{-/-} (*right*) aortic arch (*upper*) and descending aorta (*lower*). Plaque deposition is indicated by black rings.
- B. H & E-stained aorta (left, scale bar 20 μm) and aortic branch (center, scale bar 100 μm; close-up of boxed region on right) showing plaques (*yellow arrows*) in a 6-month-old female western diet-fed *Kcne2*^{-/-} mouse.
- C. Representative images of aortic plaques (*yellow arrows*), visualized with Sudan IV solution, from mice between 5.5 and 6 months of age; genotype, diet, age and sex as indicated. Each aorta image was prepared by digital splicing of panoramic series captured with a dissection microscope-mounted digital camera.
- D. Quantification of the mean ± SEM percentage of 5-7-month-old mouse aorta surface area covered by plaque as assessed by Sudan IV staining. *n* = 5-7, male control diet; 6-8, male western diet; 4-7, female control diet; 3-6, female western diet; *p* values are for 1-tailed, unpaired t-tests for inter-genotype comparisons within equivalent sex and diet groups.



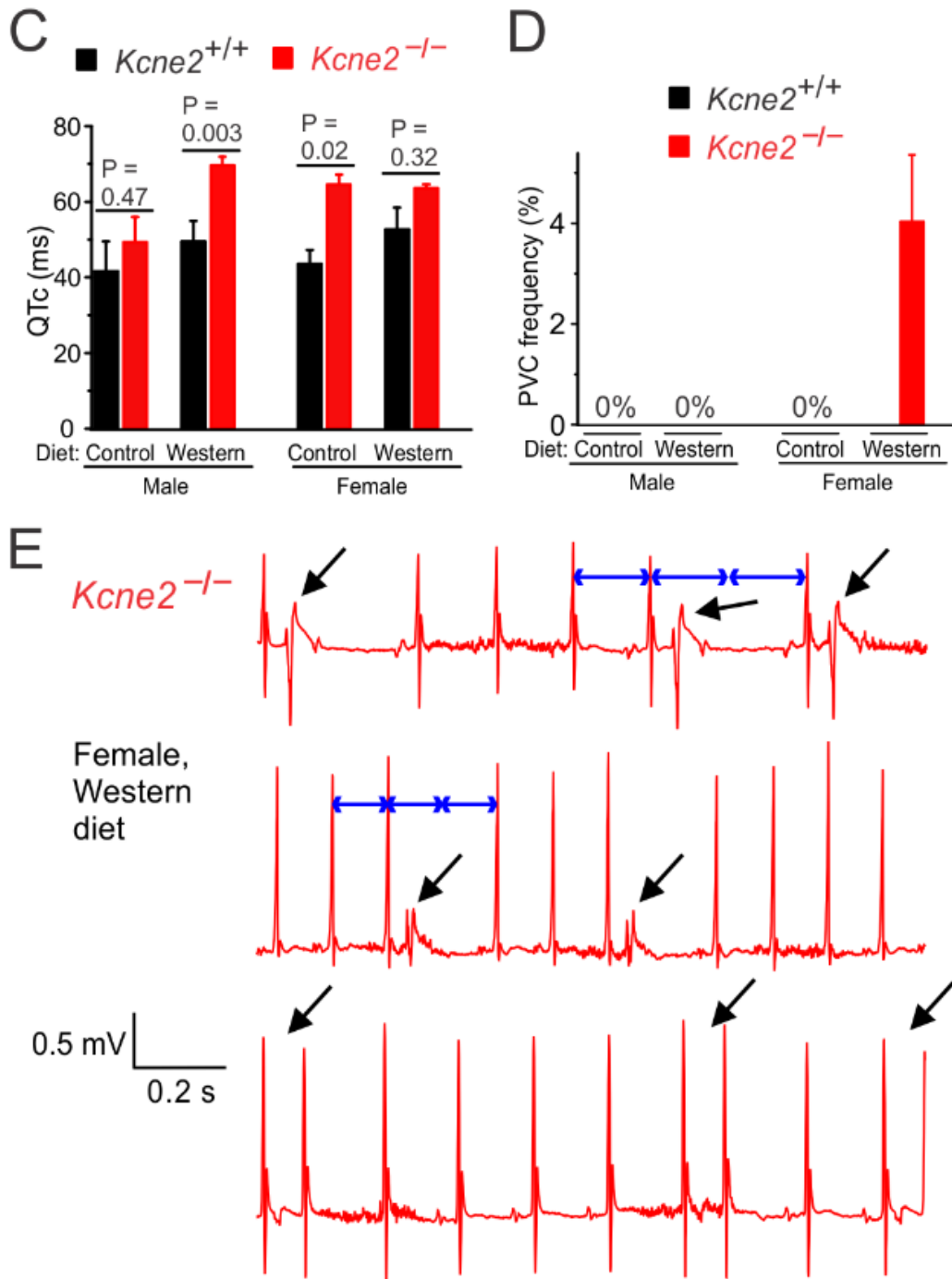


Figure 2. *Kcne2* deletion causes diet- and sex-dependent premature ventricular complexes and sudden death.

- A. Effects of *Kcne2* deletion and a western diet on % survival of female ($n = 7-13$) and male ($n = 6-14$) mice. Log rank test of survival rates: * female *Kcne2*^{-/-} western diet versus female *Kcne2*^{+/+} control diet survival ($p = 0.0028$), versus female *Kcne2*^{+/+} western diet survival ($p = 0.018$), and versus male *Kcne2*^{-/-} western diet survival ($p = 0.034$); all other comparisons $p > 0.05$.
- B. Representative ECGs recorded from control- or western-diet-fed *Kcne2*^{+/+} and *Kcne2*^{-/-} mice.
- C. Mean (\pm SEM) QTc values quantified from ECGs as in panel B ($n = 3-8$ mice per group).
- D. Mean premature ventricular complex (PVC) incidence quantified for all groups, showing 4% (4 PVCs per 100 beats) for female western diet-fed *Kcne2*^{-/-} mice and 0% incidence for all other groups.
- E. Representative ECG segments for all three western-diet-fed *Kcne2*^{-/-} female mice that survived sufficiently long for ECG recordings. Black arrows: PVCs; blue arrows, spacers demonstrating a full compensatory pause following PVCs.

References

1. World Health Organization. 2012. <http://www.who.int/mediacentre/factsheets/fs310/en/>
The top 10 causes of death.
2. Roberts R, and Stewart AF. Genetics of coronary artery disease in the 21st century. *Clinical cardiology*. 2012;35(9):536-40.
3. George AL, Jr. Molecular and genetic basis of sudden cardiac death. *The Journal of clinical investigation*. 2013;123(1):75-83.
4. Abbott GW. KCNE genetics and pharmacogenomics in cardiac arrhythmias: much ado about nothing? *Expert review of clinical pharmacology*. 2013;6(1):49-60.
5. Abbott GW, Sesti F, Splawski I, Buck ME, Lehmann MH, Timothy KW, Keating MT, and Goldstein SA. MiRP1 forms IKr potassium channels with HERG and is associated with cardiac arrhythmia. *Cell*. 1999;97(2):175-87.
6. Abbott GW. Biology of the KCNQ1 potassium channel. *New Journal of Science*. 2014;2014(
7. Neyroud N, Tesson F, Denjoy I, Leibovici M, Donger C, Barhanin J, Faure S, Gary F, Coumel P, Petit C, et al. A novel mutation in the potassium channel gene KVLQT1 causes the Jervell and Lange-Nielsen cardioauditory syndrome. *Nature genetics*. 1997;15(2):186-9.
8. Hu Z, Kant R, Anand M, King EC, Krogh-Madsen T, Christini DJ, and Abbott GW. Kcne2 deletion creates a multisystem syndrome predisposing to sudden cardiac death. *Circulation Cardiovascular genetics*. 2014;7(1):33-42.
9. Roepke TK, Anantharam A, Kirchhoff P, Busque SM, Young JB, Geibel JP, Lerner DJ, and Abbott GW. The KCNE2 potassium channel ancillary subunit is essential for gastric

- acid secretion. *The Journal of biological chemistry*. 2006;281(33):23740-7.
10. Roepke TK, Kanda VA, Purtell K, King EC, Lerner DJ, and Abbott GW. KCNE2 forms potassium channels with KCNA3 and KCNQ1 in the choroid plexus epithelium. *The FASEB journal : official publication of the Federation of American Societies for Experimental Biology*. 2011;25(12):4264-73.
 11. Roepke TK, King EC, Reyna-Neyra A, Paroder M, Purtell K, Koba W, Fine E, Lerner DJ, Carrasco N, and Abbott GW. Kcne2 deletion uncovers its crucial role in thyroid hormone biosynthesis. *Nature medicine*. 2009;15(10):1186-94.
 12. Kathiresan S, Voight BF, Purcell S, Musunuru K, Ardissino D, Mannucci PM, Anand S, Engert JC, Samani NJ, Schunkert H, et al. Genome-wide association of early-onset myocardial infarction with single nucleotide polymorphisms and copy number variants. *Nature genetics*. 2009;41(3):334-41.
 13. Szpakowicz A, Kiliszek M, Pepinski W, Waszkiewicz E, Franaszczyk M, Skawronska M, Dobrzycki S, Niemcunowicz-Janica A, Ploski R, Opolski G, et al. The rs9982601 polymorphism of the region between the SLC5A3/MRPS6 and KCNE2 genes associated with a prevalence of myocardial infarction and subsequent long-term mortality. *Polskie Archiwum Medycyny Wewnętrznej*. 2015;125(4):240-8.
 14. Sabater-Lleal M, Malarstig A, Folkersen L, Soler Artigas M, Baldassarre D, Kavousi M, Almgren P, Veglia F, Brusselle G, Hofman A, et al. Common genetic determinants of lung function, subclinical atherosclerosis and risk of coronary artery disease. *PloS one*. 2014;9(8):e104082.
 15. Franco OH, Steyerberg EW, Hu FB, Mackenbach J, and Nusselder W. Associations of diabetes mellitus with total life expectancy and life expectancy with and without cardiovascular disease. *Archives of internal medicine*. 2007;167(11):1145-51.
 16. Danesh J, Wheeler JG, Hirschfield GM, Eda S, Eiriksdottir G, Rumley A, Lowe GD, Pepys MB, and Gudnason V. C-reactive protein and other circulating markers of

- inflammation in the prediction of coronary heart disease. *The New England journal of medicine*. 2004;350(14):1387-97.
17. Roepke TK, King EC, Purtell K, Kanda VA, Lerner DJ, and Abbott GW. Genetic dissection reveals unexpected influence of beta subunits on KCNQ1 K⁺ channel polarized trafficking in vivo. *The FASEB journal : official publication of the Federation of American Societies for Experimental Biology*. 2011;25(2):727-36.
 18. Malinow MR. Hyperhomocyst(e)inemia. A common and easily reversible risk factor for occlusive atherosclerosis. *Circulation*. 1990;81(6):2004-6.
 19. Salsbury G, Cambridge EL, McIntyre Z, Arends MJ, Karp NA, Isherwood C, Shannon C, Hooks Y, Ramirez-Solis R, Adams DJ, et al. Disruption of the potassium channel regulatory subunit KCNE2 causes iron-deficient anemia. *Experimental hematology*. 2014;42(12):1053-8 e1.
 20. Ahmed U, Latham PS, and Oates PS. Interactions between hepatic iron and lipid metabolism with possible relevance to steatohepatitis. *World journal of gastroenterology : WJG*. 2012;18(34):4651-8.
 21. Targher G, Day CP, and Bonora E. Risk of cardiovascular disease in patients with nonalcoholic fatty liver disease. *The New England journal of medicine*. 2010;363(14):1341-50.
 22. Roepke TK, Kontogeorgis A, Ovanez C, Xu X, Young JB, Purtell K, Goldstein PA, Christini DJ, Peters NS, Akar FG, et al. Targeted deletion of kcne2 impairs ventricular repolarization via disruption of I(K,slow1) and I(to,f). *The FASEB journal : official publication of the Federation of American Societies for Experimental Biology*. 2008;22(10):3648-60.
 23. Gordon E, Panaghie G, Deng L, Bee KJ, Roepke TK, Krogh-Madsen T, Christini DJ, Ostrer H, Basson CT, Chung W, et al. A KCNE2 mutation in a patient with cardiac arrhythmia induced by auditory stimuli and serum electrolyte imbalance. *Cardiovascular*

- research*. 2008;77(1):98-106.
24. Sesti F, Abbott GW, Wei J, Murray KT, Saksena S, Schwartz PJ, Priori SG, Roden DM, George AL, Jr., and Goldstein SA. A common polymorphism associated with antibiotic-induced cardiac arrhythmia. *Proceedings of the National Academy of Sciences of the United States of America*. 2000;97(19):10613-8.
 25. Plump AS, Smith JD, Hayek T, Aalto-Setälä K, Walsh A, Verstuyft JG, Rubin EM, and Breslow JL. Severe hypercholesterolemia and atherosclerosis in apolipoprotein E-deficient mice created by homologous recombination in ES cells. *Cell*. 1992;71(2):343-53.
 26. Zhang SH, Reddick RL, Piedrahita JA, and Maeda N. Spontaneous hypercholesterolemia and arterial lesions in mice lacking apolipoprotein E. *Science*. 1992;258(5081):468-71.
 27. Ishibashi S, Goldstein JL, Brown MS, Herz J, and Burns DK. Massive xanthomatosis and atherosclerosis in cholesterol-fed low density lipoprotein receptor-negative mice. *The Journal of clinical investigation*. 1994;93(5):1885-93.
 28. Teupser D, Persky AD, and Breslow JL. Induction of atherosclerosis by low-fat, semisynthetic diets in LDL receptor-deficient C57BL/6J and FVB/NJ mice: comparison of lesions of the aortic root, brachiocephalic artery, and whole aorta (en face measurement). *Arteriosclerosis, thrombosis, and vascular biology*. 2003;23(10):1907-13.
 29. Abbott GW. KCNE2 and the K (+) channel: The tail wagging the dog. *Channels (Austin)*. 2012;6(1).
 30. Mishkel MA, and Crowther SM. Hypothyroidism, an important cause of reversible hyperlipidemia. *Clinica chimica acta; international journal of clinical chemistry*. 1977;74(2):139-51.
 31. Alvarez A, Ibiza S, Hernandez C, Alvarez-Barrientos A, Esplugues JV, and Calatayud S. Gastrin induces leukocyte-endothelial cell interactions in vivo and contributes to the

- inflammation caused by *Helicobacter pylori*. *The FASEB journal : official publication of the Federation of American Societies for Experimental Biology*. 2006;20(13):2396-8.
32. da Silva AR, Fraga-Silva RA, Stergiopoulos N, Montecucco F, and Mach F. Update on the role of angiotensin in the pathophysiology of coronary atherothrombosis. *European journal of clinical investigation*. 2015;45(3):274-87.
 33. Vos MA, Gorenek B, Verduyn SC, van der Hulst FF, Leunissen JD, Dohmen L, and Wellens HJ. Observations on the onset of torsade de pointes arrhythmias in the acquired long QT syndrome. *Cardiovascular research*. 2000;48(3):421-9.
 34. Massing MW, Simpson RJ, Jr., Rautaharju PM, Schreiner PJ, Crow R, and Heiss G. Usefulness of ventricular premature complexes to predict coronary heart disease events and mortality (from the Atherosclerosis Risk In Communities cohort). *The American journal of cardiology*. 2006;98(12):1609-12.
 35. Cheriya P, He F, Peters I, Li X, Alagona P, Jr., Wu C, Pu M, Cascio WE, and Liao D. Relation of atrial and/or ventricular premature complexes on a two-minute rhythm strip to the risk of sudden cardiac death (the Atherosclerosis Risk in Communities [ARIC] study). *The American journal of cardiology*. 2011;107(2):151-5.
 36. Kundu P, Ciobotaru A, Foroughi S, Toro L, Stefani E, and Eghbali M. Hormonal regulation of cardiac KCNE2 gene expression. *Molecular and cellular endocrinology*. 2008;292(1-2):50-62.
 37. Mitchell GF, Jeron A, and Koren G. Measurement of heart rate and Q-T interval in the conscious mouse. *The American journal of physiology*. 1998;274(3 Pt 2):H747-51.

Chapter 2

***Kcne2* deletion causes early-onset nonalcoholic fatty liver disease via iron deficiency**

ABSTRACT

Nonalcoholic fatty liver disease (NAFLD) is an increasing health problem worldwide, with genetic, epigenetic, and environmental components. In Chapter 2, we describe the first example of NAFLD caused by genetic disruption of a mammalian potassium channel subunit. Mice with germline deletion of the KCNE2 potassium channel β subunit exhibited NAFLD as early as postnatal day 7. Using *Kcne2*^{-/-} mouse genetics, histology, liver damage assays and transcriptomics we discovered that iron deficiency arising from KCNE2-dependent achlorhydria is a major factor in early-onset NAFLD in mice, while two other KCNE2-dependent defects did not initiate NAFLD. The findings uncover a novel genetic basis for NAFLD and an unexpected potential factor in human KCNE2-associated cardiovascular pathologies, including atherosclerosis.

Introduction

NAFLD is the predominant liver disorder in many developed and developing countries, affecting as much as a third of the United States population (1). Characterized by abnormally high hepatic lipid accumulation, NAFLD is of particular importance because it can progress to more dangerous disorders including nonalcoholic steatohepatitis (NASH) and potentially fatal liver cirrhosis (2). NAFLD is commonly associated with metabolic syndrome, hypercholesterolemia and hypertriglyceridemia, and is often observed in obese or diabetic individuals, those with poor eating habits, or people who have experienced rapid weight loss. In addition, people without these risk factors can also develop NAFLD, and the incidence and severity of the disease is influenced by a variety of genetic and epigenetic factors in addition to lifestyle and other environmental influences (1).

Sequence variants in six genes have been both linked to human NAFLD and independently validated (for review see 1). The I148M variant in *PNPLA3*, which encodes patatin-like phospholipase domain-containing protein 3, is the major recognized genetic basis for NAFLD in human populations (3). When the *PNPLA3* I148M human NAFLD-associated polymorphism (rs738409) is overexpressed in mice, it results in triacylglycerol (TAG) accumulation. Similar results are obtained by targeted hepatic overexpression of wild-type *PNPLA3* in mice, via increased TAG and fatty acid synthesis and impaired hydrolysis of TAG; a relative depletion of long-chain polyunsaturated forms of TAG was also observed (4,5). The other five genes are *GCKR* (which regulates glucokinase activity and hepatic glucose intake) (6); *PEMT*, a catalyst for phosphatidylcholine synthesis (7); *SOD2* (which clears mitochondrial reactive oxygen species and protects against cell death) (8); *KLF6* (a

transcription factor that influences fibrogenesis) (9); and ATGR1 (angiotensin type 1 receptor) (10). In addition to these genetic factors and metabolic syndrome, hepatic iron also influences lipid metabolism and hepatic steatosis. Iron overload can cause oxidative stress and lipid peroxidation, and can, for example, increase the formation of intracellular lipid droplets in liver cells *in vitro*. Conversely, iron deficiency has been shown to increase lipogenesis in rat liver, resulting in triglyceride accumulation and steatosis (11). Thus, NAFLD is a common and highly complex pathological state affected by many different interacting factors that can potentially influence its onset and development into more severe diseases.

We previously found that targeted deletion of the *Kcne2* gene causes iron deficiency anemia, and also hypercholesterolemia (12). KCNE2 is a potassium channel β subunit linked to cardiac arrhythmias and atherosclerosis (13,14,15). The five-strong KCNE gene family comprises single transmembrane span proteins (KCNE subunits, also referred to as Mink-related peptides or MiRPs) that co-assemble with and alter the functional attributes of voltage-gated potassium (Kv) channel pore-forming (α) subunits (16). Like other KCNE subunits, KCNE2 is widely expressed in a variety of tissues, and can promiscuously associate with several different Kv α subunits (17).

Aside from its roles in cardiac myocytes, where KCNE2 regulates hERG, Kv4.2, Kv1.5 and Kv2.1 depending on the species (13,18,19,20,21), KCNE2 also co-assembles with the KCNQ1 α subunit (22). This complex is important for various epithelial tissues, including the stomach, thyroid and choroid plexus (18,19,23,24). Importantly, *Kcne2*^{-/-} mice exhibit achlorhydria, because KCNQ1-KCNE2 channels are required for normal function of the parietal cell H⁺/K⁺-ATPase, and therefore gastric acid secretion (24,25). *Kcne2* deletion results in mis-trafficking of KCNQ1 channels to the basolateral side of parietal cells, where they cannot fulfil their normal function, and ultimately leads to gastritis cystica profunda and

gastric neoplasia (26,27). Because the *Kcne2*-linked achlorhydria impairs iron uptake and causes iron deficiency anemia, a potential cause of abnormalities in hepatic lipid metabolism, here we investigated *Kcne2*-dependent hepatic lipid content and transcriptome remodeling, and discovered that *Kcne2* deletion causes NAFLD.

Methods

Generation of mice and study protocol

The *Kcne2*^{-/-} mouse line was generated as we previously described (24), and mice used in this study were bred by crossing *Kcne2*^{+/-} mice which had been backcrossed >10 times into the C57BL/6 strain. After being genotyped and weaned at 3 weeks of age, mice pups were assigned to, and maintained on, either a control diet (2020X, Harlan, 16% kcal from fat; 19.1% protein, 2.7% crude fiber, 12.3% neutral detergent fiber and 0% cholesterol) or western diet (TD.88137, Harlan, 42% kcal from fat, >60% of which is saturated; 34% sucrose; 0.2% cholesterol). Cardiac-specific *Kcne2*^{-/-} mice, used as a control in the liver analyses, were generated using a mouse line expressing Cre-recombinase under the control of the α MHC (alpha myosin heavy chain) promoter; a full phenotypic description of this mouse line will appear in a separate, future study. Mouse tissue and blood serum were then collected for further analysis or stored at -80 °C.

Whole-transcript Microarray analysis

Mice were euthanized, and then tissue was harvested and preserved in RNA^{later} (Invitrogen) until use. Total RNA was collected from the liver, reverse-transcribed into cDNA and analyzed by “whole-transcript transcriptomics” using the GeneAtlas microarray system (Affymetrix) and manufacturer’s protocols. MoGene 1.1 ST array strips (Affymetrix) were used to hybridize to newly synthesized sscDNA. Each array comprised 770,317 distinct 25-mer probes to probe an estimated 28,853 transcripts, with a median 27 probes per gene. Gene expression changes associated with *Kcne2* deletion were analyzed using Ingenuity Pathway Analysis (Qiagen) to identify biological networks, pathways, processes and diseases that were most highly represented in the differentially expressed gene (DEGs) identified. Expression changes of ≥ 1.5 fold and $p < 0.05$ were included in the analysis.

RNA isolation and Real-Time qPCR

Mice were euthanized by CO₂ asphyxiation. Gastric fundus tissue was harvested and washed with PBS; livers were harvested, washed and perfused through left ventricle with PBS + heparin, then all tissue either processed or stored at -80 °C until use. RNA was extracted using 1 ml of Trizol (Invitrogen) per 100 mg of tissue and purified using the RNeasy Mini Kit (Qiagen) according to the manufacturer's protocol. RNA samples with A₂₆₀/A₂₈₀ absorbance ratios between 2.00–2.20 were used for further synthesis. 500 ng to 1 µg of RNA was used for cDNA synthesis (Qiagen's Quantitect Reverse Transcriptase) and stored at -20 °C until use. Primer pairs for target gene *Kcne2* (NCBI Gene ID: 246133) and *Gapdh* (NCBI Gene ID: 14433) produced amplicons of 175 bp and 123 bp respectively. The qPCR primer sequences were as follows:

Kcne2, forward 5'-CACATTAGCCAATTTGACCCAG-3', and reverse 5'-GAACATGCCGATCATCACCAT-3'; *Gapdh*, forward 5'-AGGTCGGTGTGAACGGATTTG-3'; and reverse 5'-TGTAGACCATGTAGTTGAGGTCA-3. Primers (0.05 µm synthesis scale, HPLC purified) were acquired from Sigma. Real-time qPCR analysis was performed using the CFX Connect System, iTaq Universal SYBR Green Supermix (BioRad) and 96-well clear plates. Thermocycling parameters were set according to manufacturer's protocol for iTaq. Samples were run in triplicate as a quality control measure and triplicates with a standard deviation of 0.6 or higher were repeated. Melting curves were assessed for verification of a single product. $\Delta\Delta Cq$ values were normalized to those obtained for the *Kcne2*^{+/+} stomach tissue.

Iron supplementation study

To determine the potential beneficial effects of alleviating iron-deficiency anemia, post-partum dams were first intraperitoneally (IP) injected with iron dextran (25 mg/kg) or vehicle control (saline) on the day their pups were born. Mouse pups were then injected with iron dextran (12.5 mg/kg) or vehicle control (saline) at P7 and P14. Whole livers and blood serum

were then harvested for analysis at P21. Liver section oil red O staining was performed by UC Irvine pathology core facility, and then the extent of staining was quantified by a scorer blinded to genotype, treatment, and hypothesis. Representative images were then chosen based on the mean score for each group.

Blood analysis

To quantify triglycerides, serum was collected after euthanasia from 3-week-old male mouse pups and then analyzed using a glycerol oxidation-based colorimetric assay (Abcam, United Kingdom). CRP and homocysteine were quantified in serum collected after sacrificing 6–9-month-old mice, using ELISA (R&D systems, MN) and the Mouse Homocysteine Assay kit (quantifying hydrogen sulfide resulting from degradation of homocysteine by homocysteinase) (Crystal Chem, IL, USA), respectively. Alanine transaminase (ALT), aspartate transaminase (AST), and total and direct (conjugated) bilirubin concentrations in P21 mouse serum were quantified using a Mindray BS-120 Chemistry Analyzer (Mindray Medical Corporation, Shenzhen, China).

Statistical analysis

Statistical analyses (student's t-test or ANOVA, as indicated in the figure legends) were performed assuming statistical significance with p values <0.05.

Study approval

All mice were housed in pathogen-free facilities and the study was approved by the Animal Care and Use Committee at University of California, Irvine. Studies were performed during the light cycle and were carried out in strict accordance with the recommendations in the Guide for the Care and Use of Laboratory Animals of the National Institutes of Health.

Results and Discussion

Postnatal day 21 (P21) *Kcne2*^{-/-} pups exhibited lower bodyweight compared to wild-type (*Kcne2*^{+/+}) counterparts (**Figure 1 A**), but had elevated serum triglycerides (**Figure 1 B**). Serum ALT and AST levels were also elevated in P21 *Kcne2*^{-/-} pups (**Figure 1 C**) whereas bilirubin was unchanged (**Figure 1 D**). These findings were consistent with early NAFLD, which was further explored using histology. Livers from P21 *Kcne2*^{-/-} pups had a more vacuolated appearance than those from wild-type pups (**Figure 1 E**) and *Kcne2* deletion caused marked accumulation of lipid in both P7 (**Figure 1 F**) and P21 (**Figure 1 G, H**) pup livers, confirming that *Kcne2*^{-/-} pups had early-onset NAFLD.

Microarray transcriptome analysis followed by regulator effect analysis (*Ingenuity Pathway Analysis*, Qiagen) of differentially expressed genes (DEGs) in livers of P21 *Kcne2*^{-/-} pups compared to *Kcne2*^{+/+} littermates identified the network with the highest consistency score as one including beta-oxidation of fatty acids, glucose concentration and hepatic steatosis, controlled by the transcriptional co-activator and regulator of genes important for energy metabolism, Peroxisome proliferator-activated receptor gamma co-activator 1- α (PGC-1 α , encoded by PPARGC1A) (**Figure 2A**). The specific transcriptional changes observed within functional gene networks in the liver were highly consistent with remodeling in response to lipid accumulation, i.e., increased beta-oxidation of fatty acids in response to the lipid accumulation, increased glucose-6 phosphatase expression (knockout of which causes hepatic steatosis in mice (28). Thus, the associated transcriptome changes were likely not causing the NAFLD but were the result of remodeling in response to it, indicating that the *Kcne2*^{-/-} liver was responding (albeit insufficiently) to abnormally high lipid accumulation. These changes occurred despite the

lack of *Kcne2* expression in *Kcne2*^{+/+} mouse liver (**Figure 2B**), suggesting that *Kcne2*-dependent NAFLD arose via an initially extrahepatic defect.

Kcne2 deletion-linked achlorhydria (24) causes iron-deficiency anemia (12,29), which can predispose to dyslipidemia and NAFLD (11). Although data vary depending on the animal model studied, iron deficiency in rats, for example, has been reported to increase hepatic lipogenesis, causing steatosis; this may occur via increased *de novo* lipogenesis from glucose (30). Here, to investigate the possible role of iron deficiency in *Kcne2* deletion-linked NAFLD, we initially utilized transcriptomic analysis in conjunction with iron supplementation. Non-treated P21 *Kcne2*^{-/-} livers exhibited extensive transcriptome remodeling indicative of NAFLD and anemia. The 6 top-ranked DEG networks as identified by pathway analysis were: increased beta oxidation of fatty acids, elevated carbohydrates, hepatic steatosis, survival of erythroid progenitor cells and red blood cells, and proliferation of embryonic stem cells (**Figure 3**). Strikingly, supplementation with injectable iron (iron dextran) eliminated the differences in concerted gene expression caused by *Kcne2* deletion that are associated with anemia (demonstrating that the iron supplementation we employed was effective in restoring iron levels and preventing anemia) and also the gene expression changes associated with NAFLD. Thus, only 5 of the 116 DEGs in the top 6 DEG networks were still differentially expressed in *Kcne2*^{-/-} livers after iron treatment (**Figure 3**).

Consistent with the finding that iron supplementation prevented the transcriptome changes associated with NAFLD in *Kcne2*^{-/-} pups, iron supplementation also prevented excessive vacuolation in the liver and eliminated *Kcne2*-dependent differences in hepatic lipid accumulation in the liver (**Figure 4 A-C**). A comparison of hepatic oil red O staining in iron-treated versus non-treated *Kcne2*^{-/-} pups indicated successful alleviation of hepatic steatosis by iron supplementation (one-way ANOVA, $p = 0.03$). Thus, iron deficiency is a major factor in

Kcne2-dependent, early-onset NAFLD. Note that the moderate *increase* in hepatic lipids of *Kcne2*^{+/+} pups treated with iron likely arose from iron overload which, as with iron deficiency, can also cause hepatic steatosis (11).

To increase confidence that iron deficiency played the major role in *Kcne2*-dependent NAFLD, we examined other potential causes. *Kcne2* deletion also causes cardiac dysfunction, which can lead to right-heart failure and associated liver fibrosis (12,19,20). Although the livers studied here were from global *Kcne2*^{-/-} pups at P21, at which age they do not show signs of heart failure (12,19,20), we next examined livers isolated from mice with a cardiac-specific *Kcne2* deletion, to rule out a direct role for cardiac dysfunction in *Kcne2*-dependent NAFLD. Accordingly, only 15/116 DEGs in the top 6 DEG networks identified in global *Kcne2*^{-/-} mouse livers were also differentially expressed in cardiac-specific *Kcne2*^{-/-} mouse livers, strongly suggesting against a cardiac role in *Kcne2*^{-/-} NAFLD initiation (**Figure 3**).

Kcne2 deletion also results in hypothyroidism because KCNQ1-KCNE2 channels facilitate thyroid iodide uptake by the sodium iodide symporter (19,31). Pups of *Kcne2*^{-/-} dams are hypothyroid regardless of their own genotype because they rely on milk for iodide and/or thyroid hormones, whereas *Kcne2*^{-/-} mice bred from *Kcne2*^{+/-} dams do not exhibit signs of hypothyroidism until adulthood (19). However, because hypothyroidism is a risk factor for NAFLD and even upper-normal levels of TSH associate with human NAFLD (32), and because we previously observed findings suggestive of liver fibrosis in hypothyroid *Kcne2*^{-/-} mice (19), here we nevertheless examined this possibility, by comparing livers of P21 *Kcne2*^{-/-} pups bred from *Kcne2*^{+/-} versus *Kcne2*^{-/-} dams. Only 14 DEGs identified when comparing livers of *Kcne2*^{-/-} pups versus those of *Kcne2*^{+/+} pups (**Figure 3**) were also identified as being differentially expressed in *Kcne2*^{-/-} pups from *Kcne2*^{-/-} dams versus those from *Kcne2*^{+/-} dams (**Figure 5A**), and none of these were within the 6 identified anemia/NAFLD networks (**Figure 3**).

Furthermore, network analysis of DEGs in livers of *Kcne2*^{-/-} pups from *Kcne2*^{-/-} dams versus those from *Kcne2*^{+/-} dams revealed less-populated networks, spanning a range of physiological processes and not biased toward NAFLD (**Figure 5B**). *Kcne2*-dependent NAFLD in pups from heterozygous dams, as we used in the current study, is therefore *not* initiated by hypothyroidism.

Taken together, our data support a primary role for iron deficiency, but not hypothyroidism or heart failure, in initiating *Kcne2*-dependent NAFLD. Similarly, iron deficiency can predispose to dyslipidemia and NAFLD in human populations (11), both of which are risk factors for atherosclerosis (33), as are certain human KCNE2 polymorphisms (3).

In addition, we found that serum CRP, an atherosclerotic biomarker released by the liver in response to inflammation, was elevated in *Kcne2*^{-/-} mice - most prominently in western diet-fed females (**Figure 6A**). This correlates with recently-discovered atherosclerotic predisposition in *Kcne2*^{-/-} mice (15) and is also consistent with presence of NAFLD, although elevated CRP is not a specific biomarker for NAFLD (34). Achlorhydria also causes hyperhomocysteinemia, another atherosclerosis risk factor (35); accordingly, *Kcne2* deletion increased serum homocysteine (**Figure 6B**), providing another possible mechanistic link between achlorhydria (impairing vitamin B absorption, causing hyperhomocysteinemia) and atherosclerosis in *Kcne2*^{-/-} mice. Importantly, hyperhomocysteinemia has also been positively correlated with NAFLD in human populations, and in mouse models has been suggested to lead to hepatic steatosis via abnormal lipid metabolism (36). Thus, although iron supplementation prevents hepatic steatosis in *Kcne2*^{-/-} mice, it is possible that their hyperhomocysteinemia also contributes or predisposes to NAFLD in the setting of anemia (perhaps in a double-hit scenario).

In conclusion, our data support a substantial role for *Kcne2*-linked iron deficiency in the development of NAFLD in mice. Future studies will determine if this novel genetic link is recapitulated in humans, and investigate potential interactions between KCNE2-associated atherosclerosis, dyslipidemia, NAFLD, and diet-dependent cardiac arrhythmogenesis and sudden death (15).

Figures

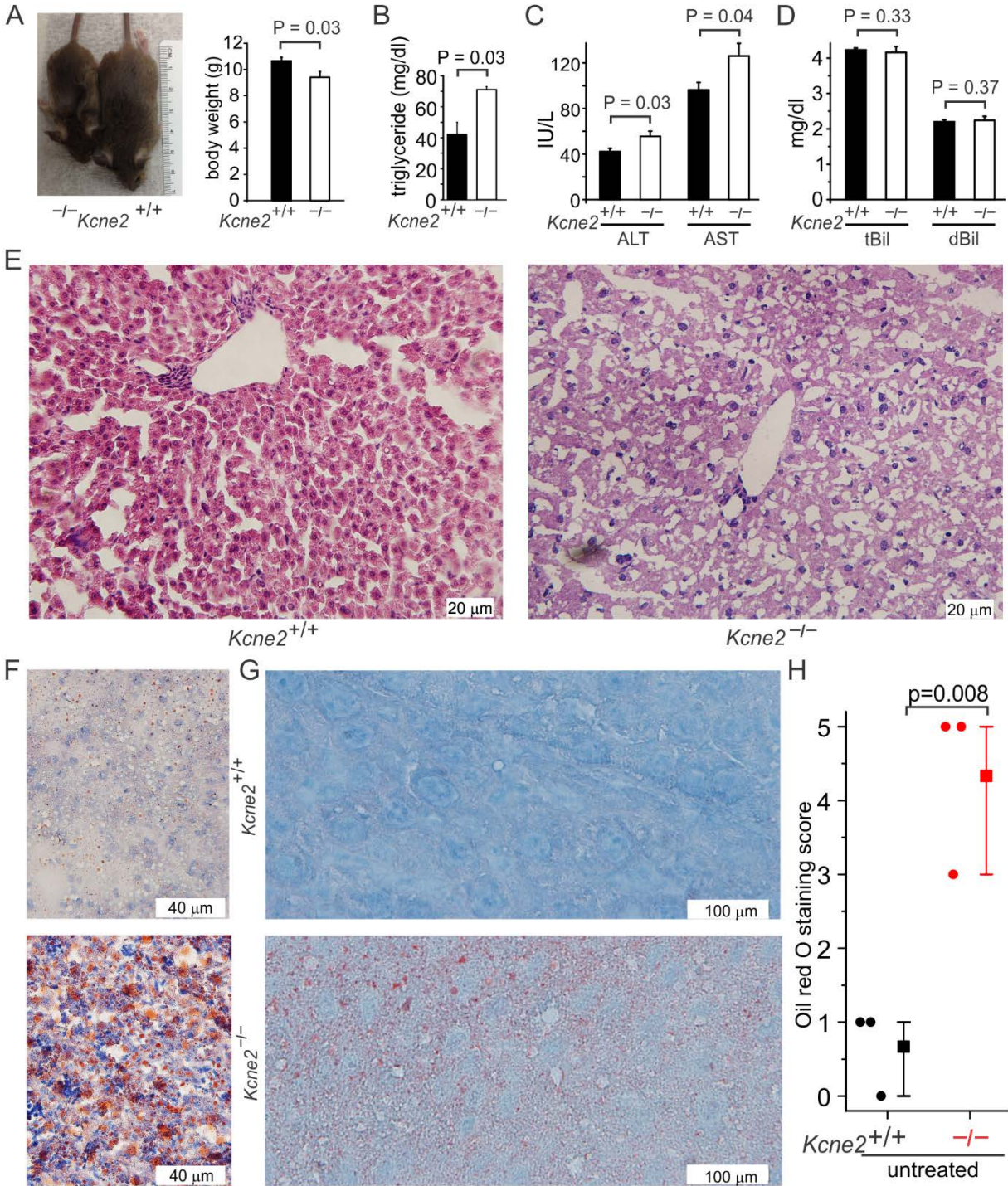


Figure 1. *Kcne2* deletion causes NAFLD.

- A. Representative image (*left*) and mean body weight (*right*) of 3-week-old male *Kcne2*^{+/+} and *Kcne2*^{-/-} mice (*n* = 8). Statistical analysis was by 2-tailed student's t-test.
- B. Mean serum triglyceride concentration for normal diet-fed 3-week-old male *Kcne2*^{+/+} and *Kcne2*^{-/-} mice (*n* = 3 per group). Statistical analysis was by 2-tailed student's t-test.
- C. Mean serum ALT and AST concentrations for normal diet-fed 3-week-old *Kcne2*^{+/+} and *Kcne2*^{-/-} mice (*n* = 6-7 per group). Statistical analysis was by 2-tailed student's t-test.
- D. Mean serum total (t) and direct (d) bilirubin (Bil) concentration for normal diet-fed 3-week-old male *Kcne2*^{+/+} and *Kcne2*^{-/-} mice (*n* = 5-7 per group). Statistical analysis was by 2-tailed student's t-test.
- E. Representative images of hematoxylin and eosin-stained liver left lobe sections from 3-week-old *Kcne2*^{+/+} and *Kcne2*^{-/-} mice (*n* = 3).
- F. Representative images of oil red O stained liver left lobe sections from 1-week-old *Kcne2*^{+/+} and *Kcne2*^{-/-} mice (*n* = 3).
- G. Representative images of oil red O stained liver left lobe sections from 3-week-old *Kcne2*^{+/+} and *Kcne2*^{-/-} mice (*n* = 3).
- H. Oil red O stain blinded scores for images as in panel G (*n* = 3). A score of 5 indicates strongest staining.

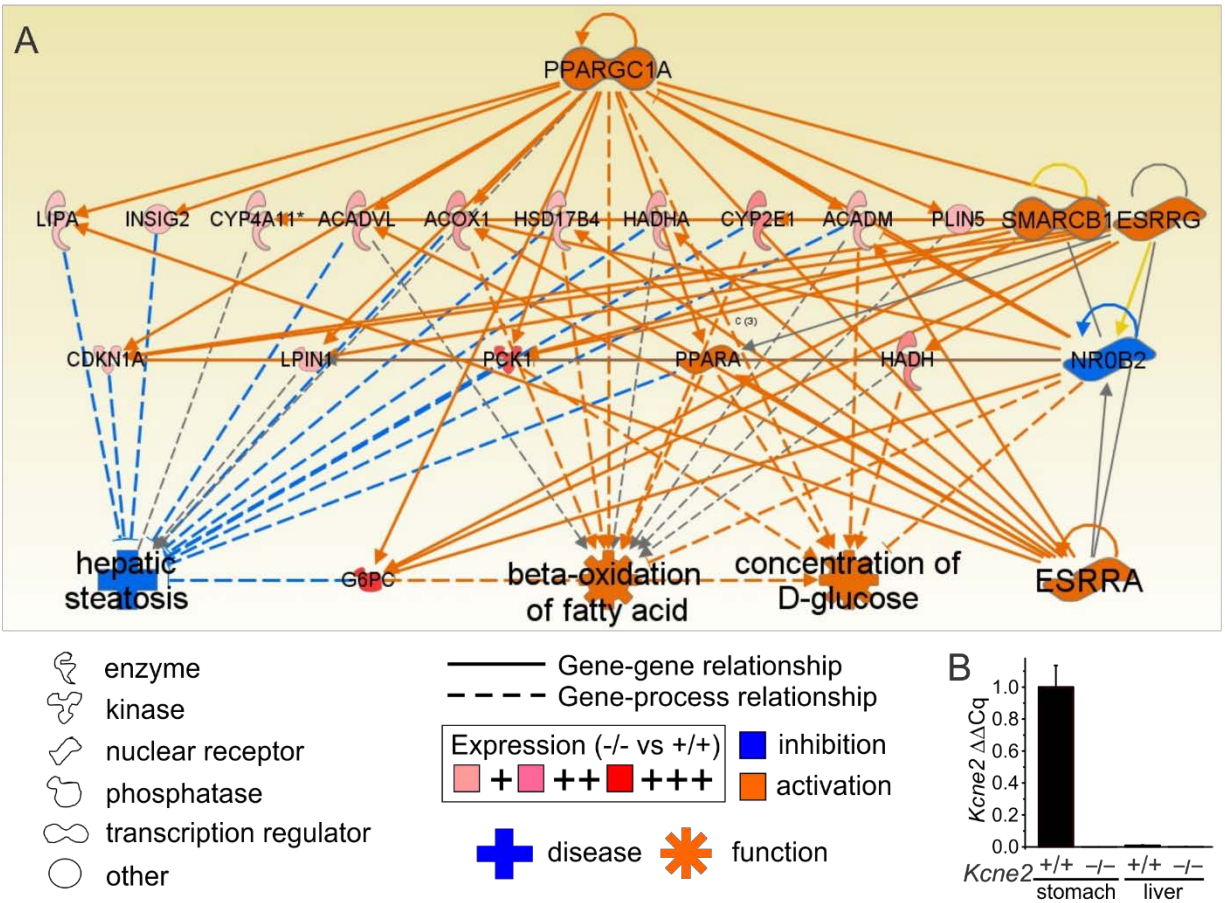


Figure 2. *Kcne2*-dependent changes in interacting hepatic gene networks

- A. The liver DEG interacting networks (after microarray transcriptome analysis of liver tissue from global *Kcne2*^{-/-} versus *Kcne2*^{+/+} mice, *n* = 8 mice per group) with the highest consistency score comprised beta-oxidation of fatty acids, glucose concentration and hepatic steatosis, with predicted hierarchical control by PPARGC1A (IPA software, Qiagen).
- B. Real-time qPCR does not detect *Kcne2* transcript expression in *Kcne2*^{+/+} mouse liver. *Kcne2*^{+/+} stomach tissue was used as a positive control, *Kcne2*^{-/-} tissue as a negative control; *n* = 3-4 mice per group, each quantified in triplicate.

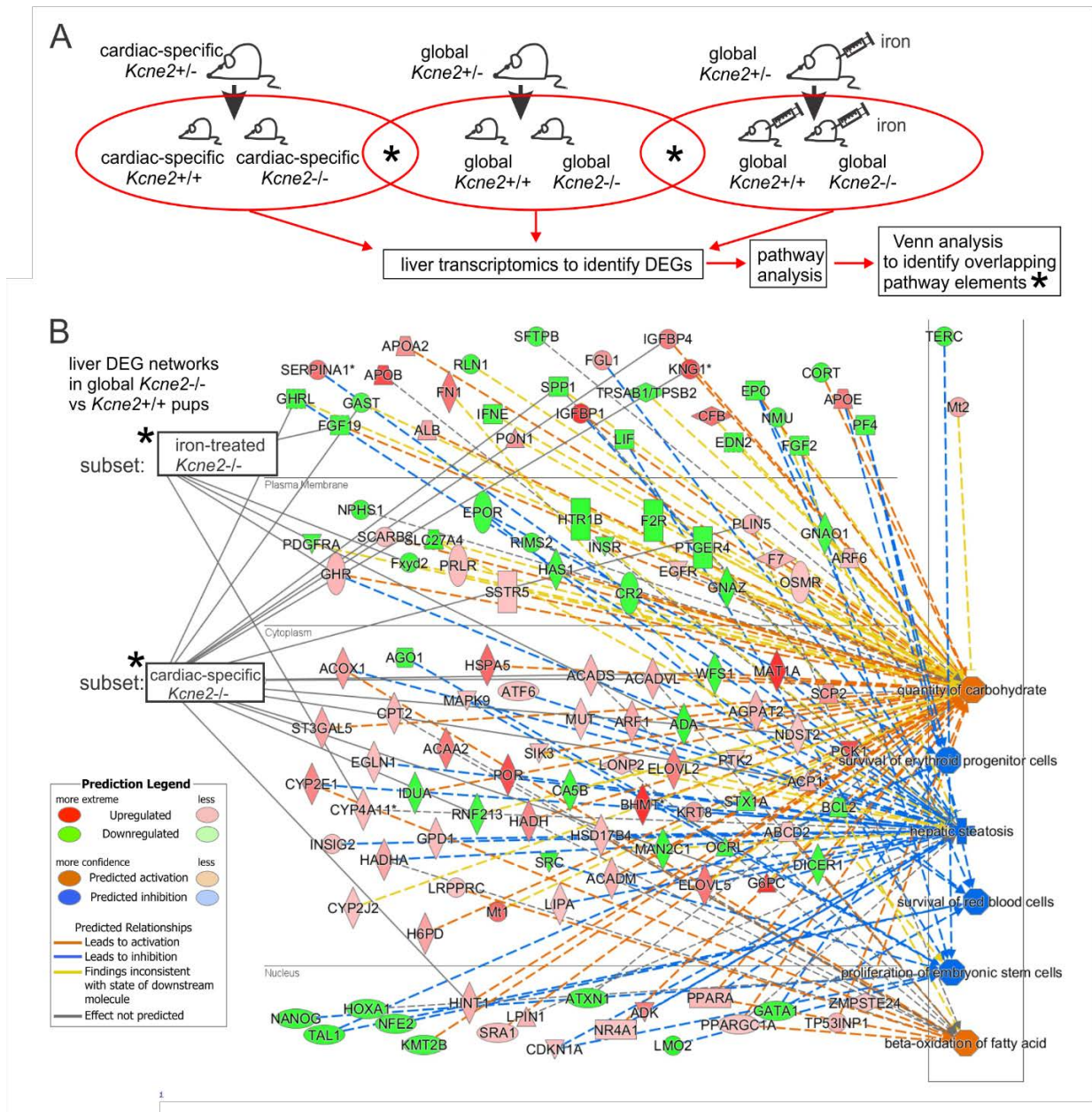


Figure 3. Iron supplementation prevents NAFLD-associated transcriptome changes in *Kcne2*^{-/-} mouse livers.

A. Schema showing genotypes, treatment and analyses for *Kcne2*-dependent hepatic transcriptome analysis.

B. DEG networks (IPA software, Qiagen) when comparing liver tissue harvested from 3-week-old global-knockout *Kcne2*^{-/-} versus *Kcne2*^{+/+} pups (organized by cellular compartment), after

microarray transcriptome analysis ($n = 8$ mice per group). Red, upregulated; green, downregulated, in $Kcne2^{-/-}$ versus $Kcne2^{+/+}$ livers. Venn analysis revealed that iron supplementation from birth eliminated all but 5 transcript changes (subset: iron treated) and that cardiac-specific $Kcne2$ deletion resulted in only 15 liver DEGs (subset: cardiac-specific $Kcne2^{-/-}$) common to those altered by global $Kcne2$ deletion.

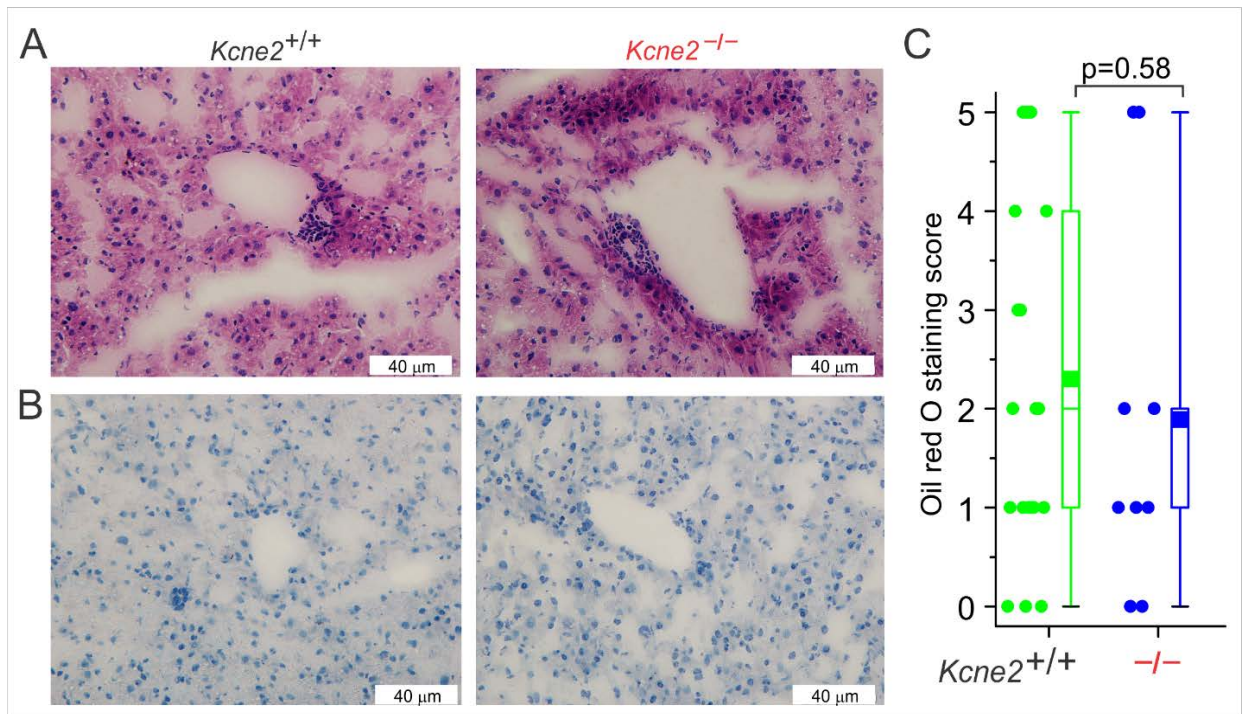
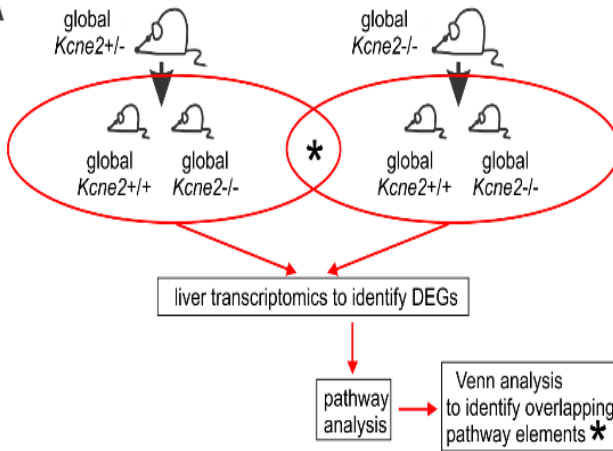


Figure 4. Iron supplementation prevents *Kcne2* deletion-associated NAFLD.

- A. Representative images of hematoxylin and eosin-stained liver left-lobe sections from iron dextran-treated P21 global *Kcne2*^{-/-} versus *Kcne2*^{+/+} mice ($n = 9-16$).
- B. Representative images of oil-red-O-stained liver left-lobe sections from iron dextran-treated P21 global *Kcne2*^{-/-} versus *Kcne2*^{+/+} mice ($n = 9-16$).
- C. Oil red O stain blinded scores for images as in panel B ($n = 9-16$). A score of 5 indicates strongest staining.

A



- ACOT4* Acyl-CoA Thioesterase 4
- ATP5F1* ATPase subunit b
- CDC23* Cell Division Cycle 23
- COG8* Component Of Oligomeric Golgi Complex 8
- DFNA5* Deafness, Autosomal Dominant 5
- FGGY* FGGY carbohydrate kinase domain-containing protein
- HIST1H2BI* Histone Cluster 1, H2bi
- HIST1H2BL* Histone Cluster 1, H2bl
- HLA-A* Major Histocompatibility Complex, Class I, A
- MYO18B* Myosin XVIIIIB
- n-R5s136* nuclear encoded rRNA 5S 136
- Snord49a* Small Nucleolar RNA, C/D Box 49A
- TMEM38B* Transmembrane Protein 38B
- Vaultrc5* Vault RNA component 5

B

liver DEG networks
in global *Kcne2*^{-/-} pups
from *Kcne2*^{-/-} dams
vs global *Kcne2*^{-/-} pups
from *Kcne2*^{+/-} dams
(maternal genotype effect)

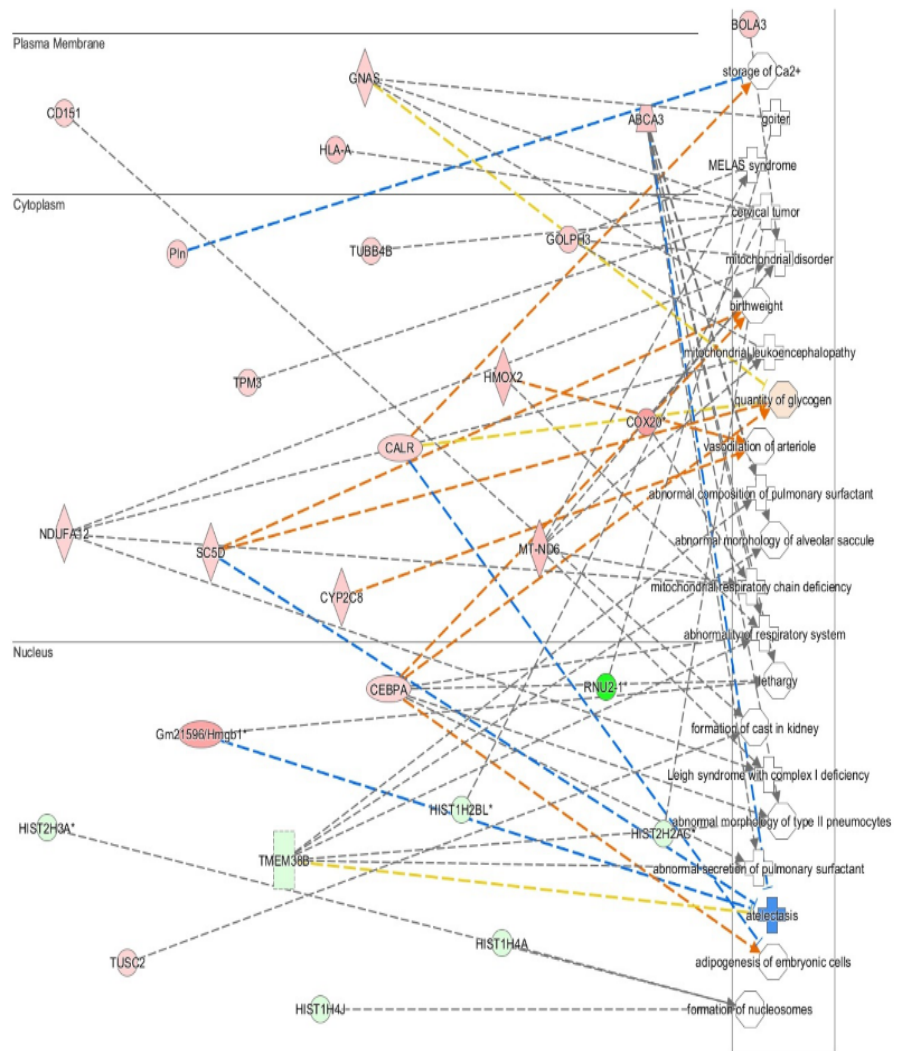
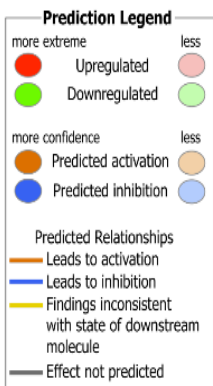


Figure 5. NAFLD in P21 *Kcne2*^{-/-} pups is not altered by maternal genotype.

A. *Left*, schema showing genotypes, treatment and analyses for effects of maternal genotype on *Kcne2*-dependent hepatic steatosis study. *Right*, the 14 DEGs identified when comparing livers of *Kcne2*^{-/-} pups versus those of *Kcne2*^{+/-} pups (**Figure 3**) that were also differentially expressed in *Kcne2*^{-/-} pups from *Kcne2*^{-/-} dams versus those from *Kcne2*^{+/-} dams; none of these were within the 6 identified anemia/NAFLD networks from **Figure 3**).

B. DEG networks (IPA software, Qiagen) when comparing liver tissue harvested from 3-week-old global-knockout $Kcne2^{-/-}$ pups from $Kcne2^{-/-}$ dams versus $Kcne2^{-/-}$ pups from $Kcne2^{+/-}$ dams (organized by cellular compartment), after microarray transcriptome analysis ($n = 8$ mice per group). Red, upregulated; green, downregulated, in $Kcne2^{-/-}$ versus $Kcne2^{+/+}$ livers.

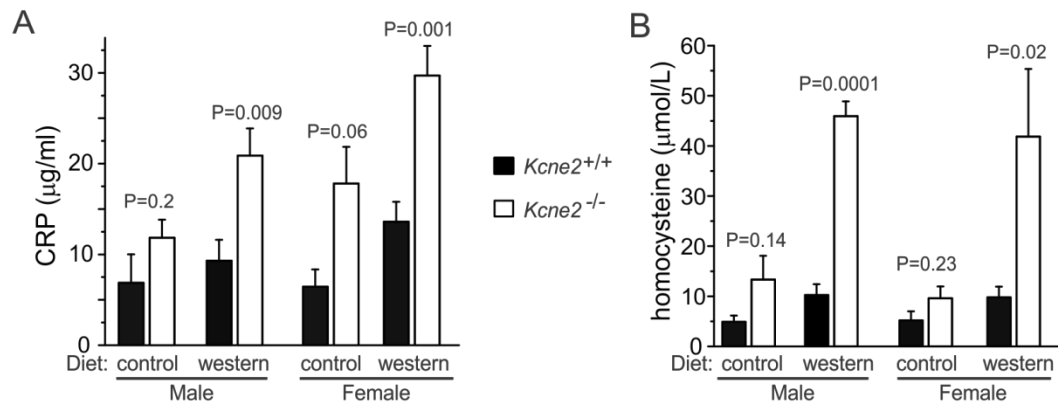


Figure 6. *Kcne2* deletion causes elevated serum CRP and homocysteine.

- A. Mean serum C-reactive protein (CRP) concentration for 6-9 month-old $Kcne2^{+/+}$ and $Kcne2^{-/-}$ mice. $n = 7-10$, male control diet; $n = 8$, male western diet; $n = 4-7$, female control diet; $n = 8$, female western diet; P values are for 2-tailed, unpaired t-tests for inter-genotype comparisons within equivalent sex and diet groups.
- B. Mean serum homocysteine concentration for $Kcne2^{+/+}$ and $Kcne2^{-/-}$ mice. $n = 4$, male control diet; 4, male western diet; 3-4, female control diet; 3-5, female western diet; p values are for 2-tailed, unpaired t-tests for inter-genotype comparisons within equivalent sex and diet groups.

References

- 1 Anstee, Q. M. & Day, C. P. The genetics of NAFLD. *Nat Rev Gastroenterol Hepatol* **10**, 645-655, doi:10.1038/nrgastro.2013.182 (2013).
- 2 Clark, J. M. & Diehl, A. M. Hepatic steatosis and type 2 diabetes mellitus. *Curr Diab Rep* **2**, 210-215 (2002).
- 3 Dongiovanni, P. & Valenti, L. Genetics of nonalcoholic fatty liver disease. *Metabolism: clinical and experimental*, doi:10.1016/j.metabol.2015.08.018 (2015).
- 4 He, S. *et al.* A sequence variation (I148M) in PNPLA3 associated with nonalcoholic fatty liver disease disrupts triglyceride hydrolysis. *The Journal of biological chemistry* **285**, 6706-6715, doi:10.1074/jbc.M109.064501 (2010).
- 5 Li, J. Z. *et al.* Chronic overexpression of PNPLA3I148M in mouse liver causes hepatic steatosis. *The Journal of clinical investigation* **122**, 4130-4144, doi:10.1172/JCI65179 (2012).
- 6 Yang, Z. *et al.* Genetic variation in the GCKR gene is associated with non-alcoholic fatty liver disease in Chinese people. *Molecular biology reports* **38**, 1145-1150, doi:10.1007/s11033-010-0212-1 (2011).
- 7 Song, J. *et al.* Polymorphism of the PEMT gene and susceptibility to nonalcoholic fatty liver disease (NAFLD). *The FASEB journal : official publication of the Federation of American Societies for Experimental Biology* **19**, 1266-1271, doi:10.1096/fj.04-3580com (2005).
- 8 Al-Serri, A. *et al.* The SOD2 C47T polymorphism influences NAFLD fibrosis severity: evidence from case-control and intra-familial allele association studies. *Journal of hepatology* **56**, 448-454, doi:10.1016/j.jhep.2011.05.029 (2012).

- 9 Watanabe, K., Ohnishi, S., Manabe, I., Nagai, R. & Kadowaki, T. KLF6 in nonalcoholic fatty liver disease: role of fibrogenesis and carcinogenesis. *Gastroenterology* **135**, 309-312, doi:10.1053/j.gastro.2008.06.014 (2008).
- 10 Yoneda, M. *et al.* Association between angiotensin II type 1 receptor polymorphisms and the occurrence of nonalcoholic fatty liver disease. *Liver Int* **29**, 1078-1085, doi:10.1111/j.1478-3231.2009.01988.x (2009).
- 11 Ahmed, U., Latham, P. S. & Oates, P. S. Interactions between hepatic iron and lipid metabolism with possible relevance to steatohepatitis. *World journal of gastroenterology : WJG* **18**, 4651-4658, doi:10.3748/wjg.v18.i34.4651 (2012).
- 12 Hu, Z. *et al.* Kcne2 deletion creates a multisystem syndrome predisposing to sudden cardiac death. *Circulation. Cardiovascular genetics* **7**, 33-42, doi:10.1161/CIRCGENETICS.113.000315 (2014).
- 13 Abbott, G. W. *et al.* MiRP1 forms IKr potassium channels with HERG and is associated with cardiac arrhythmia. *Cell* **97**, 175-187 (1999).
- 14 Sabater-Lleal, M. *et al.* Common genetic determinants of lung function, subclinical atherosclerosis and risk of coronary artery disease. *PloS one* **9**, e104082, doi:10.1371/journal.pone.0104082 (2014).
- 15 Lee, S. M., Nguyen, D., Hu, Z. & Abbott, G. W. Kcne2 deletion promotes atherosclerosis and diet-dependent sudden death. *Journal of molecular and cellular cardiology*, doi:10.1016/j.yjmcc.2015.08.013 (2015).
- 16 McCrossan, Z. A. & Abbott, G. W. The MinK-related peptides. *Neuropharmacology* **47**, 787-821, doi:10.1016/j.neuropharm.2004.06.018 (2004).
- 17 Abbott, G. W. The KCNE2 K(+) channel regulatory subunit: Ubiquitous influence, complex pathobiology. *Gene* **569**, 162-172, doi:10.1016/j.gene.2015.06.061 (2015).
- 18 Roepke, T. K. *et al.* KCNE2 forms potassium channels with KCNA3 and KCNQ1 in the choroid plexus epithelium. *The FASEB journal : official publication of the Federation of*

- American Societies for Experimental Biology* **25**, 4264-4273 (2011).
- 19 Roepke, T. K. *et al.* Kcne2 deletion uncovers its crucial role in thyroid hormone biosynthesis. *Nature medicine* **15**, 1186-1194, doi:10.1038/nm.2029 (2009).
- 20 Roepke, T. K. *et al.* Targeted deletion of kcne2 impairs ventricular repolarization via disruption of I(K,slow1) and I(to,f). *The FASEB journal : official publication of the Federation of American Societies for Experimental Biology* **22**, 3648-3660, doi:10.1096/fj.08-110171 (2008).
- 21 McCrossan, Z. A., Roepke, T. K., Lewis, A., Panaghie, G. & Abbott, G. W. Regulation of the Kv2.1 potassium channel by MinK and MiRP1. *The Journal of membrane biology* **228**, 1-14, doi:10.1007/s00232-009-9154-8 (2009).
- 22 Tinel, N., Diochot, S., Borsotto, M., Lazdunski, M. & Barhanin, J. KCNE2 confers background current characteristics to the cardiac KCNQ1 potassium channel. *The EMBO journal* **19**, 6326-6330, doi:10.1093/emboj/19.23.6326 (2000).
- 23 Abbott, G. W. *et al.* KCNQ1, KCNE2, and Na⁺-Coupled Solute Transporters Form Reciprocally Regulating Complexes That Affect Neuronal Excitability. *Science signaling* **7**, ra22, doi:10.1126/scisignal.2005025 (2014).
- 24 Roepke, T. K. *et al.* The KCNE2 potassium channel ancillary subunit is essential for gastric acid secretion. *The Journal of biological chemistry* **281**, 23740-23747, doi:10.1074/jbc.M604155200 (2006).
- 25 Lee, M. P. *et al.* Targeted disruption of the Kvlqt1 gene causes deafness and gastric hyperplasia in mice. *The Journal of clinical investigation* **106**, 1447-1455, doi:10.1172/JCI10897 (2000).
- 26 Roepke, T. K. *et al.* Genetic dissection reveals unexpected influence of beta subunits on KCNQ1 K⁺ channel polarized trafficking in vivo. *The FASEB journal : official publication of the Federation of American Societies for Experimental Biology* **25**, 727-736, doi:10.1096/fj.10-173682 (2011).

- 27 Roepke, T. K. *et al.* Targeted deletion of *Kcne2* causes gastritis cystica profunda and gastric neoplasia. *PloS one* **5**, e11451, doi:10.1371/journal.pone.0011451 (2010).
- 28 Mutel, E. *et al.* Targeted deletion of liver glucose-6 phosphatase mimics glycogen storage disease type 1a including development of multiple adenomas. *Journal of hepatology* **54**, 529-537, doi:10.1016/j.jhep.2010.08.014 (2011).
- 29 Salsbury, G. *et al.* Disruption of the potassium channel regulatory subunit KCNE2 causes iron-deficient anemia. *Experimental hematology* **42**, 1053-1058 e1051, doi:10.1016/j.exphem.2014.07.269 (2014).
- 30 Sherman, A. R., Guthrie, H. A., Wolinsky, I. & Zulak, I. M. Iron deficiency hyperlipidemia in 18-day-old rat pups: effects of milk lipids, lipoprotein lipase, and triglyceride synthesis. *The Journal of nutrition* **108**, 152-162 (1978).
- 31 Purtell, K. *et al.* The KCNQ1-KCNE2 K⁺ channel is required for adequate thyroid I⁻ uptake. *The FASEB journal : official publication of the Federation of American Societies for Experimental Biology*, doi:10.1096/fj.12-206110 (2012).
- 32 Chung, G. E. *et al.* Non-alcoholic fatty liver disease across the spectrum of hypothyroidism. *Journal of hepatology* **57**, 150-156, doi:10.1016/j.jhep.2012.02.027 (2012).
- 33 Targher, G., Day, C. P. & Bonora, E. Risk of cardiovascular disease in patients with nonalcoholic fatty liver disease. *The New England journal of medicine* **363**, 1341-1350, doi:10.1056/NEJMra0912063 (2010).
- 34 Dogru, T., Genc, H. & Bagci, S. C reactive protein levels in non-alcoholic fatty liver disease. *Journal of hepatology* **56**, 507-508; author reply 508-510, doi:10.1016/j.jhep.2011.06.030 (2012).
- 35 Malinow, M. R. Hyperhomocyst(e)inemia. A common and easily reversible risk factor for occlusive atherosclerosis. *Circulation* **81**, 2004-2006 (1990).
- 36 Namekata, K. *et al.* Abnormal lipid metabolism in cystathionine beta-synthase-deficient

mice, an animal model for hyperhomocysteinemia. *The Journal of biological chemistry* **279**, 52961-52969, doi:10.1074/jbc.M406820200 (2004).

Chapter 3

***Kcne2* deletion Type II Diabetes Mellitus via a primary defect in insulin secretion**

Abstract

Type II diabetes mellitus (T2DM) represents a rapidly increasing threat to global public health. T2DM arises largely from obesity, poor diet, and lack of exercise, but also involves genetic predisposition. We previously detected glucose intolerance in adult mice with germline deletion of *Kcne2*, which encodes a K⁺ channel ancillary subunit. In Chapter 3, we show that germline *Kcne2* deletion in mice impairs glucose tolerance as early as 5 weeks of age in pups fed a western diet, ultimately causing diabetes. In adult mice fed normal chow, skeletal muscle insulin receptor β and IRS-1 expression was downregulated by *Kcne2* deletion, characteristic of T2DM. *Kcne2* deletion also caused extensive pancreatic transcriptome changes consistent with T2DM, including ER stress, inflammation and hyperproliferation. *Kcne2* transcript was islet cell-specific in mouse pancreas. *Kcne2* deletion impaired isolated β -cell insulin secretion *in vitro* up to 8-fold, and diminished β -cell peak outward K⁺ current at positive membrane potentials, but also left-shifted its voltage dependence and reduced inactivation. Thus, KCNE2 is crucial for normal β -cell electrical activity and insulin secretion, and its deletion causes T2DM. KCNE2 may regulate multiple β -cell K⁺ channels, including human T2DM-linked KCNQ1.

Introduction

T2DM prevalence is increasing globally, due in large part to alterations in lifestyle including poor diet and lack of exercise. T2DM is thus often part of a larger syndrome, termed metabolic syndrome, which often includes obesity, nonalcoholic fatty liver disease (NAFLD), hypercholesterolemia and coronary artery disease (CAD) (1). However, not all individuals with T2DM are obese, and there are other contributing factors, including genetic predisposition. For example, a large number of studies have shown that inherited polymorphisms in *KCNQ1*, which encodes a voltage-gated potassium (Kv) channel pore-forming (α) subunit, predispose to T2DM (2,3).

Unlike Type 1 diabetes, which is predominantly genetically acquired and arises from immune attack and destruction of pancreatic insulin-secreting β -cells, in T2DM the β -cells are present but cannot secrete sufficient insulin to control blood glucose levels. T2DM is a balance between insufficient insulin secretion, and insulin resistance, with the relative deficiencies in each insulin secretion and sensitivity varying between individuals (4,5). Insulin resistance in itself is not sufficient to cause diabetes, and must be combined with inadequate insulin secretion (6,7,8).

Various potassium channels play roles in β -cell function and insulin secretion. The best-characterized in these respects is the K_{ATP} channel. K_{ATP} channels are each formed from an octamer of two types of subunits – a tetramer of Kir6.2 α subunits that spans the plasma membrane and forms the pore, and a tetramer of cytosolic sulfonylurea receptors (SURs) that facilitates sensing of the metabolic state of β -cells by the channel complex. Increased blood glucose raises intracellular ATP levels in β -cells. Intracellular ATP binds to the SURs, resulting in inhibition of the K_{ATP} channel. Because K_{ATP} channels are weak inward rectifiers that are open at resting membrane potential, their inhibition initiates cellular depolarization. This opens β -cell voltage-gated Ca^{2+} channels, raising intracellular Ca^{2+} levels, signaling to the cell to secrete insulin. The insulin signals to the liver to stop releasing glucose into the blood, and signals to skeletal muscle to take up glucose from the blood (9,10). Inherited mutations in the genes encoding K_{ATP} channel subunits can contribute to diabetes. Mutations that moderately increase K_{ATP} channel activity can predispose to T2DM in adults. Mutations that dramatically increase K_{ATP} channel activity to the extent that glucose-dependent insulin secretion is essentially prevented can cause syndromic neonatal diabetes (11).

Several Kv channels are also expressed in β -cells, and are involved in the repolarization phase of β -cell action potentials and/or in regulation of insulin secretion. Inhibition of the repolarizing K^+ currents the Kv channels generate augments insulin secretion. Kv1.4, Kv1.5, Kv2.1, Kv2.2, Kv3.1 and Kv3.2 α subunits have been detected in the insulin-secreting cell line, INS-1. Their inhibition by classic Kv channel blockers 4-aminopyridine, tetraethylammonium and tetrapentyl ammonium enhanced tolbutamide-stimulated insulin secretion, but not basal insulin secretion (12). Interestingly, Kv2.1 directly interacts with the exocytotic machinery of β -cells via syntaxin 1A, and this activity was recently postulated to be more important than its electrical activity in

terms of effects on insulin secretion (13,14,15). Inhibition of Kv2.1 has been suggested as a potential therapy for T2DM (16). Selective KCNQ1 inhibition using chromanol 293B also augments glucose-stimulated insulin secretion from INS-1 cells (17) and mouse β -cells *in vivo* and *ex vivo* (18).

Interestingly, KCNQ1, Kv1.4, Kv1.5, Kv2.1, Kv3.1 and Kv3.2 are all known to be regulated by the KCNE2 single transmembrane domain ion channel ancillary subunit (19,20,21,22,23,24). KCNE2, part of the five-member *KCNE* gene family, is ubiquitously expressed in both excitable cells and in non-excitable secretory epithelial cells, and can exert marked effects on the channels it regulates. These effects include altering voltage dependence and kinetics of gating, trafficking, regulation by other factors, and pharmacology (25,26). In Chapters 1 and 2, we showed that *Kcne2* deletion in mice results in impaired glucose tolerance as part of a broader syndrome that includes hypercholesterolemia, NAFLD, and atherosclerosis (27,28,29), but we did not elucidate the mechanistic basis for glucose intolerance. Therefore, in Chapter 3, we describe direct analysis of the effects of *Kcne2* deletion on pancreatic function. We report the discovery that KCNE2 is required for normal β -cell electrical activity and insulin secretion, and that *Kcne2* deletion causes T2DM.

Methods

Generation of mice and study protocol

The *Kcne2*^{-/-} mouse line was generated as we previously described (30), and mice used in this study were bred by crossing *Kcne2*^{+/-} mice which had been backcrossed >10 times into the C57BL/6 strain. After being genotyped and weaned at 3 weeks of age, mice pups were assigned to, and maintained on, either a control diet (2020X, Harlan, 16% kcal from fat; 19.1% protein, 2.7% crude fiber, 12.3% neutral detergent fiber and 0% cholesterol) or western diet (TD.88137, Harlan, 42% kcal from fat, >60% of which is saturated; 34% sucrose; 0.2% cholesterol). All mice were subjected to fortnightly 6-hr fasts prior to glucose tolerance tests. Some cohorts had an additional fortnightly 20 to 24-hour fast commencing the morning after glucose tolerance tests, between weeks 5 through 15-17, with similar fasting protocols for mice of each diet and genotype. Mouse tissue and blood serum were then collected for further analysis or stored at -80°C.

Islet isolation

For each isolation, a pancreas each from a *Kcne2*^{+/+} and a *Kcne2*^{-/-} mouse were harvested and prepared in parallel, with both being placed in vials of collagenase solution containing (in mmol/l) 2.25 D-glucose, 1.26 CaCl₂, 0.49 MgCl₂·6H₂O, 0.41 MgSO₄·7H₂O, 5.3 KCl, 0.44 KH₂PO₄, 4.2 NaHCO₃, 137.9 NaCl, 0.34 Na₂HPO₄ [solution 1]; 0.1% collagenase P ; 0.2 % BSA) at the same time, and then the vials were placed in a 37 °C water bath. The vials were observed for 14-16 minutes and shaken every 2 minutes. The duration of the warm-up was dependent upon the amount of tissue present. Afterwards, the vials were placed in a centrifuge at 500 rcf for 8 minutes at 4 °C, to pellet the cells. The supernatant was then removed and the

cells were filtered three times through cell strainers into 50 mL vials using [solution 1]. The cells were then pelleted once more, 3 mL of solution 1 added, and then the mixture was added to 3 mL of Histopaque 1.100 (54% 1.119 density histopaque, 46% 1.077 density histopaque) in a 15 mL vial. The vials were then centrifuged for 18 minutes at 900 rcf at 4 °C as previously described (31).

Whole cell patch electrophysiological recording.

We recorded β -cell K^+ currents by patch-clamping in the whole-cell configuration using an Axopatch 200B amplifier and pCLAMP 9 software (Molecular Devices). Patch electrodes (2–4 M Ω) were loaded with intracellular solution containing (in mmol/l) 140 KCl, 1 MgCl₂[(H₂O)₆], 10 EGTA, 10 HEPES, 5 MgATP (adjusted to pH 7.25 with KOH). Islet cells were perfused with an extracellular bath solution containing (in mmol/l) 20 (D)-glucose, 119 NaCl, 2 CaCl₂[(H₂O)₆], 4.7 KCl, 10 HEPES, 1.2 MgSO₄, 1.2 KH₂PO₄, (adjusted to pH 7.3 with NaOH). β -cells were identified based on their morphology and response to glucose concentration.

Insulin secretion by isolated pancreatic islets.

After isolation, islet cells were used immediately for quantification of insulin secretion. Cells (in 200 μ l per batch) were removed using a micropipette and placed into two vials. Two mL of 3 mM glucose Krebs-Ringer Bicarbonate (KRB) solution containing (in mmol/l) 119 NaCl, 2 CaCl₂[(H₂O)₆], 4.7 KCl, 10 HEPES, 1.2 MgSO₄, 1.2 KH₂PO₄, (adjusted to pH 7.3 with NaOH) (presaturated in 5% CO₂ to buffer the cells) was added. The solution was centrifuged and the supernatant removed, leaving solely the cells. KRB media (2 mL) was again added and the vials incubated in a shaking water bath at 37 °C and rotating at 50-70 rpm. The vials were then removed, centrifuged at 1.2 rpm for 0.5-1 minutes, and the supernatant removed. The cells were counted using trypan blue and AO/PI (acridine orange and propidium iodide) dye to ensure that the same amount of cells were being examined for each sample; if one had a substantially

larger amount of cells present, then the solution was diluted. The number of cells for paired *Kcne2*^{+/+} and *Kcne2*^{-/-} mouse pancreases was thus adjusted to a more equal ratio. For insulin secretion in response to glucose, 200 µl of cell solution was mixed with 200 µl of 0, 6 and 16 mM glucose KRB media for 30 minutes at 37 °C. . The vials were then incubated for another 30 minutes at 37 °C.. The vials were centrifuged, and the supernatants extracted and stored in an -80° C freezer pending analysis by ELISA according to manufacturer's instructions (EMD Millipore, St. Charles, MO, USA). ELISA plates were analyzed using a VERSA max plate reader with SoftMax Pro 5.3 data system SoftMax Pro 5.3 data system (Molecular Devices, Silicon Valley, CA, USA)

RNA isolation and Real-Time qPCR

Mice were euthanized by CO₂ asphyxiation. Gastric fundus tissue was harvested and washed with PBS; Pancreas were harvested, washed and perfused through left ventricle with PBS, then all tissue either processed or stored at -80 °C until use. For islet and non-islet cells, pancreas samples were pooled from 4 mice per experiments and then isolated islet cells as protocol of isolation islet cells. RNA was extracted using 1 ml of Trizol (Invitrogen) per 100 mg of tissue and purified using the RNeasy Mini Kit (Qiagen) according to the manufacturer's protocol. RNA samples with A₂₆₀/A₂₈₀ absorbance ratios between 2.00–2.20 were used for further synthesis. 100 ng to 1 µg of RNA was used for cDNA synthesis (Qiagen's Quantitect Reverse Transcriptase) and stored at -20 °C until use. Primer pairs for target gene *Kcne2* (NCBI Gene ID: 246133) and *Gapdh* (NCBI Gene ID: 14433) produced amplicons of 175 bp and 123 bp respectively. The qPCR primer sequences were as follows:

Kcne2, forward 5'-CACATTAGCCAATTTGACCCAG-3', and reverse 5'-GAACATGCCGATCATCACCAT-3'; *Gapdh*, forward 5'-AGGTCGGTGTGAACGGATTTG-3'; and reverse 5'-TGTAGACCATGTAGTTGAGGTCA-3. Primers (0.05 µm synthesis scale, HPLC purified) were acquired from Sigma. Real-time qPCR analysis was performed using the CFX

Connect System, iTaq Universal SYBR Green Supermix (BioRad) and 96-well clear plates. Thermocycling parameters were set according to manufacturer's protocol for iTaq. Samples were run in triplicate as a quality control measure and triplicates with a standard deviation of 0.6 or higher were repeated. Melting curves were assessed for verification of a single product. $\Delta\Delta Cq$ values were normalized to those obtained for the *Kcne2*^{+/+} stomach tissue.

Islet cell RNA isolation and whole-transcript Microarray analysis

Mice were euthanized, and then islet cells were isolated. RNA was extracted using Trizol (Invitrogen) and purified using the RNeasy Mini Kit (Qiagen) according to the manufacturer's protocol. RNA samples with A_{260}/A_{280} absorbance ratios between 2.00-2.20 were stored at -80°C until being used for further synthesis. Reverse-transcribed cDNA was analyzed by "whole-transcript transcriptomics" with the GeneAtlas microarray system (Affymetrix) and manufacturer's protocols. MoGene 1.1 ST array strips (Affymetrix) were used to hybridize to newly synthesized sscDNA. Each array comprised 770,317 distinct 25-mer probes to probe an estimated 28,853 transcripts, with a median 27 probes per gene. Gene expression changes associated with *Kcne2* deletion were analyzed using Ingenuity Pathway Analysis (Qiagen) to identify biological networks, pathways, processes and diseases that were most highly represented in the islet cell differentially expressed gene (DEGs) identified. Expression changes of ≥ 2 fold and $p < 0.05$ were included in the analysis.

Western-blotting

For quantification of insulin receptor β protein expression, skeletal muscle tissue from *Kcne2*^{+/+} and *Kcne2*^{-/-} mice was homogenized using a dounce homogenizer with 5 mL ice-cold lysis buffer (150 mM NaCl, 10 mM Tris (pH 7.4), 1 mM EDTA, 1mM EGTA, 1% Triton x-100, 0.5% Nonidet P-40, 100 mM NaF, 10 mM sodium orthovanadate). Fresh protease inhibitor mini tablets (Pierce) were added for every 10 mL of lysis buffer. After homogenization, samples were

kept ice for 30 minutes, then centrifuged at 600 rpm (29 rcf) for 20 minutes at 4 °C. Supernatant was centrifuged again at 13,000 rpm (13,793 rcf) for 45 minutes at 4°C and then the final lysate was collected. For quantification of Insulin receptor substrate 1 (IRS-1), skeletal muscle was homogenized using a dounce homogenizer with 2.5 mL ice-cold lysis buffer. Lysis buffer was composed of 20mM Tris (pH 8.0), 137 mM NaCl, 2.7 mM KCl, 10mM NaF, 1 mM MgCl, 1mM Na₃VO₄, 10% glycerol, 1% Triton X-100. Fresh protease inhibitor mini tablets (Pierce) were added for every 10 mL of lysis buffer. After homogenization, samples were kept rotating in 4°C for one hour then centrifuged at 12,000 rpm (11,752 rcf) for 10 minutes at 4°C, and final lysate was collected. Subsequent steps were identical for all samples. The final lysate was collected and protein concentration was quantified using BCA Protein Assay (Thermo Fisher, Rockford, IL, USA). Samples of equal target protein concentration were separated on NuPAGE 4-12% Bis-Tris gels and transferred onto PDVF membranes. Primary insulin receptor β -subunit, IRS1, and phospho-IRS1 antibodies (EMD Millipore) were diluted 1:1000 in 5% milk in Tris Buffered Saline with 1% Tween-20 (TBST) and incubated either at room temperature for 2 hours or overnight in 4°C on a rocker. GAPDH antibody (Abcam) was used as loading control in 1:1000 dilution. Secondary antibodies (BioRad) were added at 1:5000 dilutions in 3% milk in TBST. Antibodies were incubated at room temperature on a rocker for 1 -2 hours. Membranes were then exposed to HRP substrate (EMD Millipore) for 5 minutes at room temperature, and chemiluminescence visualized with on a Gbox system (Syngene, Frederick, MD, USA). Images were saved and analyzed with ImageJ (National Institutes of Health, Bethesda, MD, USA).

Glucose tolerance test

Glucose tolerance tests were performed fortnightly after weaning. Mice were injected intraperitoneally (IP) with 20% glucose in 0.9% NaCl solution (2g of glucose/kg body weight) following a 6-hour fast. Blood samples were taken via tail vein before injection as well as 15, 30, 60, 90, and 120 minutes after injection for determination of blood glucose metabolism. Blood

glucose in tail-vein blood samples was quantified using OneTouch Ultra Glucose Monitors (LifeScan, Milpitas, CA, USA). The corresponding relative area under the curve (AUC) for glucose concentration was calculated using the trapezoid rule.

Statistical analysis

Statistical analyses (student's t-test or ANOVA, as indicated in the figure legends) were performed assuming significance with p values < 0.05. Bonferroni and Holm corrections were used for multiple comparisons.

Study approval

All mice were housed in pathogen-free facilities and the study was approved by the Animal Care and Use Committee at University of California, Irvine. Studies were performed during the light cycle and were carried out in strict accordance with the recommendations in the Guide for the Care and Use of Laboratory Animals of the National Institutes of Health.

Results

Kcne2 deletion causes T2DM in mice

We previously found that *Kcne2* deletion impairs glucose tolerance in adult mice fed regular mouse chow (27). Here, we discovered that feeding with a western diet has a dramatic effect on glucose tolerance of *Kcne2*^{-/-} pups, causing glucose intolerance within 2 weeks, by 5 weeks of age, versus no effect in *Kcne2*^{+/+} pups at this age (**Figure 1 A**). By 21 weeks, after 18 weeks on the western diet, *Kcne2*^{-/-} mice were diabetic (baseline serum concentration of >200 mg/dl, and serum glucose concentration of >400 mg/dl measured 2 hours after injection) whereas *Kcne2*^{+/+} mice were only moderately less glucose tolerant than those on a control diet (**Figure 1 B**).

Given the severity of effects of *Kcne2* deletion on glucose tolerance, we tested for hallmarks of T2DM in *Kcne2*^{-/-} mice. All other experiments in this study utilized adult mice fed regular mouse chow. Decreased skeletal muscle expression of insulin receptor β (IR β), and insulin receptor substrate 1 (IRS-1), is indicative of insulin resistance and characteristic of T2DM (32,33). Here, using western blotting analyses demonstrated that *Kcne2* deletion decreases IR β and IRS-1 expression twofold in skeletal muscle (**Figure 2**).

We also performed microarray analysis of the islet cell transcriptomes of *Kcne2*^{+/+} and *Kcne2*^{-/-} mice. From a total of 35556 gene transcripts, 1426 were found to be differentially expressed between female *Kcne2*^{-/-} and *Kcne2*^{+/+} mice using default filter criteria: fold change (linear) < -2 or > 2, and ANOVA p-value < 0.05. A total of 653 genes were up-regulated and 773 genes were down-regulated in *Kcne2*^{-/-} compared to *Kcne2*^{+/+} mice (**Figure 3**). The transcriptome changes in *Kcne2*^{-/-} mice were highly consistent with T2DM, and included altered expression of

T2DM markers, and gene expression changes indicative of islet cell proliferation, ER stress, increased ATP synthesis, and inflammation (**Figure 4**). Furthermore, pathway analysis of islet cell *Kcne2* deletion-associated DEG networks showed changes highly consistent with T2DM, including islet cell proliferation (networks associated with protein synthesis and metabolism; **Supplementary Figure 1**) and ER stress (EIF2 and EIF4 signaling pathways were the top two canonical signaling pathways activated; **Supplementary Figures 2 and 3**). In addition, gene networks associated with amyloid precursor protein (APP) and ERK signaling were notably altered in *Kcne2*^{-/-} mice (**Supplementary Figures 4 and 5**).

Kcne2 is expressed in pancreatic islets and its deletion impairs insulin secretion

We previously detected *Kcne2* transcript expression in mouse pancreas by real-time qPCR (27). Here, we discovered that pancreatic *Kcne2* transcript is expressed exclusively in mouse pancreas islet cells, and is undetectable in pancreatic non-islet cells (**Figure 5**). Crucially, germline *Kcne2* deletion resulted in dramatically impaired glucose-stimulated insulin secretion by β -cells freshly isolated from mouse pancreas. β -cells isolated from 3-5 month-old mice showed a *Kcne2* deletion-dependent 8-fold lower insulin secretion in response to 12 mM glucose, and lesser insulin secretion deficits at baseline and 4.5 mM glucose (**Figure 6**).

Kcne2 deletion impairs β -cell K^+ currents

Finally, we examined the effects of *Kcne2* deletion on freshly isolated β -cell K^+ currents, using whole-cell patch clamp. Peak outward current at +40 mV was 30% lower in β -cells isolated from 3-6 month-old *Kcne2*^{-/-} mice compared to those from age-matched *Kcne2*^{+/+} mice, but *Kcne2* deletion also produced a crossover of the IV relationships at -10 to -30 mV because of a left-shift in the voltage dependence of the K^+ current in this range (**Figure 7 A-B**). This left-shift, of about 10 mV, was also apparent from normalized tail current-voltage relationships (**Figure 7**

C). In β -cells isolated from 10-13 month-old mice, current densities were lower than in β -cells isolated from same-genotype 3-6 month-old mice, but *Kcne2* deletion had an even greater effect on peak K^+ current than in younger mice, diminishing it by 45% at +40 mV (**Figure 8 A, B**). *Kcne2* deletion in older mice again resulted in a left-shift of voltage dependence to whole-cell K^+ current, this time in the wider range of -10 to -80 mV (**Figure 8 B**). Interestingly, *Kcne2* deletion reduced the amount of current decay during depolarizing pulses, only in 10-13 month-old mice (**Figure 8 C**).

Discussion

KCNE2 is widely expressed in mammalian tissues and is associated with a variety of disease states in both humans and mice. The promiscuity of KCNE2 makes defining its exact physiological roles and the molecular etiology of its associated disease states quite challenging (26). Human KCNE2 polymorphisms within the coding region are associated with inherited and acquired (drug-induced) Long QT syndrome, with the primary mechanism probably being direct disruption of K⁺ currents generated by KCNE2 and various ventricular myocyte Kv channels with which it forms heteromeric complexes, the prime candidates being hERG and Kv4.2/3 (23,34,35,36,37). KCNE2 polymorphisms outside the coding region, and also one near the KCNE2 locus, are associated with atherosclerosis, early-onset myocardial infarction, and coronary artery disease (38,39,40). The precise mechanism for these associations is unclear, but we recently found that *Kcne2* deletion also causes atherosclerosis in mice, establishing causality (29). *Kcne2*^{-/-} mice also exhibit hypercholesterolemia, hypokalemia and non-alcoholic fatty liver disease (NAFLD), as part of a multisystem syndrome (27,28). Further, they exhibit increased susceptibility to stringent ischemia/reperfusion-induced sudden cardiac death (27), yet in cases of less stringent induced ischemia/reperfusion injury, they paradoxically exhibit less cardiac tissue damage, because of chronic upregulation of cardioprotective pathways involving GSK-3β inactivation (41).

The NAFLD in *Kcne2*^{-/-} mice arises at least in part from iron deficiency caused by achlorhydria, which in turn arises because KCNE2-KCNQ1 channels are required for normal function of the gastric parietal cell H⁺/K⁺-ATPase that acidifies the stomach lumen(28,30). In addition, KCNE2-KCNQ1 channels are required for efficient functioning of the sodium/iodide symporter in thyroid

epithelial cells; thus, *Kcne2* deletion also causes hypothyroidism in pregnant and lactating dams, and in their pups (42). By adulthood, non-gestating/lactating *Kcne2*^{-/-} mice are euthyroid but can begin to show further signs of hypothyroidism at advanced age (>1 year).

We also previously found that *Kcne2*^{-/-} mice are glucose-intolerant and deficient in regulating glucose levels after fasting (27), but we did not pursue the mechanism until now. Despite the wide range of tissue defects caused by *Kcne2* deletion, in the current study we have been able to establish that *Kcne2*^{-/-} mice become diabetic as young adults when on a western diet, and that *Kcne2* deletion causes a primary defect in β -cell insulin secretion, in mice fed regular mouse chow. Young adult *Kcne2*^{-/-} mice exhibit classic signs of T2DM, including the combination of impaired insulin secretion by the pancreas, and impaired insulin sensitivity of skeletal muscle, together contributing to glucose intolerance.

Microarray analysis of islet cells revealed that *Kcne2* deletion causes remodeling highly consistent with what is known of the molecular pathology of T2DM. We detected in *Kcne2*^{-/-} mice islet cells changes in the transcripts and/or signaling networks of a number of markers of T2DM, including cystatin C (43), vitronectin (44), keratin 8 (45), and APP (46) (**Figure 4 A and Supplementary Figure 4**). ER stress, transcriptomic signatures for which were prominent in the islet cells of *Kcne2*^{-/-} mice (**Figure 4B; Supplementary Figures 2 and 3**), results from glucolipotoxicity and is considered to be one of the main mechanisms underlying β -cell failure in T2DM (47,48,49,50). Detection of the EIF2 pathway as the predominant canonical signaling pathways altered in islet cells of *Kcne2*^{-/-} mice is highly consistent with its known role in islet cell ER stress and islet cell development, physiology and survival (51), and identification of EIF4 related signaling as the second-highest altered pathway is also of interest with respect to beta

cell function (52). Inflammation, also suggested by transcript expression changes in our microarray data (**Figure 4 C**) is another source of β -cell dysfunction in T2DM (53); the same applies to mitochondrial dysfunction (**Figure 4 D**) (49). Hyperproliferation, transcript changes associated with which we also detected in *Kcne2*^{-/-} islets (**Figure 4 E, Supplementary Figure 1**), is also characteristic of T2DM (54).

Further, we found that β -cells from young adult *Kcne2*^{-/-} mice exhibit a K⁺ current signature distinct from that of their wild-type littermates, with reduced peak currents at depolarized potentials but relatively more current at mildly negative potentials. Interestingly, we show for the first time, to our knowledge, that aging of mice (to 10-13 months) reduces β -cell K⁺ current density even in wild-type mice, and that this is further diminished in *Kcne2*^{-/-} mice.

The K⁺ current changes are suggestive of two events. First, we speculate that the reduced peak current at depolarized potentials arises from loss of KCNE2 from complexes with one or more of the various Kv channel α subunits that are both expressed in islet cells, and known to be upregulated by KCNE2. One possible candidate is Kv1.5, given that KCNE2 increases Kv1.5 activity 2-fold *in vitro*, *Kcne2* deletion decreases Kv1.5 current ~2-fold in mouse ventricular myocytes (23), and Kv1.5 is expressed in β -cells (55). Another less likely candidate would be Kv2.1, although we previously found that KCNE2 co-expression inhibits Kv2.1 *in vitro*, and reduces its inactivation (22), so this does not match with our β -cell data (which shows similar effects but for deletion of KCNE2, not addition). It is possible, that Kv2.1 forms complexes with, for example, Kv6.4 in β -cells, but these heteromers are not noticeably affected by KCNE2 *in vitro* (David JP et al Sci Rep 5:12813, 2015) and so this is also an unlikely explanation for the effects we observe in mouse pancreas..

Second, we suggest that the relative increase in K⁺ current at mildly hyperpolarized potentials arises at least partly from loss of KCNE2 from complexes with KCNQ1. Although co-assembly with KCNE2 converts KCNQ1 to a channel with left-shifted voltage dependence, able to remain constitutively open at resting membrane potentials, KCNE2 reduces KCNQ1 current magnitude 2-3-fold between -50 and 0 mV (24). KCNE2 co-expression *in vitro* also inhibits Kv2.1, as mentioned above, and so removal of this inhibition could also contribute; however, Kv2.1 activates ~10-20 mV more positively than KCNQ1 (in our hands), and so increased Kv2.1 current would not explain current increase in β -cells from *Kcne2*^{-/-} mice across the entire voltage range it is observed (-80 to -10 mV in 10-13-month-old adult mice). At this stage, the technical difficulties encountered in isolating sufficient β -cells, maintaining them in healthy condition, and recording from them, has limited the scope of our analyses to defining the changes in whole cell current associated with *Kcne2* deletion, but future analyses may involve identification of the specific Kv α subunits affected.

Previous studies showed that pharmacological inhibition of Kv1.5 or Kv2.1 increased insulin secretion and also diminished β -cell apoptosis (12). Likewise, inhibition of KCNQ1 with chromanol 293B enhanced glucose-stimulated insulin secretion in mice and in INS-1 cells (17,18). Germline deletion of *Kcnq1* in mice was previously found to enhance insulin sensitivity in the liver (56), but recently to not alter insulin secretion from pancreatic islets (57). However, *Kcnq1* deletion did impair glucose tolerance and reduce β -cell mass when parental origin of the null allele was taken into account, and was associated with paternal heterozygous transmission. This was deduced to arise from loss of imprinting control and associated epigenetic modification of neighboring gene *Cdkn1c*. This is because the *Kcnq1* gene is overlapped by the noncoding RNA KCNQ1 overlapping transcript (*Kcnq1ot1*) which regulates neighboring genes on the

paternal allele. For this reason, it has been very difficult to ascertain the mechanisms underlying the mechanisms by which KCNQ1 regulates pancreatic function and diabetes, via its role as an ion channel or otherwise.

Our finding that *Kcne2* deletion impairs insulin secretion and insulin sensitivity tallies well with a role for KCNE2-KCNQ1 complexes in regulating insulin secretion, as by enhancing KCNQ1 currents in the moderately hyperpolarized range, we would be predicted to obtain results opposite to pharmacological inhibition of KCNQ1, which we did. If a role for KCNE2-KCNQ1 complexes in regulation of insulin secretion is further supported in future studies, it could have important implications for new therapeutic avenues, and for avoidance of side-effects if targeting KCNQ1 channels in other tissues, given that each KCNE isoform lends specific attributes to KCNQ1 pharmacology (58,59,60). Interestingly, I_{Ks} channels, formed by KCNQ1 and KCNE1, are activated by increased intracellular ATP, independent of the augmenting effects of PIP_2 on KCNQ1 (61). This effect is opposite to that of K_{ATP} channels, which are inhibited by ATP to trigger the cascade of events that induces insulin secretion. Therefore, we hypothesize that KCNE2-KCNQ1 channels in β -cells could provide a brake to prevent excessive insulin secretion and help return β -cells to resting membrane potential. By deleting *Kcne2*, we may have increased the activity of this brake at mildly negative potentials, to the extent that insulin secretion is impaired. This hypothesis would also fit with previous findings that inhibition of KCNQ1 increases insulin secretion (18), and that overexpression of KCNQ1 in the MIN6 β -cell line impairs insulin secretion (62).

Figures

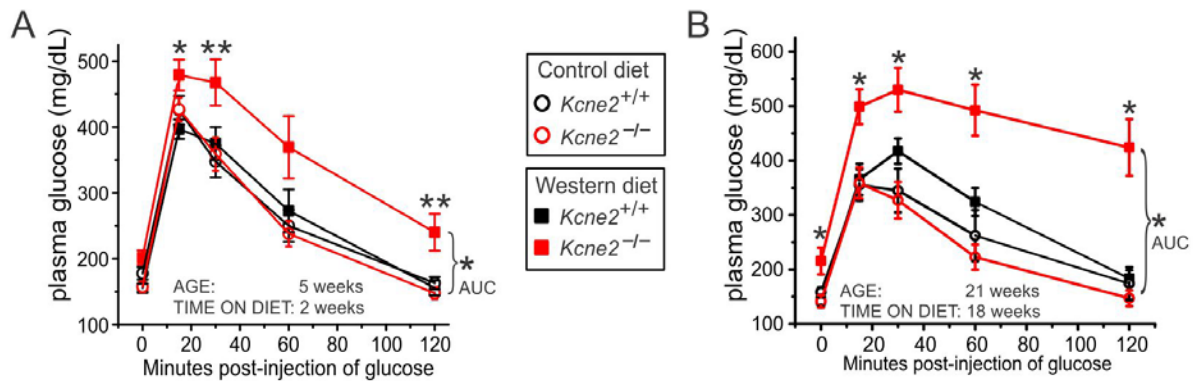


Figure 1. *Kcne2* deletion causes western diet-exacerbated glucose intolerance

Glucose tolerance tests in 5-week-old pups fed a control or western diet for 2 weeks. * $P < 0.05$; ** $P < 0.01$, for western diet-fed *Kcne2*^{-/-} mice compared to all other groups. AUC (Area Under the Curve) by ANOVA. Values are expressed as mean \pm SEM; $n = 14-18$ per group (A).

Glucose tolerance tests in 21-week-old mice fed a control or western diet for 18 weeks. * $P < 0.05$; ** $P < 0.01$, by ANOVA, for western diet-fed *Kcne2*^{-/-} mice compared to all other groups. Values are expressed as mean \pm SEM; $n = 8-11$ per group (B).

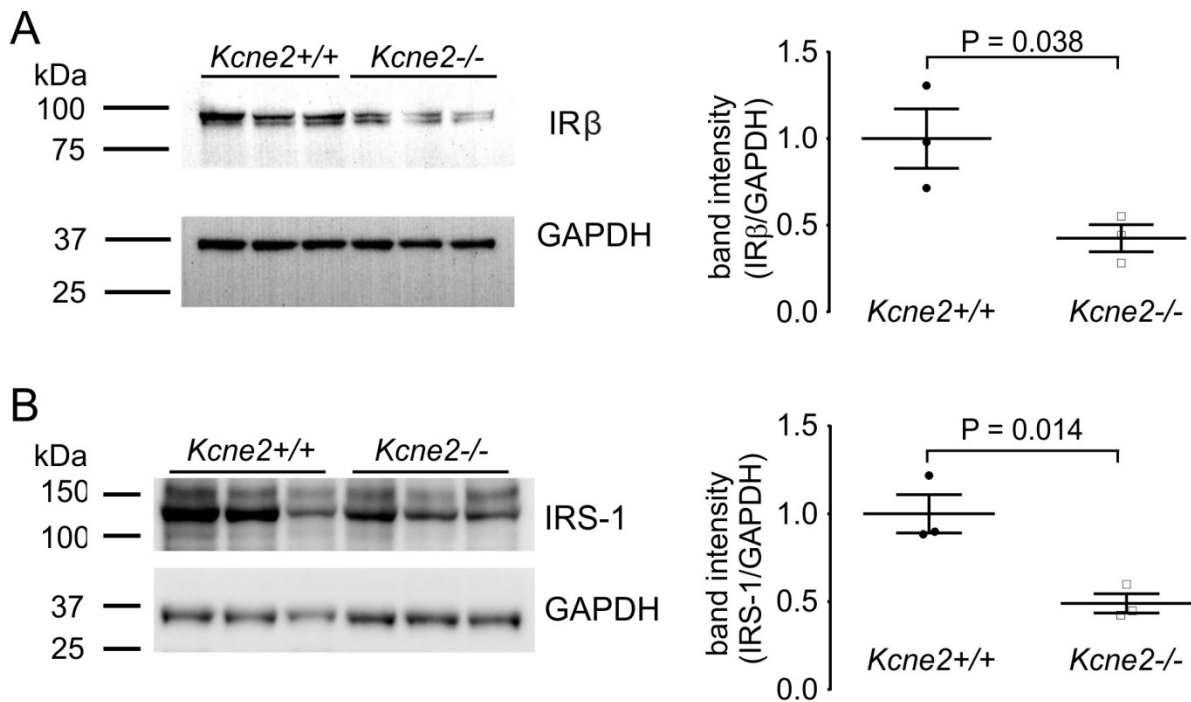


Figure 2. *Kcne2* deletion reduces expression of insulin receptor β and insulin receptor substrate-1 in skeletal muscle.

Left panels, western blots of *Kcne2*^{+/+} ($n = 3$) and *Kcne2*^{-/-} ($n = 3$) mice skeletal muscle lysates showing expression of (A) insulin receptor β (IR β) and (B) insulin receptor substrate 1 (IRS-1), and glyceraldehyde-3-phosphate dehydrogenase (GAPDH) as a loading control (each lane using lysate from a different mouse). *Right panels*, mean GAPDH-normalized band intensities quantified from blots on left. Error bars represent SEM. P values are for 2-tailed, unpaired t-tests for inter-genotype comparisons.

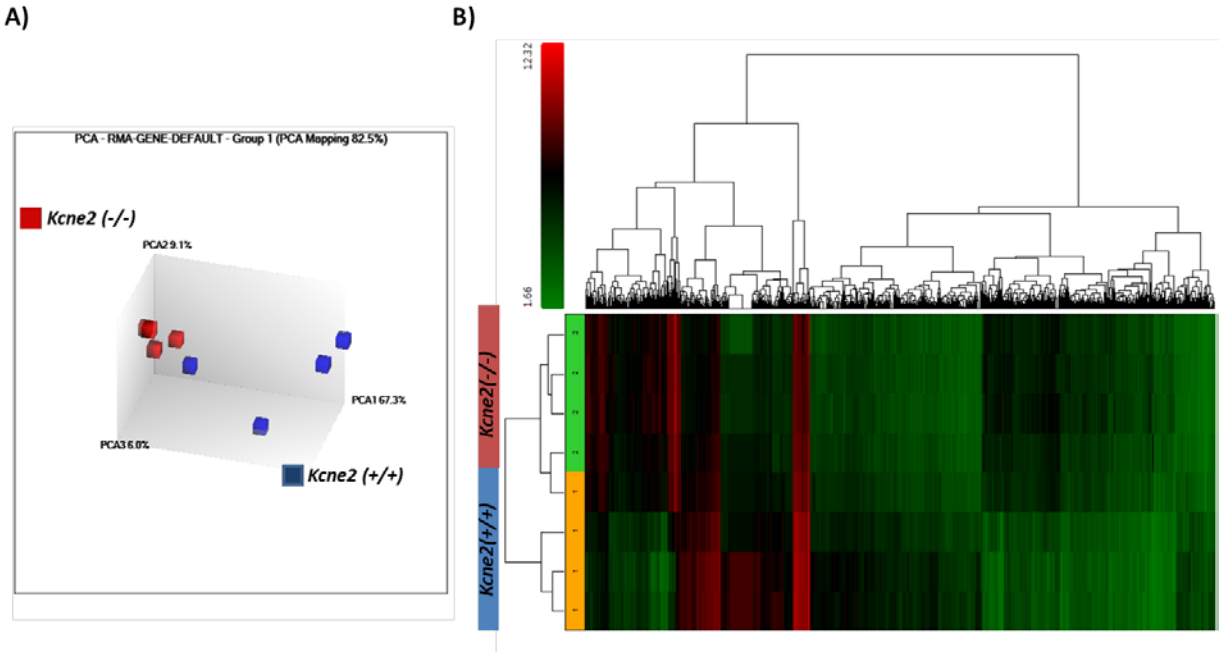


Figure 3. Whole-transcript microarray of islet cells from 5~6-month-old *Kcne2*^{+/+} and *Kcne2*^{-/-} mice. A) Principle component analysis (PCA); B) heat map display of global transcript expression differences, after microarray analysis of the pancreas islet transcriptomes of *Kcne2*^{+/+} (*n* = 4) and *Kcne2*^{-/-} (*n* = 4) mice.

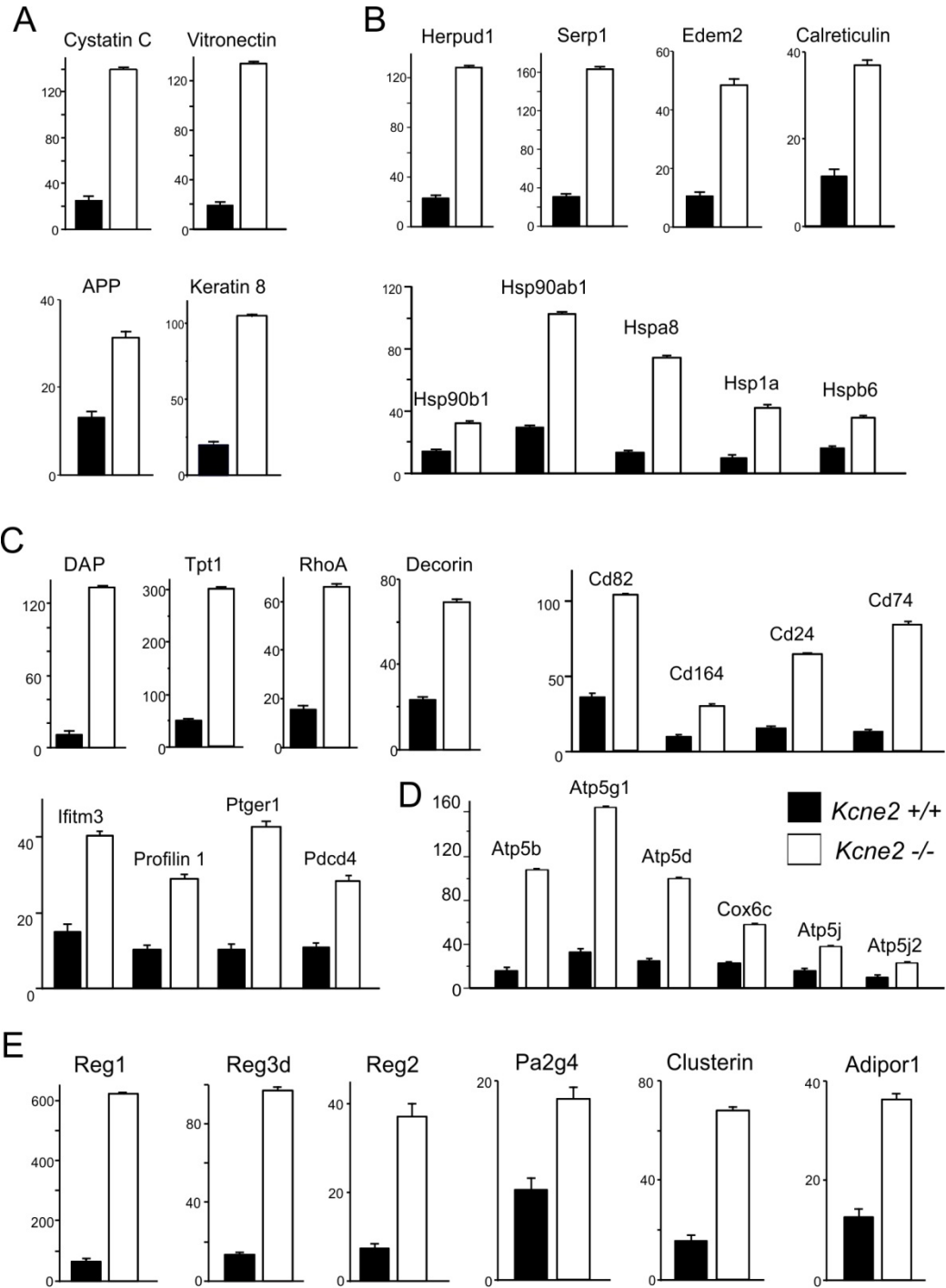


Figure 4. *Kcne2* deletion causes concerted islet cell transcriptomic changes characteristic of T2DM.

Graphs show Tukey's Biweight signals of differentially expressed genes (DEGs) (quantified by microarray analysis, all changes show reached the $P < 0.05$ significance level, $n = 4$ mice per group) in islet cells isolated from 6 month-old *Kcne2*^{+/+} (solid columns) and *Kcne2*^{-/-} mice (open columns).

A. *Kcne2* deletion alters expression of known T2DM marker genes. **APP**: amyloid β precursor protein.

B. *Kcne2* deletion causes transcript expression changes consistent with islet ER stress.

Herpud1: homocysteine-inducible, endoplasmic reticulum stress-inducible, ubiquitin-like domain member 1, **Serp1**: stress-associated endoplasmic reticulum protein 1, **Edem2**: ER degradation enhancer, mannosidase alpha-like 2, **Hsp90b1**: heat shock protein 90, β (Grp94), member 1, **Hsp90ab1**: heat shock protein 90 alpha (cytosolic), class B member 1, **Hspa8**: heat shock protein 8, **Hspa1a**: heat shock protein 1A, **Hspb6**: heat shock protein, alpha-crystallin-related, B6

C. *Kcne2* deletion causes transcript expression changes consistent with islet inflammation.

DAP: death-associated protein, **Tpt1**: tumor protein, translationally-controlled 1, **RhoA**: ras homolog gene family, member A, **Ifitm3**: interferon induced transmembrane protein 3, **Ptger1**: prostaglandin E receptor 1, **Pdcd4**: programmed cell death 4.

D. *Kcne2* deletion increases islet expression of mitochondrial ATP synthesis-related genes.

Atp5b: ATP synthase, H⁺ transporting mitochondrial F1 complex, β subunit, **Atp5g1**: ATP synthase, H⁺ transporting, mitochondrial F0 complex, subunit c1 (subunit 9), **Atp5d**: ATP synthase, H⁺ transporting, mitochondrial F1 complex, delta subunit, **Cox6c**: cytochrome c oxidase, subunit Vic, **Atp5j**: ATP synthase, H⁺ transporting, mitochondrial F0 complex, subunit F, **Atp5j2**: ATP synthase, H⁺ transporting, mitochondrial F0 complex, subunit F2.

E. *Kcne2* deletion increases expression of proliferation-related genes in islets. **Reg1**: regenerating islet-derived 1, **Reg3d**: regenerating islet-derived 3 delta, **Reg2**: regenerating islet-derived 2, **Pa2g4**: proliferation-associated 2G4, **Adipor1**: adiponectin receptor 1.

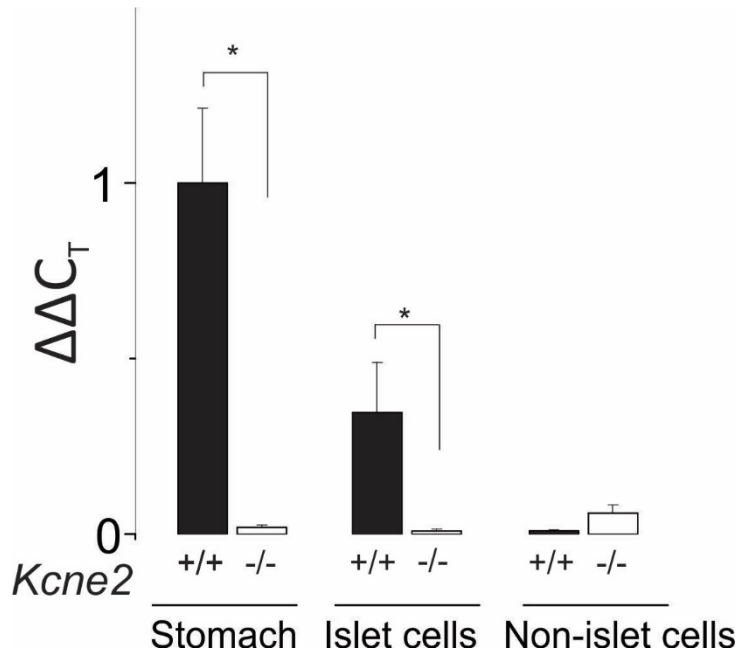


Figure 5. *Kcne2* location in mouse pancreas.

Kcne2 transcript was detected by real-time qPCR in *Kcne2*^{+/+} but not *Kcne2*^{-/-} mouse pancreas islet cells, and was not detectable in non-islet cells. Stomach tissue data are shown for comparison. Data are means of $n = 6$ independent measurements per group. Each independent measurement was itself a mean of triplicate quantifications from cells isolated from 4 mice and pooled (total of 24 mice used per group).

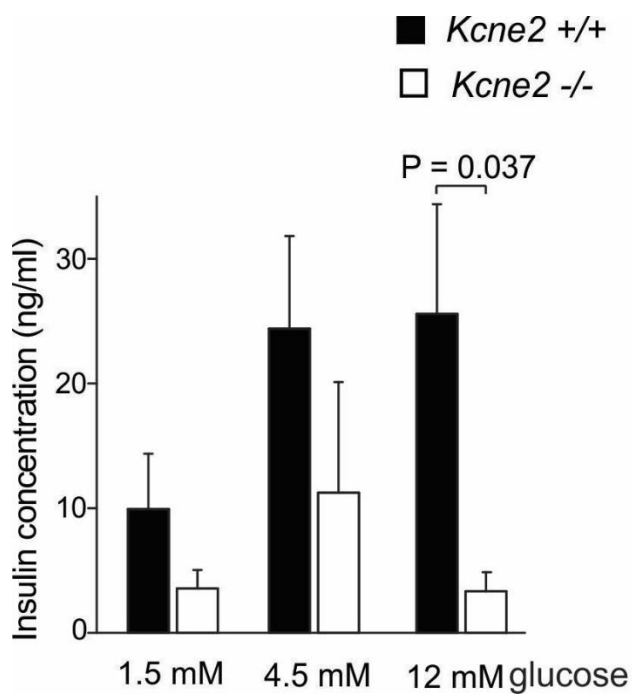


Figure 6. *Kcne2* deletion impairs glucose-stimulated insulin secretion by isolated β -cells.

Mean insulin secretion from islet β -cells were incubated in buffer containing 1.5, 4.5, or 12 mM D-glucose from 3-4 month-old *Kcne2*^{+/+} and *Kcne2*^{-/-} mice ($n = 5$ mice per genotype). Error bars indicate SEM. P values are for 2-tailed, unpaired t-tests for inter-genotype comparisons.

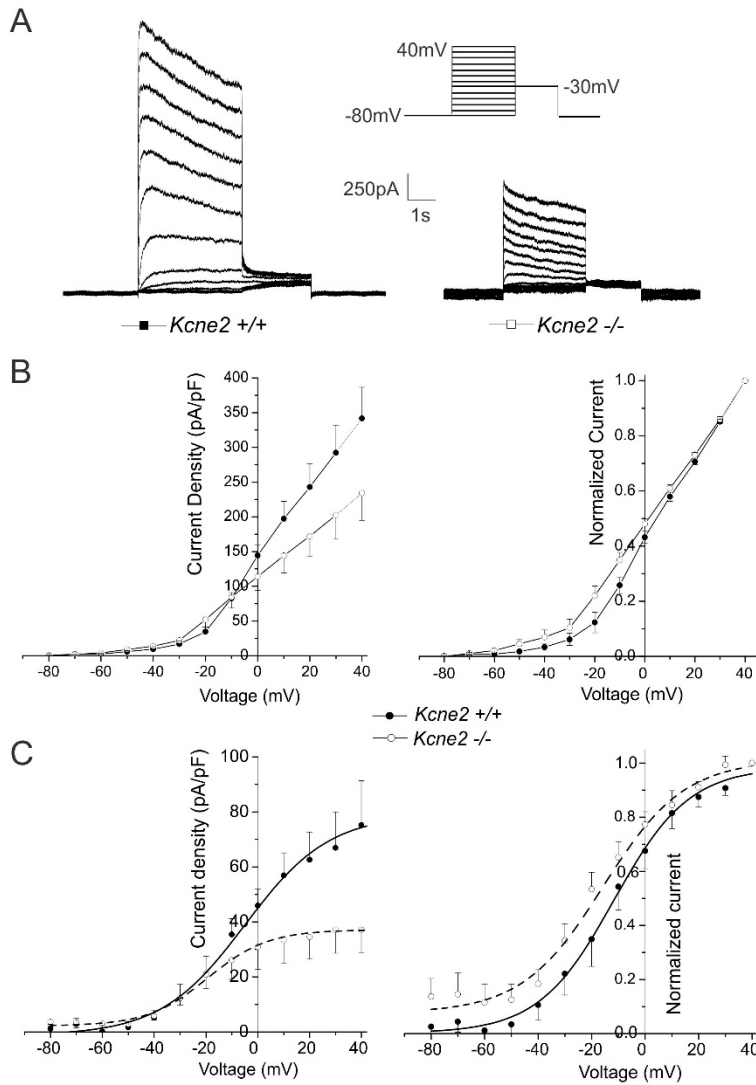


Figure 7. *Kcne2* deletion diminishes delayed rectifier K^+ currents in β -cells isolated from young adult mice.

A. Exemplar current traces recorded in response to depolarization in 10 mV increments from -80 mV to +40 mV in islet β -cells from 3-5 month-old *Kcne2*^{+/+} ($n = 9$) and *Kcne2*^{-/-} ($n = 8$) mice.

B. Mean raw current-voltage relationship (*left*) and normalized current-voltage relationship (*right*) from cells as in panel A ($n = 8-9$ cells from 4 mice). Error bars indicate SEM.

C. Mean raw (*left*) and normalized (*right*) -30 mV tail current versus prepulse voltage relationship for cells as in panel A. ($n = 8-9$ cells from 4 mice). Error bars indicate SEM.

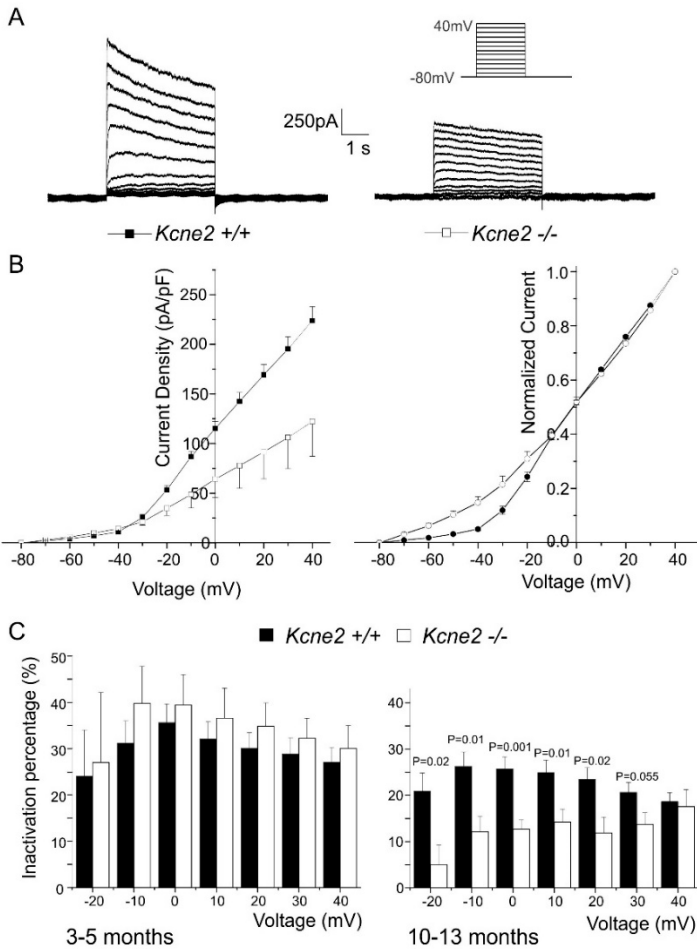
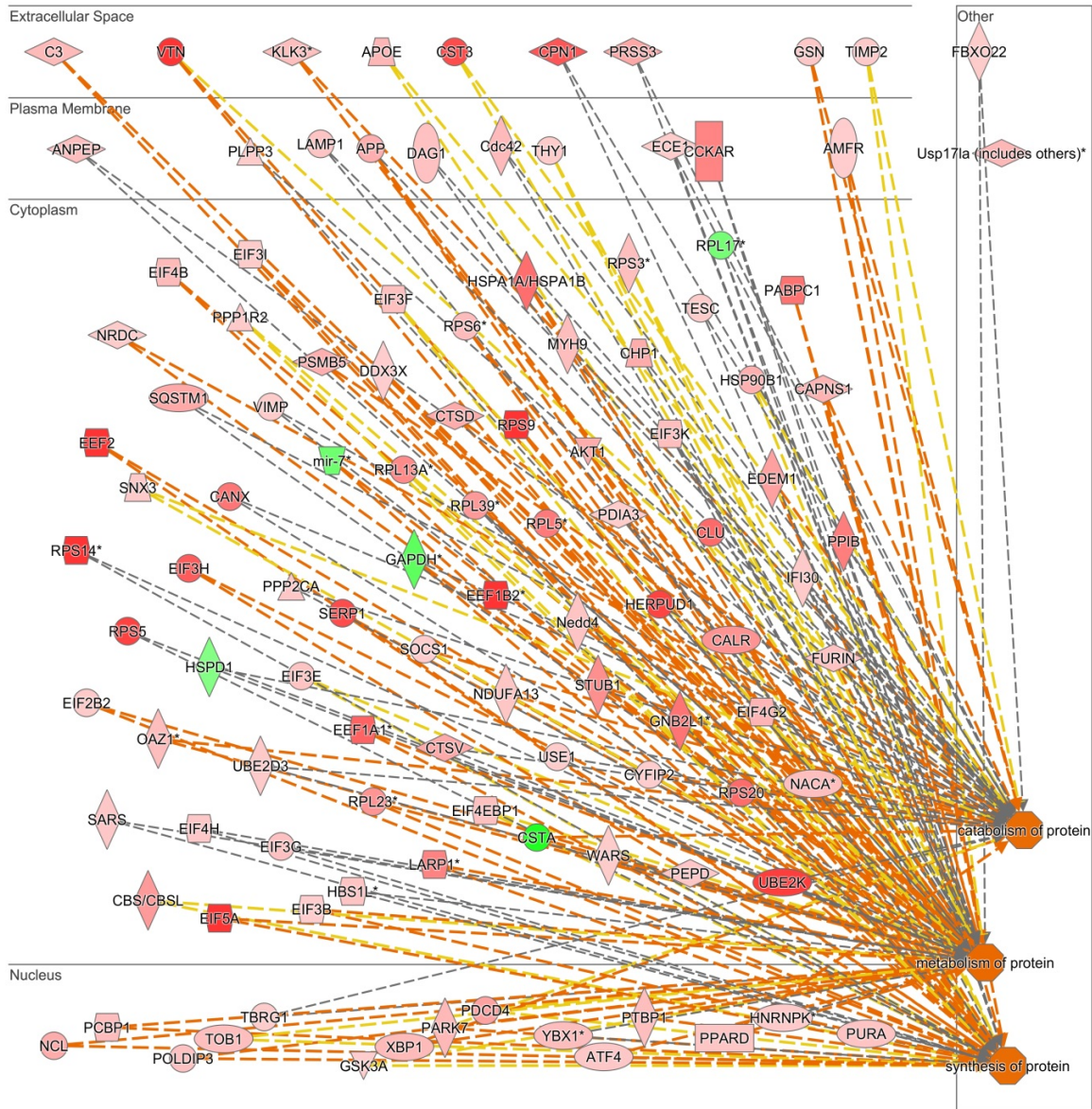


Figure 8. Aging and *Kcne2* deletion diminish delayed rectifier K^+ currents in β -cells isolated from older adult mice.

A. Exemplar current traces recorded in response to depolarization in 10 mV increments from -80mV to +40mV in islet β -cells from 10-13 month-old *Kcne2*^{+/+} ($n = 15$) and *Kcne2*^{-/-} ($n = 7$) mice.

B. Mean raw current-voltage relationship (*left*) and normalized current-voltage relationship (*right*) from cells as in panel A ($n = 7-15$ cells from 4 mice). Error bars indicate SEM.



























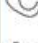

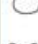










C. Mean % decay (inactivation) over 4 seconds of K^+ currents recorded as in panel A from (left) 3-5 month-old and (right) 10-13 month-old *Kcne2*^{+/+} and *Kcne2*^{-/-} mice ($n = 7-15$ cells from 4 mice). P values are for 2-tailed, unpaired t-tests for inter-genotype comparisons.



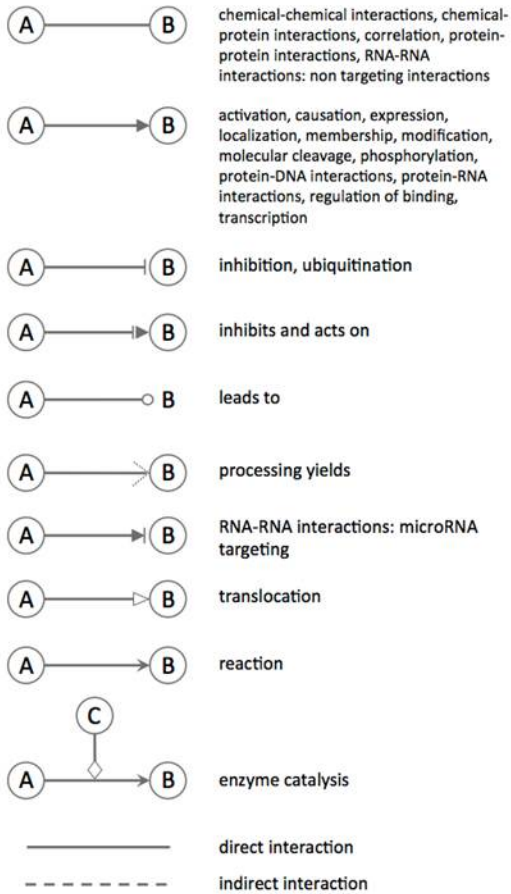
© 2000-2016 QIAGEN. All rights reserved.

Supplementary Figure 1. The top 3 biological processes altered by *Kcne2* deletion in islet cells. The 3 processes identified by pathway analysis of microarray data as containing the greatest net change in transcript expression were catabolism, metabolism, and synthesis of protein.

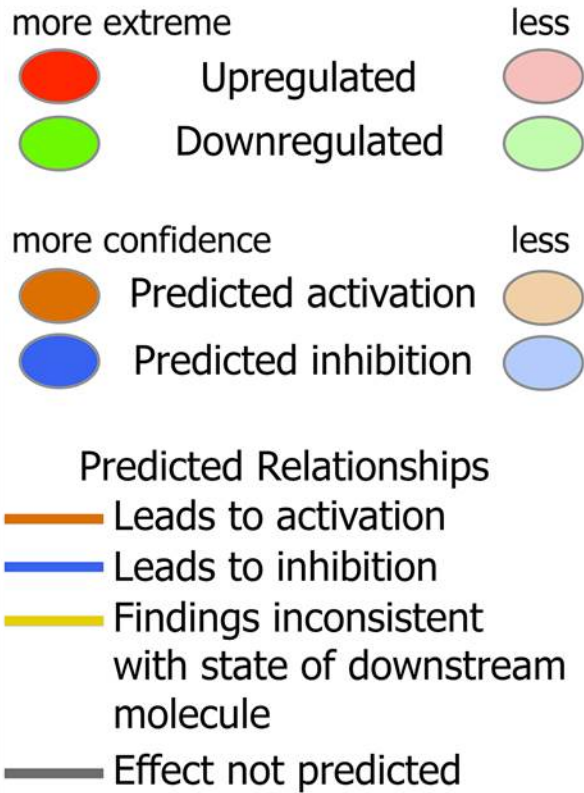
Molecule Shapes

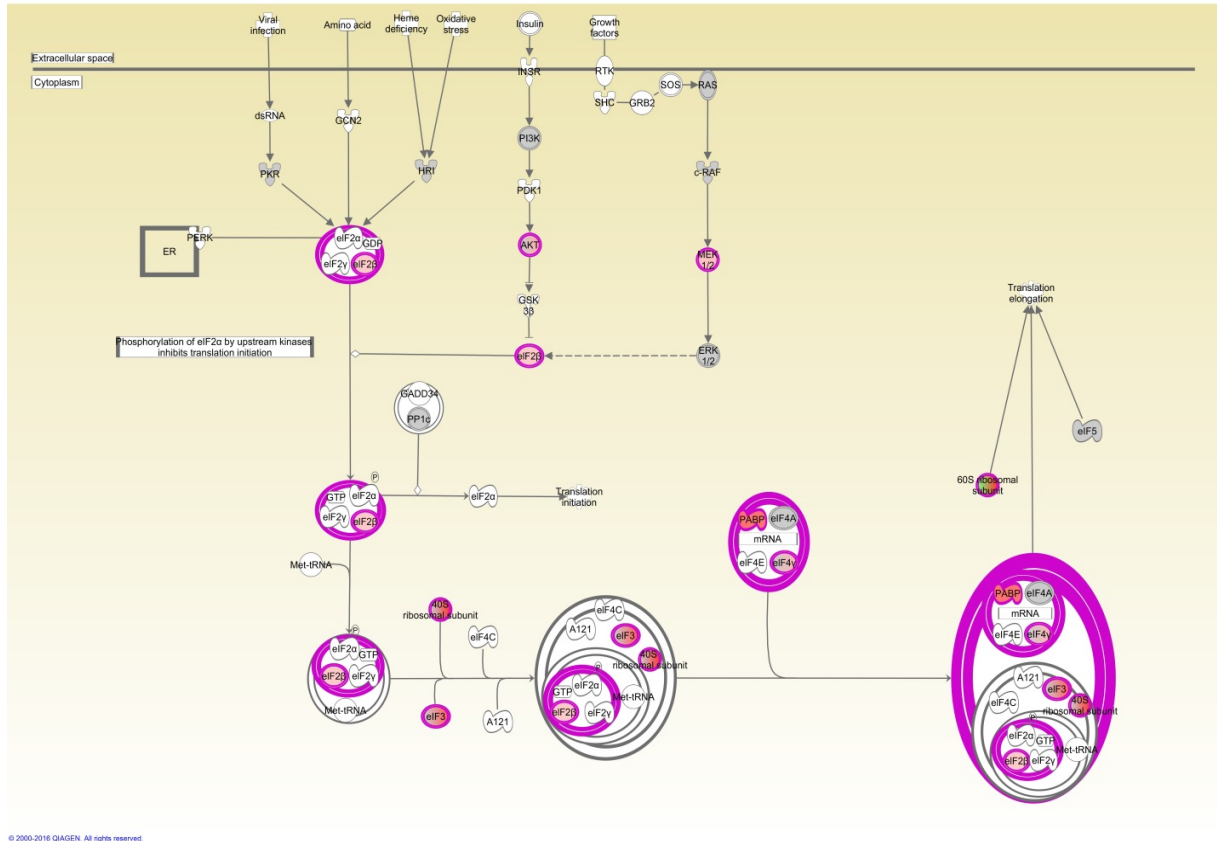
Path Designer Shapes	Network Shapes
 Complex/Group/Other	 Complex/Group
 Chemical/Toxicant	 Chemical/Drug/Toxicant
 Cytokine/Growth Factor	 Cytokine
 Disease	 Disease
 Drug	 Enzyme
 Enzyme	 Function
 Function	 G-protein Coupled Receptor
 G-protein Coupled Receptor	 Growth Factor
 Ion Channel	 Ion Channel
 Kinase	 Kinase
 Ligand-dependent Nuclear Receptor	 Ligand-dependent Nuclear Receptor
 Mature microRNA	 Mature microRNA
 microRNA	 microRNA
 Peptidase	 Other
 Phosphatase	 Peptidase
 Transcription Regulator	 Phosphatase
 Translation Regulator	 Transcription Regulator
 Transmembrane Receptor	 Translation Regulator
 Transporter	 Transmembrane Receptor
	 Transporter

Relationships



Prediction Legend

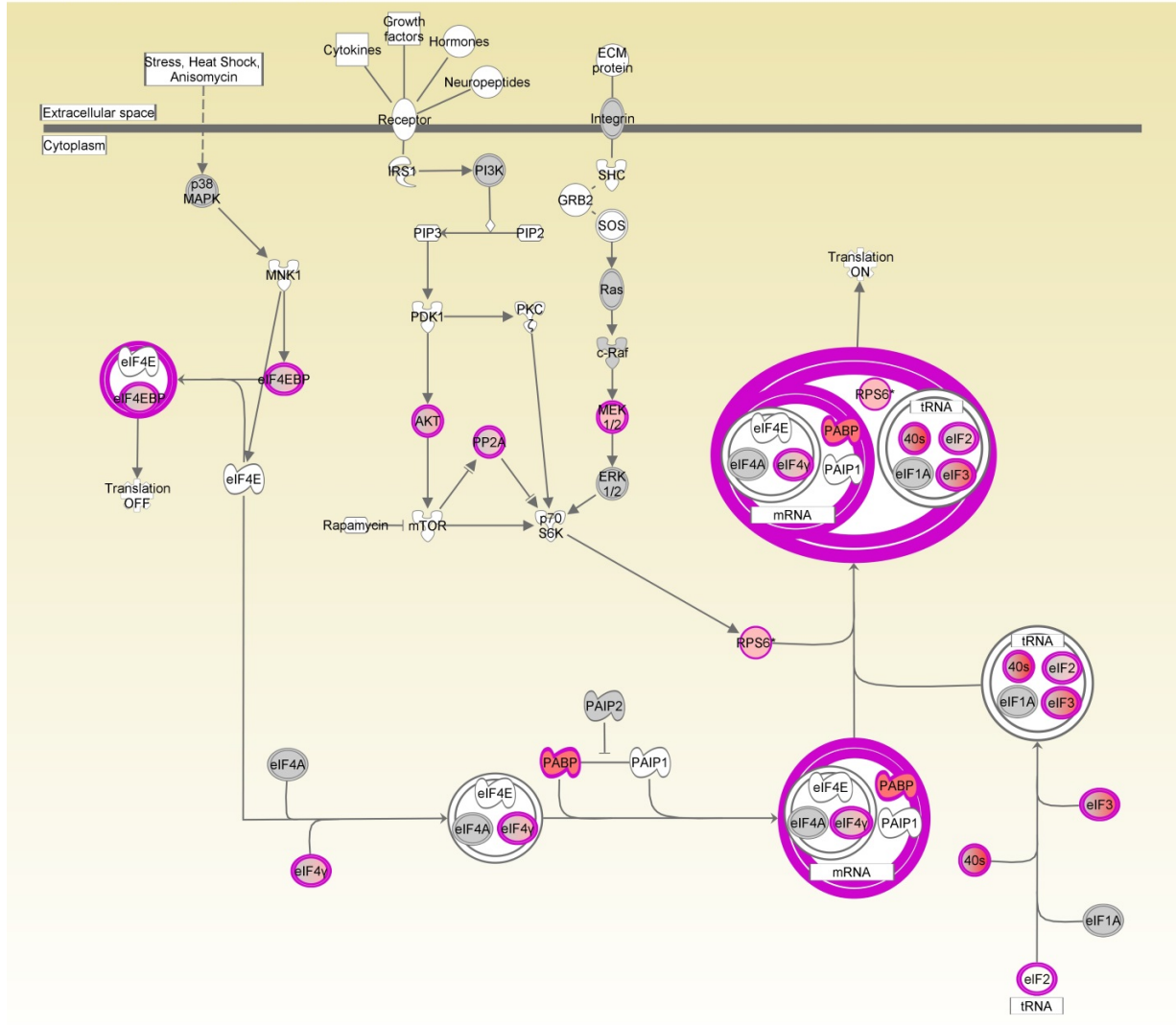




© 2000-2016 QIAGEN. All rights reserved.

Supplementary Figure 2. *Kcne2* deletion activates EIF2 signaling pathway in islet cells.

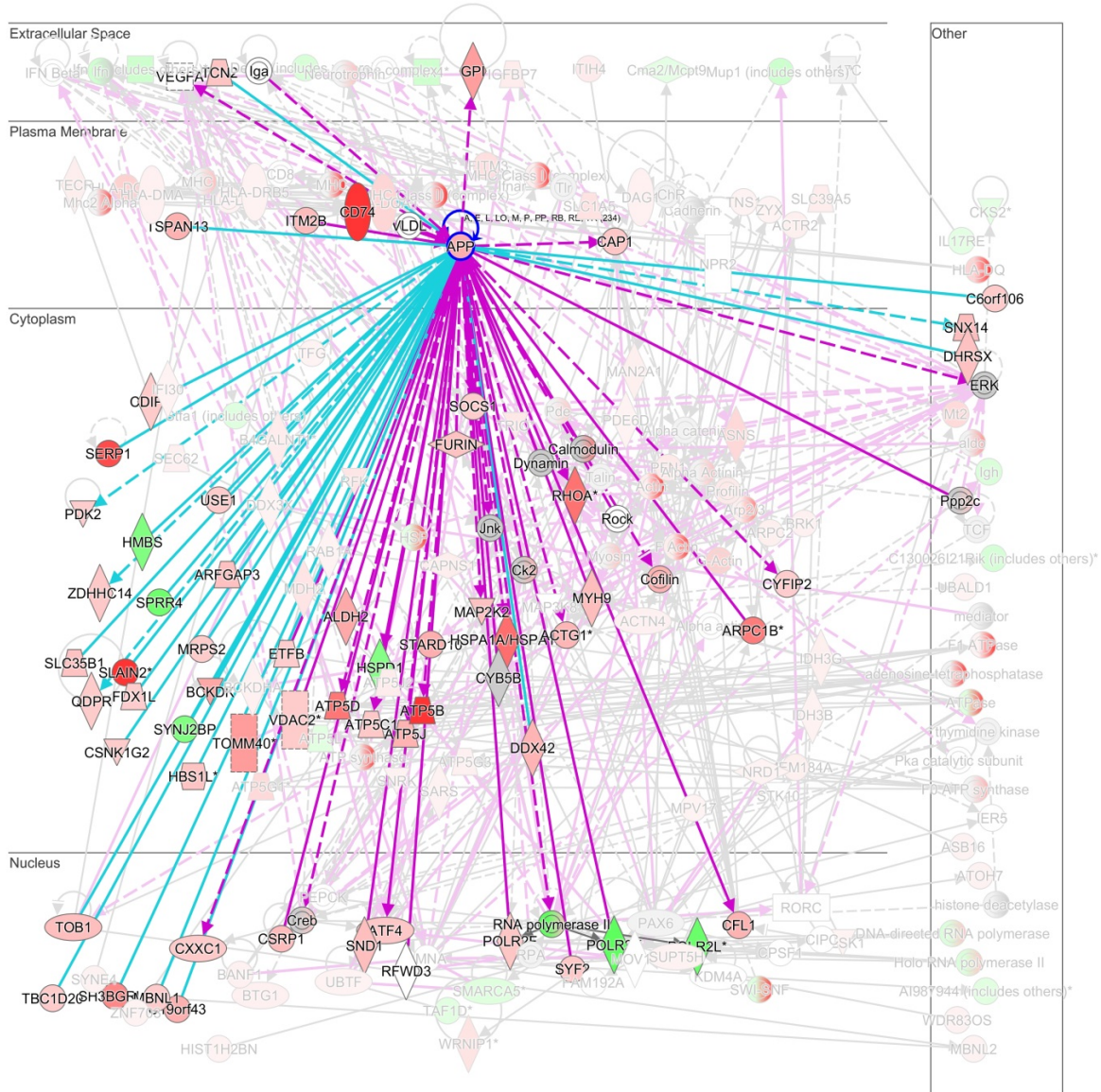
The EIF2 signaling pathway, which is activated during ER stress, was the top canonical pathway (by z-score) activated by *Kcne2* deletion in mouse islet cells, identified by pathway analysis of microarray data. Magenta lines surround affected parts of the pathway; colors within gene-labeled symbols reflect degree of activation (red indicates highest upregulation; green indicates highest downregulation).



© 2000-2016 QIAGEN. All rights reserved.

Supplementary Figure 3. *Kcne2* deletion activates EIF4 signaling pathway in islet cells.

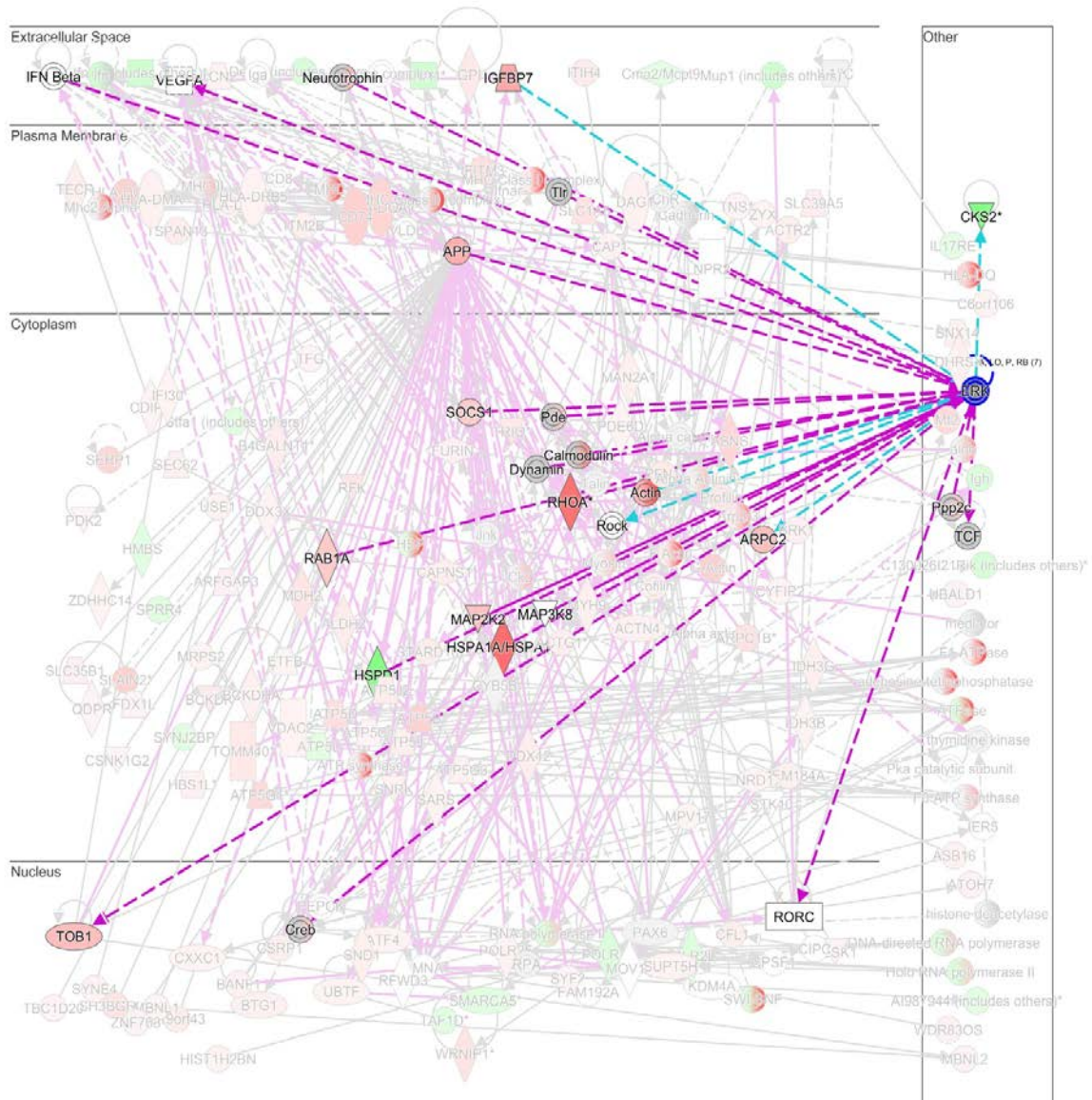
The EIF4 signaling pathway, which is activated during ER stress, was the second highest (by z-score) canonical pathway activated by *Kcne2* deletion in mouse islet cells, identified by pathway analysis of microarray data. Magenta lines surround affected parts of the pathway; colors within gene-labeled symbols reflect degree of activation (red indicates highest upregulation; green indicates highest downregulation).



© 2000-2016 QIAGEN. All rights reserved.

Supplementary Figure 4. *Kcne2* deletion alters the APP signaling network in islet cells.

Pathway analysis revealed one super-network of 6 connected networks, shown here. The DEG with the most connections within the 6 networks was amyloid precursor protein (APP), highlighted. Solid lines, direct interactions; dashed lines, indirect interactions.



© 2000-2016 QIAGEN. All rights reserved.

Supplementary Figure 5. *Kcne2* deletion alters the ERK signaling pathway in islet cells.

Pathway analysis revealed one super-network of 6 connected networks, shown here. The DEG with the second-most connections within the 6 networks was ERK, highlighted. Solid lines, direct interactions; dashed lines, indirect interactions.

References

- 1 DeFronzo, R. A. & Ferrannini, E. Insulin resistance. A multifaceted syndrome responsible for NIDDM, obesity, hypertension, dyslipidemia, and atherosclerotic cardiovascular disease. *Diabetes care* **14**, 173-194 (1991).
- 2 Unoki, H. *et al.* SNPs in KCNQ1 are associated with susceptibility to type 2 diabetes in East Asian and European populations. *Nature genetics* **40**, 1098-1102, doi:10.1038/ng.208 (2008).
- 3 Yasuda, K. *et al.* Variants in KCNQ1 are associated with susceptibility to type 2 diabetes mellitus. *Nature genetics* **40**, 1092-1097, doi:10.1038/ng.207 (2008).
- 4 Virkamaki, A., Ueki, K. & Kahn, C. R. Protein-protein interaction in insulin signaling and the molecular mechanisms of insulin resistance. *The Journal of clinical investigation* **103**, 931-943, doi:10.1172/JCI6609 (1999).
- 5 Warram, J. H., Martin, B. C., Krolewski, A. S., Soeldner, J. S. & Kahn, C. R. Slow glucose removal rate and hyperinsulinemia precede the development of type II diabetes in the offspring of diabetic parents. *Annals of internal medicine* **113**, 909-915 (1990).
- 6 Olefsky, J. M. & Nolan, J. J. Insulin resistance and non-insulin-dependent diabetes mellitus: cellular and molecular mechanisms. *The American journal of clinical nutrition* **61**, 980S-986S (1995).
- 7 Chiasson, J. L. & Rabasa-Lhoret, R. Prevention of type 2 diabetes: insulin resistance and beta-cell function. *Diabetes* **53 Suppl 3**, S34-38 (2004).
- 8 Gerich, J. E. Is insulin resistance the principal cause of type 2 diabetes? *Diabetes, obesity & metabolism* **1**, 257-263 (1999).

- 9 Tucker, S. J., Gribble, F. M., Zhao, C., Trapp, S. & Ashcroft, F. M. Truncation of Kir6.2 produces ATP-sensitive K⁺ channels in the absence of the sulphonylurea receptor. *Nature* **387**, 179-183, doi:10.1038/387179a0 (1997).
- 10 Nichols, C. G. & Koster, J. C. Diabetes and insulin secretion: whither KATP? *American journal of physiology. Endocrinology and metabolism* **283**, E403-412, doi:10.1152/ajpendo.00168.2002 (2002).
- 11 Tarasov, A. I. *et al.* A Kir6.2 mutation causing neonatal diabetes impairs electrical activity and insulin secretion from INS-1 beta-cells. *Diabetes* **55**, 3075-3082, doi:10.2337/db06-0637 (2006).
- 12 Su, J., Yu, H., Lenka, N., Hescheler, J. & Ullrich, S. The expression and regulation of depolarization-activated K⁺ channels in the insulin-secreting cell line INS-1. *Pflugers Archiv : European journal of physiology* **442**, 49-56 (2001).
- 13 Dai, X. Q. *et al.* The voltage-dependent potassium channel subunit Kv2.1 regulates insulin secretion from rodent and human islets independently of its electrical function. *Diabetologia* **55**, 1709-1720, doi:10.1007/s00125-012-2512-6 (2012).
- 14 Leung, Y. M. *et al.* Syntaxin 1A binds to the cytoplasmic C terminus of Kv2.1 to regulate channel gating and trafficking. *The Journal of biological chemistry* **278**, 17532-17538, doi:10.1074/jbc.M213088200 (2003).
- 15 MacDonald, P. E. *et al.* Synaptosome-associated protein of 25 kilodaltons modulates Kv2.1 voltage-dependent K⁽⁺⁾ channels in neuroendocrine islet beta-cells through an interaction with the channel N terminus. *Mol Endocrinol* **16**, 2452-2461, doi:10.1210/me.2002-0058 (2002).
- 16 Li, X. N. *et al.* The role of voltage-gated potassium channels Kv2.1 and Kv2.2 in the regulation of insulin and somatostatin release from pancreatic islets. *The Journal of pharmacology and experimental therapeutics* **344**, 407-416, doi:10.1124/jpet.112.199083 (2013).

- 17 Ullrich, S. *et al.* Effects of I(Ks) channel inhibitors in insulin-secreting INS-1 cells. *Pflugers Archiv : European journal of physiology* **451**, 428-436, doi:10.1007/s00424-005-1479-2 (2005).
- 18 Liu, L., Wang, F., Lu, H., Ren, X. & Zou, J. Chromanol 293B, an inhibitor of KCNQ1 channels, enhances glucose-stimulated insulin secretion and increases glucagon-like peptide-1 level in mice. *Islets* **6**, e962386, doi:10.4161/19382014.2014.962386 (2014).
- 19 Kanda, V. A., Lewis, A., Xu, X. & Abbott, G. W. KCNE1 and KCNE2 provide a checkpoint governing voltage-gated potassium channel alpha-subunit composition. *Biophysical journal* **101**, 1364-1375, doi:10.1016/j.bpj.2011.08.014 (2011).
- 20 Kanda, V. A., Lewis, A., Xu, X. & Abbott, G. W. KCNE1 and KCNE2 inhibit forward trafficking of homomeric N-type voltage-gated potassium channels. *Biophysical journal* **101**, 1354-1363, doi:10.1016/j.bpj.2011.08.015 (2011).
- 21 Lewis, A., McCrossan, Z. A. & Abbott, G. W. MinK, MiRP1, and MiRP2 diversify Kv3.1 and Kv3.2 potassium channel gating. *The Journal of biological chemistry* **279**, 7884-7892, doi:10.1074/jbc.M310501200 (2004).
- 22 McCrossan, Z. A., Roepke, T. K., Lewis, A., Panaghie, G. & Abbott, G. W. Regulation of the Kv2.1 potassium channel by MinK and MiRP1. *The Journal of membrane biology* **228**, 1-14, doi:10.1007/s00232-009-9154-8 (2009).
- 23 Roepke, T. K. *et al.* Targeted deletion of *kcne2* impairs ventricular repolarization via disruption of I(K,slow1) and I(to,f). *The FASEB journal : official publication of the Federation of American Societies for Experimental Biology* **22**, 3648-3660, doi:10.1096/fj.08-110171 (2008).
- 24 Tinel, N., Diochot, S., Borsotto, M., Lazdunski, M. & Barhanin, J. KCNE2 confers background current characteristics to the cardiac KCNQ1 potassium channel. *The EMBO journal* **19**, 6326-6330, doi:10.1093/emboj/19.23.6326 (2000).

- 25 Abbott, G. W. KCNE2 and the K (+) channel: The tail wagging the dog. *Channels (Austin)* **6** (2012).
- 26 Abbott, G. W. The KCNE2 K(+) channel regulatory subunit: Ubiquitous influence, complex pathobiology. *Gene* **569**, 162-172, doi:10.1016/j.gene.2015.06.061 (2015).
- 27 Hu, Z. *et al.* Kcne2 deletion creates a multisystem syndrome predisposing to sudden cardiac death. *Circulation. Cardiovascular genetics* **7**, 33-42, doi:10.1161/CIRCGENETICS.113.000315 (2014).
- 28 Lee, S. M. *et al.* Kcne2 deletion causes early-onset nonalcoholic fatty liver disease via iron deficiency anemia. *Scientific Reports* **6**, 23118, doi:10.1038/srep23118 (2016).
- 29 Lee, S. M., Nguyen, D., Hu, Z. & Abbott, G. W. Kcne2 deletion promotes atherosclerosis and diet-dependent sudden death. *Journal of molecular and cellular cardiology* **87**, 148-151, doi:10.1016/j.yjmcc.2015.08.013 (2015).
- 30 Roepke, T. K. *et al.* The KCNE2 potassium channel ancillary subunit is essential for gastric acid secretion. *The Journal of biological chemistry* **281**, 23740-23747, doi:10.1074/jbc.M604155200 (2006).
- 31 Li, D. S., Yuan, Y. H., Tu, H. J., Liang, Q. L. & Dai, L. J. A protocol for islet isolation from mouse pancreas. *Nature protocols* **4**, 1649-1652, doi:10.1038/nprot.2009.150 (2009).
- 32 Caro, J. F. *et al.* Insulin receptor kinase in human skeletal muscle from obese subjects with and without noninsulin dependent diabetes. *The Journal of clinical investigation* **79**, 1330-1337, doi:10.1172/JCI112958 (1987).
- 33 Kerouz, N. J., Horsch, D., Pons, S. & Kahn, C. R. Differential regulation of insulin receptor substrates-1 and -2 (IRS-1 and IRS-2) and phosphatidylinositol 3-kinase isoforms in liver and muscle of the obese diabetic (ob/ob) mouse. *The Journal of clinical investigation* **100**, 3164-3172, doi:10.1172/JCI119872 (1997).
- 34 Abbott, G. W. *et al.* MiRP1 forms IKr potassium channels with HERG and is associated with cardiac arrhythmia. *Cell* **97**, 175-187 (1999).

- 35 Zhang, M., Jiang, M. & Tseng, G. N. minK-related peptide 1 associates with Kv4.2 and modulates its gating function: potential role as beta subunit of cardiac transient outward channel? *Circulation research* **88**, 1012-1019 (2001).
- 36 Isbrandt, D. *et al.* Identification and functional characterization of a novel KCNE2 (MiRP1) mutation that alters HERG channel kinetics. *J Mol Med (Berl)* **80**, 524-532, doi:10.1007/s00109-002-0364-0 (2002).
- 37 Gordon, E. *et al.* A KCNE2 mutation in a patient with cardiac arrhythmia induced by auditory stimuli and serum electrolyte imbalance. *Cardiovascular research* **77**, 98-106, doi:10.1093/cvr/cvm030 (2008).
- 38 Kathiresan, S. *et al.* Genome-wide association of early-onset myocardial infarction with single nucleotide polymorphisms and copy number variants. *Nature genetics* **41**, 334-341, doi:10.1038/ng.327 (2009).
- 39 Szpakowicz, A. *et al.* The rs9982601 polymorphism of the region between the SLC5A3/MRPS6 and KCNE2 genes associated with a prevalence of myocardial infarction and subsequent long-term mortality. *Polskie Archiwum Medycyny Wewnętrznej* **125**, 240-248 (2015).
- 40 Wakil, S. M. *et al.* A genome-wide association study reveals susceptibility loci for myocardial infarction/coronary artery disease in Saudi Arabs. *Atherosclerosis* **245**, 62-70, doi:10.1016/j.atherosclerosis.2015.11.019 (2016).
- 41 Hu, Z., Crump, S. M., Zhang, P. & Abbott, G. W. Kcne2 deletion attenuates acute post-ischaemia/reperfusion myocardial infarction. *Cardiovascular research* **110**, 227-237, doi:10.1093/cvr/cvw048 (2016).
- 42 Roepke, T. K. *et al.* Kcne2 deletion uncovers its crucial role in thyroid hormone biosynthesis. *Nature medicine* **15**, 1186-1194, doi:10.1038/nm.2029 (2009).
- 43 Reutens, A. T. *et al.* The association between cystatin C and incident type 2 diabetes is related to central adiposity. *Nephrology, dialysis, transplantation : official publication of*

- the European Dialysis and Transplant Association - European Renal Association* **28**, 1820-1829, doi:10.1093/ndt/gfs561 (2013).
- 44 Morioka, S., Makino, H., Shikata, K. & Ota, Z. Changes in plasma concentrations of vitronectin in patients with diabetic nephropathy. *Acta medica Okayama* **48**, 137-142 (1994).
- 45 Alam, C. M. *et al.* Keratin 8 modulates beta-cell stress responses and normoglycaemia. *Journal of cell science* **126**, 5635-5644, doi:10.1242/jcs.132795 (2013).
- 46 Westermark, P., Andersson, A. & Westermark, G. T. Islet amyloid polypeptide, islet amyloid, and diabetes mellitus. *Physiological reviews* **91**, 795-826, doi:10.1152/physrev.00042.2009 (2011).
- 47 Marcu, M. G. *et al.* Heat shock protein 90 modulates the unfolded protein response by stabilizing IRE1alpha. *Molecular and cellular biology* **22**, 8506-8513 (2002).
- 48 Ramos, R. R., Swanson, A. J. & Bass, J. Calreticulin and Hsp90 stabilize the human insulin receptor and promote its mobility in the endoplasmic reticulum. *Proceedings of the National Academy of Sciences of the United States of America* **104**, 10470-10475, doi:10.1073/pnas.0701114104 (2007).
- 49 Back, S. H. & Kaufman, R. J. Endoplasmic reticulum stress and type 2 diabetes. *Annual review of biochemistry* **81**, 767-793, doi:10.1146/annurev-biochem-072909-095555 (2012).
- 50 Eletto, D., Dersh, D. & Argon, Y. GRP94 in ER quality control and stress responses. *Seminars in cell & developmental biology* **21**, 479-485, doi:10.1016/j.semcd.2010.03.004 (2010).
- 51 Harding, H. P. & Ron, D. Endoplasmic reticulum stress and the development of diabetes: a review. *Diabetes* **51 Suppl 3**, S455-461 (2002).

- 52 Thierry, M. *et al.* Early adaptive response of the retina to a pro-diabetogenic diet: Impairment of cone response and gene expression changes in high-fructose fed rats. *Experimental eye research* **135**, 37-46, doi:10.1016/j.exer.2015.04.012 (2015).
- 53 Donath, M. Y., Boni-Schnetzler, M., Ellingsgaard, H. & Ehses, J. A. Islet inflammation impairs the pancreatic beta-cell in type 2 diabetes. *Physiology (Bethesda)* **24**, 325-331, doi:10.1152/physiol.00032.2009 (2009).
- 54 Cerf, M. E. Beta cell dysfunction and insulin resistance. *Front Endocrinol (Lausanne)* **4**, 37, doi:10.3389/fendo.2013.00037 (2013).
- 55 Kim, S. J., Ao, Z., Warnock, G. & McIntosh, C. H. Incretin-stimulated interaction between beta-cell Kv1.5 and Kvbeta2 channel proteins involves acetylation/deacetylation by CBP/SirT1. *The Biochemical journal* **451**, 227-234, doi:10.1042/BJ20121669 (2013).
- 56 Boini, K. M. *et al.* Enhanced insulin sensitivity of gene-targeted mice lacking functional KCNQ1. *American journal of physiology. Regulatory, integrative and comparative physiology* **296**, R1695-1701, doi:10.1152/ajpregu.90839.2008 (2009).
- 57 Asahara, S. *et al.* Paternal allelic mutation at the Kcnq1 locus reduces pancreatic beta-cell mass by epigenetic modification of Cdkn1c. *Proceedings of the National Academy of Sciences of the United States of America* **112**, 8332-8337, doi:10.1073/pnas.1422104112 (2015).
- 58 Panaghie, G. & Abbott, G. W. The impact of ancillary subunits on small-molecule interactions with voltage-gated potassium channels. *Current pharmaceutical design* **12**, 2285-2302 (2006).
- 59 Heitzmann, D. *et al.* Heteromeric KCNE2/KCNQ1 potassium channels in the luminal membrane of gastric parietal cells. *The Journal of physiology* **561**, 547-557, doi:10.1113/jphysiol.2004.075168 (2004).

- 60 Roura-Ferrer, M. *et al.* Impact of KCNE subunits on KCNQ1 (Kv7.1) channel membrane surface targeting. *Journal of cellular physiology* **225**, 692-700, doi:10.1002/jcp.22265 (2010).
- 61 Li, Y. *et al.* Intracellular ATP binding is required to activate the slowly activating K⁺ channel I(K_s). *Proceedings of the National Academy of Sciences of the United States of America* **110**, 18922-18927, doi:10.1073/pnas.1315649110 (2013).
- 62 Yamagata, K. *et al.* Voltage-gated K⁺ channel KCNQ1 regulates insulin secretion in MIN6 beta-cell line. *Biochemical and biophysical research communications* **407**, 620-625, doi:10.1016/j.bbrc.2011.03.083 (2011).

Conclusion

The metabolic syndrome refers to a cluster of CVD risk factors that come together in a single individual. These CVD risk factors include insulin resistance, hypertension and hypertriglyceridemia. Metabolic syndrome is quite common. According to the National Health and Nutrition Examination Survey (NHANES) of 1999-2006, prevalence of metabolic syndrome is 34% of the population in the U.S (1). There are several animal models of metabolic syndrome, the *LepR^{db/db}* mouse being the most well-known. This model loses leptin receptor function due to a point mutation in the leptin receptor gene, *LepR*. This mutation causes cardiac contractile dysfunction (2, 3, 4), reduced cardiac efficiency (5,6) and other CVD risk factors including hyperglycemia at 4-8 weeks of age (7, 8, 9), insulin resistance (5, 10, 11, 12), hyperlipidemia (13, 14, 15), and hypertriglyceridemia (16).

Previous studies from the Abbott lab have shown that *Kcne2* deletion causes sudden cardiac death exhibiting elevated angiotensin II, which is a major hormone in blood pressure homeostasis (17). In Chapter 1, we showed that *Kcne2* deletion promotes atherosclerosis and diet-dependent sudden death. In Chapter 2, we showed that *Kcne2* deletion increases CVD risk factors, hypertriglyceridemia, hyperhomocysteinemia and high levels of CRP.

Metabolic syndrome is considered to be a risk factor not only for CVD but also for NAFLD and T2DM. Two key components of metabolic syndrome, glucose and triglyceride levels, are elevated in NAFLD patients. It is of little surprise then that approximately 85% of patients with

diabetes also have metabolic syndrome (18). Many risk factors for CVD are also predisposing factors for NAFLD and T2DM. Hypertriglyceridemia is also a risk factor for T2DM and conversely, and T2DM can lead to significant hypertriglyceridemia (19). Homocysteine not only degrades the formation of the components of arteries, but also causes ER stress (20,21,22) which is one of the main mechanisms underlying β -cell failure in T2DM (23,24). Homocysteine-induced ER stress also causes dysregulation of the cholesterol and triglyceride biosynthetic pathways (20). In Chapter 3, we confirmed by microarray transcriptome analysis that in islet cells, *Kcne2* deletion causes ER stress and increases expression of homocysteine-inducible, endoplasmic reticulum stress-inducible, ubiquitin-like domain member 1 (Herpud1) which plays a role in maintaining intracellular Ca^{2+} homeostasis (25,26). CRP is a substance produced by the liver in response to inflammation. Elevated CRP levels in blood may indicate CVD and pancreatitis as well as liver disease (27).

In Chapter 2, we also showed that *Kcne2* deletion causes early-onset NAFLD as early as postnatal day 7 via iron deficiency, and hypertriglyceridemia as early as postnatal day 21. Microarray transcriptome analysis showed that *Kcne2* deletion activates PGC-1 α downstream pathways including beta-oxidation of fatty acids, glucose concentration and hepatic steatosis. In Chapter 3, we demonstrated that *Kcne2* deletion impairs glucose tolerance as early as 5 weeks of age in pups fed a western diet, ultimately leading to T2DM. In adult mice fed a normal diet, *Kcne2* deletion causes T2DM, showing insufficient insulin secretion and insulin resistance.

There is a strong association between T2DM and NAFLD. T2DM and NAFLD are common conditions that regularly co-exist (more than 90% of obese patients with T2DM also have NAFLD) (28). The two symptoms can act synergistically to drive each other (28). In both conditions, insulin resistance and PGC-1 α play important roles. It has been reported that PGC-1 α is upregulated in the livers of rodents in models of T2DM, and that increased PGC-1 α expression contributes to elevated hepatic glucose output and the development of

hyperglycemia (29). In Chapter 2, we showed that *Kcne2* deletion activates PGC-1 α pathways in liver, suggesting that these activated pathways may contribute to the development of hyperglycemia. Because increased PGC-1 α by hyperglycemia also induces diabetic vascular dysfunction (30,31), activation of PGC-1 α by *Kcne2* deletion may also contribute to induction of CVD, which we described in Chapter 1. There is also a strong correlation between T2DM and CVD, wherein high blood glucose levels can lead to increased plaque formation and worsened atherosclerosis (32,33,34). Thus, hyperglycemia caused by *Kcne2* deletion may increase plaque formation in Chapter 1.

Our findings demonstrate for the first time that genetic disruption of an ion channel subunit gene can cause multiple aspects of metabolic syndrome, including atherosclerosis, NAFLD and T2DM. Each factors likely act synergistically to induce or worsen the others. These studies may potentially help in developing novel therapeutic strategies targeting KCNE2-containing Kv channel complexes for the treatment of CVD and metabolic syndrome, or in the shorter term by directing genetic screening studies to help identify those at risk. Future mechanistic studies will be directed at delineating exactly which Kv channels KCNE2 regulates in pancreatic islets, and comparing the effects of, e.g., cardiac myocyte or islet-cell-specific *Kcne2* deletion with global *Kcne2* deletion.

References

1. Mozumdar, A. *et al.*, Persistent increase of prevalence of metabolic syndrome among US adults: NHANES III to NHANES 1999-2006. *Diabetes Care*, 2011.**34**(1):216-219.
2. Aasum, E. *et al.*, Effect of BM 17.0744, a PPARalpha ligand, on the metabolism of perfused hearts from control and diabetic mice. *Can J Physiol Pharmacol*, 2005.**83**: 183-190.
3. Carley, A. N. *et al.*, Treatment of type 2diabetic *db/db* mice with a novel PPARγ agonist improves cardiac metabolism but not contractile function. *Am J Physiol Endocrinol Metab*, 2004.**286**:449-455.
4. Oakes, N. D.*et al.*, Cardiac metabolism in mice: Tracer method developments and in vivo application revealing profound metabolic inflexibility in diabetes. *Am J Physiol Endocrinol Metab*, 2006.**290**:870-881.
5. Hafstad, A. D. *et al.*, Glucose and insulin improve cardiac efficiency and postischemic functional recovery in perfused hearts from type 2 diabetic (*db/db*) mice. *Am J Physiol Endocrinol Metab*, 2007.**292**:1288-1294.
6. How, O-J. *et al.*, Increased myocardial oxygen consumption reduces cardiac efficiency in diabetic mice.*Diabetes*,2006.**55**:466-473.
7. Green, M. C. *et al.*, Genetic Variants and Strains of the Laboratory Mouse. *Stuttgart, NY: Gustav Fischer Verlag*,1981
8. Lyon, M. F. *et al.*, (1996). Genetic Variants and Strains of the Laboratory Mouse (3rd Ed.) *New York: Oxford University Press*,1996.**2**
9. Rodgers, K. E. *et al.*, Expression of intracellular filament, collagen, and collagenase

- genes in diabetic and normal skin after injury. *Wound Rep Reg*, 2006.**14**:298-305.
10. del Rey, A. *et al.*, Antidiabetic effects of interleukin 1. *Proc. Natl. Acad. Sci. USA*, 1989.**86**:5943-5947
 11. Hafstad, A. D. *et al.*, Perfused hearts from Type 2 diabetic (db/db) mice show metabolic responsiveness to insulin. *Am J Physiol Heart Circ Physiol*, 2006.**290**:1763-1769.
 12. Oakes, N. D. *et al.*, Cardiac metabolism in mice: Tracer method developments and in vivo application revealing profound metabolic inflexibility in diabetes. *Am J Physiol Endocrinol Metab*, 2006.**290**:870-881.
 13. How, O-J. *et al.*, Increased myocardial oxygen consumption reduces cardiac efficiency in diabetic mice. *Diabetes*, 2006.**55**:466-473.
 14. Jones, S. P. *et al.*, Reperfusion injury is not affected by blockade of P-selectin in the diabetic mouse heart. *Am J Physiol Heart Circ Physiol*, 1999.**277**:763-769.
 15. Zuurbier, C. J. *et al.*, Short-term hyperglycemia increases endothelial glycocalyx permeability and acutely decreases lineal density of capillaries with flowing red blood cells. *J Appl Physiol*, 2005.**99**:1471-1476.
 16. Cao, J. *et al.*, A predominant role of acyl-CoA: Monoacylglycerol acyltransferase-2 in dietary fat absorption implicated by tissue distribution, subcellular localization, and up-regulation by high fat diet. *J. Biol. Chem*, 2004.**279**:18878-18886.
 17. Hu, Z. *et al.* Kcne2 deletion creates a multisystem syndrome predisposing to sudden cardiac death. *Circulation. Cardiovascular genetics*, 2014.**7**:33-42.
 18. Alexander C.M. *et al.*, NCEP-defined metabolic syndrome, diabetes, and prevalence of coronary heart disease among NHANES III participants age 50 years and older. *Diabetes*, 2003.**52**:1210–1214.
 19. D'Agostino Jr. R.B. *et al.*, Cardiovascular disease risk factors predict the development of type 2 diabetes: the insulin resistance atherosclerosis study. *Diabetes Care*, 2004.**27**: 2234–2240.

20. Werstuck. G.H. *et al.*, Homocysteine-induced endoplasmic reticulum stress causes dysregulation of the cholesterol and triglyceride biosynthetic pathways. *J Clin Invest*, 2001.**107**(10):1263–1273.
21. Outinen P.A. *et al.*, Homocysteine-induced endoplasmic reticulum stress and growth arrest leads to specific changes in gene expression in human vascular endothelial cells. *Blood*, 1999.**94**:959–967.
22. Outinen P.A. *et al.*, Characterization of the stress-inducing effects of homocysteine. *Biochem J*, 1998.**332**:213–221.
23. Back, S. H. *et al.*, Endoplasmic reticulum stress and type 2 diabetes. *Annual review of biochemistry*, 2012.**81**:767-793.
24. Harding, H. P. *et al.*, Endoplasmic reticulum stress and the development of diabetes: a review. *Diabetes*, 2002.**51**(Suppl 3):S455-461.
25. Chigurupati. S. *et al.*, The Homocysteine-inducible Endoplasmic Reticulum Stress Protein Counteracts Calcium Store Depletion and Induction of CCAAT Enhancer-binding Protein Homologous Protein in a Neurotoxin Model of Parkinson Disease. *J. Biol. Chem*, 2009.**284**(27):18323–18333.
26. Belal C. *et al.*, The homocysteine-inducible endoplasmic reticulum (ER) stress protein Herp counteracts mutant α -synuclein-induced ER stress via the homeostatic regulation of ER-resident calcium release channel proteins. *Hum. Mol. Genet*, 2012.**21**(5):963-977.
27. David C.W. *et al.*, Metabolic syndrome: A marker of patients at high cardiovascular risk. *Can J Cardiol*, 2006.**22**(Suppl B): 85B–90B
28. Tolman, K. G. *et al.*, Spectrum of liver disease in type 2 diabetes and management of patients with diabetes and liver disease. *Diabetes Care*, 2007.**30**:734–743.
29. Yoon J.C. *et al.*, Control of hepatic gluconeogenesis through the transcriptional coactivator PGC-1. *Nature*, 2001.**413**:131–138.
30. Sawada N. *et al.*, Endothelial PGC-1 α Mediates Vascular Dysfunction in Diabetes. *Cell*

Metabolism, 2014.**19**(2):246–258.

31. Hu F.B. *et al.*, Elevated risk of cardiovascular disease prior to clinical diagnosis of type 2diabetes. *Diabetes Care*, 2002.**25**:1129–1134.
32. McGill H.C. Jr.*et al.*, Relation of glycohemoglobin and adiposity to atherosclerosis in youth. *Arterioscler Thromb Vasc Bio*, 1995.**15**:431–40.
33. McGill H.C. Jr. *et al.*, Obesity accelerates the progression of coronary atherosclerosis in young men. *Circulation*, 2002.**105**: 2712–18.
34. Nesto R.W. *et al.*, Correlation between cardiovascular disease and diabetes mellitus: Current concepts. *Am J Med*, 2004.**116**(5A):11S–22S.